# THE ROLE OF RNA BINDING PROTEINS AND CRISPR/CAS9 AS A GENE EDITING TOOL IN DROSOPHILA NOCICEPTION

A Thesis
by
ERIK FERNANDO RANGEL SILVA

Submitted to the School of Graduate Studies
at Appalachian State University
in partial fulfillment of the requirements for the degree of
MASTER OF SCIENCE

May 2023
Department of Biology

# THE ROLE OF RNA BINDING PROTEINS AND CRISPR/CAS9 AS A GENE EDITING TOOL IN DROSOPHILA NOCICEPTION

A Thesis
by
ERIK FERNANDO RANGEL SILVA
May 2023

APPROVED BY:

Andrew Charles Bellemer, Ph.D.
Chairperson, Thesis Committee

Maryam Ahmed, Ph.D.
Member, Thesis Committee

Michael Opata, Ph.D.
Member, Thesis Committee

Dr. Ava J. Udvadia, Ph.D.
Chairperson, Department of Biology

Marie Hoepfl, Ed.D.
Interim Dean, Cratis D. Williams School of Graduate Studies

**Abstract**

THE ROLE OF RNA BINDING PROTEINS AND CRISPR/CAS9 AS A GENE EDITING TOOL IN DROSOPHILA NOCICEPTION

Erik Fernando Rangel Silva
B.S., Wingate University
M.S., Appalachian State University

Chairperson: Dr. Andrew Bellemer

*Drosophila melanogaster* is a powerful model organism to study nociception. The compact and easily manipulated genome provides an opportunity to determine the function of ion channels and signaling molecules involved in basal and sensitized nociception in both larval and adult animals. Using the GAL4/UAS system, ectopic expression, genetic knockdown with RNAi, and knockout with Cas9 are possible to pinpoint specific molecular mechanisms and cellular processes within nociceptors that are implicated in nociception. The three main objectives of this work were to: elucidate the impact that three RNA binding proteins have on basal nociception, establish a transgenic fly line capable of inducing Cas9-mediated knockout of specific genes, and to validate a protocol based on a previously published assay to measure thermal nociception in adults. The expression of SC35, an exon-inclusion splicing factor; LaRP4B, a translation stimulator; and eIF2α, a regulator of translation, were each found to be required for normal thermal nociception. Cas9 expression led to unforeseen, sgRNA-independent effects such as severe defects in dendrite

morphology. The adult thermal nociception assay was sufficiently calibrated and similar results to the original publication were able to be reproduced. Importantly, the findings made in the *Drosophila* model may be directly applicable to chronic pain in humans due to DNA sequence homology and the conserved function of proteins across species.

**Acknowledgments**

This thesis would not have been possible without the continued support and grace that Dr. Bellemer provided throughout my time at App. Under his rigorous mentorship, I became a better scientist and expanded my thinking. For this, I am deeply appreciative. To my committee members, Dr. Ahmed and Dr. Opata, I thank you for your guidance and feedback throughout this entire process.

I would also like to acknowledge my fellow lab mates and graduate students, past and present, for the camaraderie and community.

My sincerest gratitude to the Cratis D. Williams School of Graduate Studies for funding through the Graduate Student Diversity Fellowship and the Out of State Tuition Scholarship. Additionally, thank you to the Office of Student Research for Research and Travel Grant funding.

## Dedication

I dedicate this work to my parents, Jose Martinez and Liliana Silva, for the incredible sacrifices they have made to support me in my journey. I also dedicate this to my sister Karla, who believed in me and went to great lengths to make my graduate studies a reality.

## Table of Contents

## List of Tables

## List of Figures

# Introduction

## The Burden of Chronic Pain Conditions

Pain is generally understood as a negative emotional experience that occurs in response to an extreme stimulus, whether it be thermal, mechanical, or chemical in nature. Indeed, the capability to recognize and respond to pain is so important, that humans without this ability have significantly higher morbidity rates (Drissi et al., 2020). Like all physiological processes, however, pain must be dynamically regulated, such that it is present in the moments preceding potential injury and linger after injury to prevent further damage, but not when noxious or painful stimuli are absent. When dysregulation of pain occurs, it may progress into a chronic pain condition, which is defined as pain that persists for more than three weeks (Drissi et al., 2020).

An estimated 20.4% of the US population, or about 50 million people, are thought to suffer from chronic pain conditions while 19.6 million are estimated to suffer from a severe form of the disease (Dahlhamer et al., 2018). A study published in 2017 found that around one third of people suffering from chronic pain also experienced symptoms associated with depression and anxiety, which considerably decreases quality of life (Kawai et al., 2017). The study also found that the those suffering from severe chronic pain and chronic pain conditions that affect multiple areas were more likely to be women of lower socioeconomic status (Kawai et al., 2017). Additionally, the resulting loss in productivity was dramatically high, particularly for those experiencing chronic pain in multiple sites which was just under 10 hours a week (Kawai et al., 2017). In the United States, the total economic burden of treating chronic pain, which considers specialized healthcare and lost productivity is estimated to range from $560 to $635 billion (Gaskin & Richard, 2012).

**Nociception Basics**

Nociception refers to an organism's ability to detect harsh stimuli that have the potential to cause tissue damage. This can be extreme temperatures, mechanical pressure, UV radiation, or exposure to chemical irritants. The nervous system is responsible for detecting and regulating sensitivity to noxious stimuli, which is mediated by specialized sensory neurons known as nociceptors. In humans, nociceptors are in peripheral sensory ganglia, which are masses of neuron cell bodies. In humans, nociceptors are the Aδ- and C-fibers of dorsal root ganglia, which project off each side of the spinal cord (Dubin & Patapoutian, 2010).

Nociceptors are morphologically polar cells with three distinct areas: dendrites, soma, and axon. Each of these areas have specific, unique functions. Nociceptor dendrites are elaborately branched cellular protrusions embedded in the skin that serve as information receptors by directly interacting with the external environment (Koltzenburg et al., 1997). This ability to detect changes in the environment is different from other sensory information such as taste and smell, which require auxiliary cells (Koltzenburg et al., 1997; Roper & Chaudhari, 2017). Information detected at the dendrites is then converted into electrical signals by ion channels. Ion channels are transmembrane proteins that are embedded in a nociceptor's plasma membrane and allow for the influx or efflux of ions. This is what gives neurons their electrical excitability. These electrical signals are then sent to the soma or cell body where they are integrated. If the signal is strong enough, it continues to and through the axon, another long, branched protrusion as an action potential. At the axon terminals, in the spinal cord, the action potential triggers the release of neurotransmitters. These neurotransmitters serve as chemical messengers that travel across a gap between neurons,

called the synaptic cleft, from the nociceptor's axon to a second order interneuron's dendrites. This process relays information from the nociceptor to the next neurons in the circuit and quickly triggers the appropriate response to the detected stimulus.

**Using *Drosophila* as a Model Organism for Nociception Studies**

Studying nociception in humans is very costly, uses subjective ratings, and requires stringent adherence to many ethical and regulatory guidelines. Therefore, using model organisms to study nociception is a very attractive option. *Drosophila melanogaster* is a valuable model organism for neurobiological studies of pain mechanisms (Im & Galko, 2012). *Drosophila* has a relatively simple genome with 3 autosomal chromosomes, which makes its compact genome particularly amenable to genetic manipulations (Ugur et al., 2016). Around 75% of the genes that cause disease in humans have a fly homolog, meaning that there is a high level of genetic conservation between the two species (Ugur et al., 2016).

This conservation is demonstrated by an investigation of the functional relationship between the fly and human ligands that stimulate the Bone Morphogenetic (BMP) pathway (Padgett et al., 1993). The *Drosophila* ligand is Dpp and the human homolog is BMP2/4 (Padgett et al., 1993). In *dpp* mutant flies, normal development is disrupted (Padgett et al., 1993). This is restored by inserting the human *BMP2/4* into the genome of *Drosophila* larvae (Padgett et al., 1993). The genetic homology between the fly and humans exhibited in this experiment validates *Drosophila* as a model organism and showcases the information that can be gained by studying pain mechanisms in *Drosophila* to understand how it functions in humans.

**Nociception in *Drosophila* larvae**

As previously mentioned, nociception in humans is mediated by Aδ- and C-fibers and in *Drosophila* larvae, there is a similar type of sensory neuron. Type II multidendritic (md) neurons in flies directly transduce somatosensory information without an accessory cell (Brewster & Bodmer, 1995). These neurons can be further subdivided into four different classes, each with increasingly complex dendritic branching (Grueber et al., 2002). Type II class IV md neurons have the most complex dendritic branching and tile the entire larval body wall (Grueber et al., 2002; Hwang et al., 2007; Robertson et al., 2013). These class IV md neurons function as nociceptors in *Drosophila* and are activated by noxious stimuli such as excessive heat and mechanical pressure (Grueber et al., 2002; Hwang et al., 2007; Robertson et al., 2013; Tracey et al., 2003).

When these neurons are activated, larvae exhibit a consistent and stereotyped response to noxious stimuli that is not present in other developmental stages (Hwang et al., 2007; Tracey et al., 2003). After stimulation with a noxious stimulus such as temperatures above 38°C or mechanical pressure greater than 30mN, larvae enact a stereotyped behavior known as nocifensive escape locomotion (NEL) (Hwang et al., 2007; Zhong et al., 2010). During NEL, larvae complete one or more 360° barrel rolls that resemble a corkscrew motion (Hwang et al., 2007). Nociception can therefore be observed and analyzed with this unique locomotion pattern. Quantification of nociception is possible by measuring the latency in seconds between exposure to noxious stimulus and completion of a barrel roll, or by calculating the percentage of larvae that respond to a noxious stimulus with NEL (Hwang et al., 2007;Tracey et al., 2003; Zhong et al., 2010).

As the temperature that larvae are exposed to increases from 38°C, their response latency decreases. In other words, as the magnitude of the stimulus increases, the larvae will react faster to avoid the stimulus through NEL. Depending on the expected outcome of a given genetic manipulation, various temperatures can be used to test larval thermal nociception. For example, testing larvae at 46°C is useful to determine what genes are required for basal nociception. As control larvae have an average latency of 2-3s at this temperature, nociceptive defects are indicated if a genotype has a delayed average latency. Larvae can also be tested at 42°C to test for a hypersensitive nociception phenotype. At this temperature, control larvae exhibit a greater average latency of around 8s. Therefore, if the genetic manipulation induces a hypersensitive phenotype, this will be represented as a lower latency compared to the controls which would not be detected during a 46°C thermal nociception assay. Another important assay that may be conducted at 42°C involves injury-induced sensitization of larvae to simulate plastic changes that occur during chronic pain conditions (Babcock et al., 2009; Follansbee et al., 2017; Im et al., 2015; Jo et al., 2017).

**Thermal Nociception in *Drosophila* Adults**

While the larval model has provided great insight into the cellular mechanisms that are involved in nociception, it is limited in its ability to demonstrate changes over an extended period. This is because the wandering third instar larval lasts for 24-48 hours before transitioning to the pupal state (Fernández-Moreno et al., 2007). After metamorphosis, adults can survive for up to a month which provides a substantial timeframe to observe changes in nociceptive function (Fernández-Moreno et al., 2007). An experimental paradigm to test adult thermal nociception uses a water bath to subject adult flies to a 46°C heat challenge

(Neely et al., 2011). After 4 minutes of being subjected to the heat challenge, the number of flies that were able to avoid incapacitation via prolonged exposure to the noxious temperature was recorded (Neely et al., 2011). A defect in nociceptive function is indicated by a fly's inability to avoid the noxious temperature and become incapacitated as a result (Neely et al., 2011). Adding this protocol to the Bellemer lab's repertoire of behavioral experiments will allow the investigation of what molecules and genes are involved in long-term changes in nociception.

## Inducing Nociceptor-Specific Manipulations to Study the Mechanisms of Nociception

### *The GAL4/UAS System*

To understand these molecular events involved in nociception, it is important to be able to make nociceptor-specific genetic manipulations, which is made possible with the GAL4/UAS system (Figure 1) (Brand & Perrimon, 1993). *Pickpocket* is expressed exclusively in nociceptors (Zhong et al., 2010). This unique expression pattern allows for targeted genetic manipulations by utilizing the GAL4/UAS system (Brand & Perrimon, 1993; Phelps & Brand, 1998). *GAL4* encodes a yeast transcription factor that can be inserted downstream of a cell-specific promotor in the fly genome. *UAS* (Upstream Activation Sequence) is a specific DNA sequence that serves as a binding site for GAL4 and activates transcription of downstream genes. This system can therefore be used to manipulate gene expression in specific cells. Integrating *GAL4* downstream of the sequence for *ppk* restricts expression of the transcription factor to class IV md neurons (Figure 1) (Ainsley et al., 2003; Phelps & Brand, 1998). A transgenic fly line with *UAS* preceding a gene of interest is created such that when a *ppk-GAL4* and *UAS-(transgene)* lines are crossed together, the progeny

express the complete system (Ainsley et al., 2003; Phelps & Brand, 1998). Expression of *GAL4* is restricted to nociceptors which will bind to *UAS* and drive expression of the desired transgene (Ainsley et al., 2003; Phelps & Brand, 1998). Using this method, robust cell-specific genetic alterations can be made through ectopic expression, knockdown with RNA interference (RNAi), or knockout with Cas9 (Heigwer et al., 2018; Meltzer et al., 2019; Phelps & Brand, 1998).

### *Using RNAi for Loss of Function Experiments*

One common genetic manipulation accomplished with the GAL4/UAS system involves RNAi-mediated gene knockdowns (Heigwer et al., 2018). With this method, RNA hairpin sequences that correspond to a gene of interest are expressed with a cell-specific *GAL4* transgene and a *UAS-RNAi* transgene (Heigwer et al., 2018). These hairpin RNAs are cleaved by Dicer-2 and associate with Argonaute 2 to form the RNA-induced silencing complex (RISC) (Heigwer et al., 2018).The RISC then uses the RNA molecule that is complimentary to the target gene mRNA to bind and degrade the mRNA transcript, preventing expression at the translational level in specific cells (Heigwer et al., 2018). Thus, the GAL4/UAS system can be used to knock down genes specifically in nociceptors that are suspected to be involved in nociception in loss-of-function experiments (Kim et al., 2012; Neely et al., 2010, 2011; Tracey et al., 2003; Zhong et al., 2010, 2012).

### *Utilizing Cas9-Mediated Mutagenesis in Drosophila*

CRISPR (Clustered Regularly Interspaced Short Palindromic Repeats)/Cas9 can be used to induce genetic mutations at specific sequences exclusively in nociceptors with the

**Figure 1**

*The ppk-GAL4/UAS System Allows for Cell-Specific Manipulations*

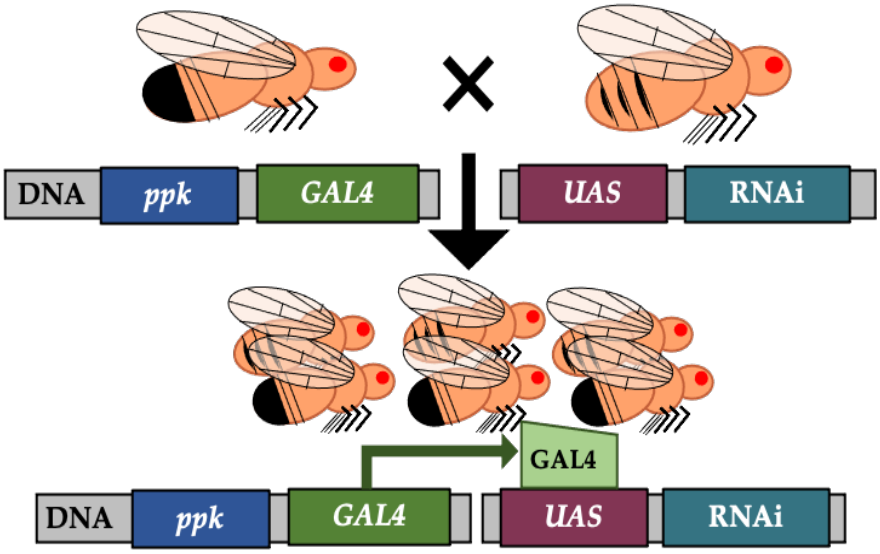


*Note:* This diagram depicts the GAL4/UAS system. pickpocket driver restricts expression of the GAL4 transcription factor to nociceptors. When expressed, GAL4 binds to the Upstream Activator Sequence (UAS) and drives expression of the desired transgene (RNAi in the depicted scenario) (Brand & Perrimon, 1993). (Adapted from Brand & Perrimon 1993)

GAL4/UAS system (Meltzer et al., 2019; Wang et al., 2016). To be used in *Drosophila*, a stock line of flies that use the GAL4/UAS system to drive expression of Cas9 only in nociceptors is needed. This modular design would allow the stock to be easily used to knock out target genes. This would be accomplished by crossing adults with the *ppk-GAL4;UAS-Cas9* genotype to a fly line that expresses UAS-"X".gRNA that targets "gene X". The progeny would then express *ppk-GAL4;UAS-Cas9,UAS-X.gRNA* and gene X would be knocked out exclusively in the nociceptors. As a novel technique, using the GAL4/UAS system for Cas9-mediated knockout can provide an additional tool for manipulating

nociceptor expression and functions (Meltzer et al., 2019). Additionally, Cas9 KO could be used to further validate findings made using RNAi, such as the defects in thermal nociception observed with *eIF2α*, *sc35*, and *LaRP4B* knockdown.

CRISPR refers to a sequence of bacterial DNA that codes an adaptive defense against viral pathogens (Wang et al., 2016). CRIPSR sequences are composed of characteristic palindromic repeats with coding "spacers" sequences in between them (Wang et al., 2016). Cas proteins and important CRISPR RNA (Gasiunas et al.) transcripts are included within these spacers (Wang et al., 2016). Endogenous bacterial Cas proteins break up segments of viral DNA and incorporate it into the host genome between the palindromic repeats as crRNA spacers (Wang et al., 2016). Once a foreign bacteriophage attempts to reinfect the bacteria, these crRNA are expressed and processed to be integrated with tracrRNA (Wang et al., 2016). The purpose of tracrRNA is to provide scaffolding for the guide RNA strand (Meltzer et al.), which is itself produced from processed crRNA transcripts (Liao & Beisel, 2021). Both tracrRNA and gRNA strands complex and form the single guide RNA (Liao & Beisel) (Wang et al., 2016). Modern applications of Cas9 hybridize the tracrRNA and crRNAs into a single synthetic guide RNA strand (Liao & Beisel) (Meltzer et al., 2019; Poe et al., 2019; Wang et al., 2016). This complex associates with the Cas9 protein, and the gRNA scans target DNA for a complimentary sequence and binds through conventional Watson-Crick base pairing (Wang et al., 2016). In order for the gRNA to bind to DNA and induce Cas9 nuclease activity, a PAM (protospacer adjacent motif) sequence must be present in the target DNA (Wang et al., 2016). Though this is absolutely required, the Cas9 variant that is commonly used is derived from *Streptococcus pyogenes* and needs a very simple

PAM, NGG, where N is any nucleotide (Wang et al., 2016). Once the gRNA has colocalized with Cas9 to the target DNA sequence, nuclease activity can occur (Wang et al., 2016).

### *Mechanisms of Cas9-Induced DSB and NHEJR*

After a gRNA strand guides Cas9 to a specific DNA sequence, a DSB is made that is repaired by the cell through either non-homologous end joining repair (NHEJR) or homology-directed repair. The Cas9 protein has two nuclease domains: the HNH and RuvC-like domains (Gasiunas et al., 2012; Wang et al., 2016). The HNH Cas9 nuclease domain is located toward the middle of the protein and cleaves the complimentary DNA strand that is bound to the gRNA (Gasiunas et al., 2012). The RuvC domain is located at the N terminus and cleaves the noncomplimentary DNA strand (Gasiunas et al., 2012). Cleavage of the target DNA sequence occurs 3nt away from the PAM and leaves blunt edges that may be repaired through one of two mechanisms (Gasiunas et al., 2012). Homology-directed repair relies on the availability of a template DNA strand so the sequence of DNA that was damaged during the DSB can be fully replaced with the original content (Kuhfittig-Kulle et al., 2007). This method is preferred since it will result in minimal, if any, mutations or variations from the original sequence (Kuhfittig-Kulle et al., 2007). As in the case of Cas9-mediated DSB, NHEJR mechanisms take place after DNA damage is detected (Gasiunas et al., 2012; Kuhfittig-Kulle et al., 2007; Scully et al., 2019; Wang et al., 2016). Various factors are required for NHEJR, but the special DNA polymerases, λ and μ are what add/remove nucleotides to the blunt edges and result in the characteristic indels that prevent expression of the targeted gene (Kuhfittig-Kulle et al., 2007; Scully et al., 2019).

### *Using GAL4/UAS for Gain of Function Experiments and Ectopic Expression*

The GAL4/UAS system is not restricted to loss of function experiments, as the model can also be used to drive overexpression by simply inserting the desired transgene downstream of the UAS element (Johnson et al., 1995; Phelps & Brand, 1998). In addition, ectopic expression of GFP reporter genes is also possible with the GAL4/UAS system. For example, visualization of nociceptors has been achieved by ectopic expression of GFP in the cell membrane using *ppk-GAL4/UAS-mCD8::GFP* (Hwang et al., 2007). mCD8::GFP is a mouse cell surface marker that is tagged with GFP. Expression of this transgene results in a strong GFP signal that is localized to the nociceptor's plasma membrane (Hwang et al., 2007). As a result, observation and quantification of dendrite morphology is possible by manually tracing images of fluorescent nociceptors captured using confocal microscopy and analyzing the length and branching of dendrites with the NeuronJ plugin in the software package, ImageJ (Meijering et al., 2004). This provides a useful way of measuring how genetic manipulations in nociceptors can affect dendrite morphology.

## Nociceptors Express Diverse Ion Channels

The use of the GAL4/UAS system allowed studies of the specialized ion channels that nociceptors use to detect various modalities of stimuli (Kim et al., 2012; Tracey et al., 2003; Zhong et al., 2010, 2012). For example, there are ion channels that open exclusively in response to mechanical stimuli, some by high temperatures, and even channels that can detect both thermal and mechanical stress (Neely et al., 2011; Tracey et al., 2003; Zhong et al., 2010, 2012).

***dTRPA1***

Early research into the ion channels that are specifically used by nociceptors led to the discovery of the Transient Receptor Potential (TRP) family of ion channels (Caterina et al., 1997). There are two major groups of ion channels within the TRP family that are involved in nociception: TRPV and TRPA. TRPV ion channels are associated with nociception only in vertebrates while TRPA proteins are associated with nociception in both vertebrates and invertebrates (Breese et al., 2005; Gu et al., 2019; Heber et al., 2019; Jordt et al., 2004; Neely et al., 2011; Saito & Tominaga, 2017; Zhong et al., 2012). Additionally, defects in these TRP ion channels have been implicated in pain disorders in humans (Saito & Tominaga, 2017). One of the major ion channels that are used by human nociceptors to detect noxious thermal and mechanical stimuli is TRPV1 (Caterina et al., 1997).

dTRPA1 is a non-selective, calcium-permeable cation channel in *Drosophila* that belongs to the Transient Receptor Potential Ankyrin Repeat (TRPA) group of TRP channels and allows for the non-specific influx of ions (Neely et al., 2011; Zhong et al., 2012). It is a homolog for the human TRPA1 ion channel (Neely et al., 2011; Story et al., 2003). dTRPA1 contains several ankyrin repeat found at the N terminal of the protein, which is characteristic of the TRPA group of ion channels (Zhong et al., 2012).

This channel is particularly interesting because it is able to respond to both thermal and mechanical stimuli. (Neely et al., 2011). When *dTrpa1* mutant larvae are exposed to a noxious temperature of 46°C, the NEL latency is significantly higher than wildtype, indicating that this receptor is necessary for basal nociception (Zhong et al., 2012). In addition, mutant larvae that were subjected to a noxious mechanical stimulus of 30mN had a significantly lower response rate than the wildtype larvae (Zhong et al., 2012). Further,

various isoforms of dTrpa1 (*dTrpA1- A-D*) were found to be created through alternative splicing (Gu et al., 2019; Zhong et al., 2012). A striking finding was that specific isoforms had different temperatures in which they were the most responsive (Zhong et al., 2012). For example, the A isoform was significantly more active at a temperature range of 34-36°C (Zhong et al., 2012). Alternative splicing could therefore be implicated as a mechanism in which nociceptors modulate their sensitivity and response to stimuli.

Further, *dTrpA1* has been found to be required for adult thermal nociception and adult nociceptive sensitization (Khuong et al., 2019; Neely et al., 2010, 2011). In $dTrpA1^{ins}$ mutant flies, avoidance percentage was drastically reduced when compared to wildtype controls. (Neely et al., 2010, 2011) Additionally, thermal nociceptive sensitization in adults was prevented in $dTrpA1^{ins}$ mutant flies (Khuong et al., 2019).

***Pickpocket***

The degenerin/epithelial sodium ion channel (DEG/ENaC) subunit Pickpocket is expressed exclusively in class IV md neurons (Zhong et al., 2010). *Drosophila* larvae that are mutant for *ppk* exhibit a severe defect in general locomotion and their ability to detect a noxious mechanical stimulus of 50mN (Zhong et al., 2010). Whereas wildtype larvae produced a response to this stimulus in about 75-80% of trials, mutant larvae responded in about 25% of trials (Zhong et al., 2010). This effect is not observed when *ppk* is knocked down in other md neuron classes (Robertson et al., 2013; Zhong et al., 2010). Interestingly, this defective phenotype of *ppk* mutants was rescued with expression *ppk* in nociceptors (Zhong et al., 2010). Further experiments showed that Pickpocket is not required for thermal

nociception, as the mutant larvae exhibited normal basal thermal nociception, indicating that these processes may require mutually exclusive proteins (Zhong et al., 2010).

***Painless***

Another member of the TRP family of ion channels expressed in larval nociceptors is Painless, which is closely related to dTRPA1 (Tracey et al., 2003). Flies that are *painless* mutants show a significant increase in response latency to a 46°C stimulus, indicating that the Painless ion channel is required for thermal nociception. A similar effect was seen in response to noxious mechanical stimulus of 50mN: wildtype flies responded in 92% of trials but mutants only responded in 13% of trials (Tracey et al., 2003). The Painless ion channel also plays a significant role in adult thermal nociception as mutants exhibited a significantly lowered avoidance percentage to noxious thermal stimuli (Neely et al., 2011; Xu et al., 2006). Although Painless does not have a direct human homolog, its discovery provides useful evidence that multiple ion channels are involved in nociception and can also serve as a positive control for experiments (Tracey et al., 2003).

***Piezo***

The ion channel Piezo was recently discovered and belongs to a distinct family of Piezo mechanosensitive cation channels that are conserved in humans (Kim et al., 2012). A version of Piezo, dPiezo, is found in *Drosophila* larval nociceptors and although it only has 24% sequence homology to the human protein, dPiezo still allows an influx of ions in human cells under mechanical pressure (Kim et al., 2012). This indicates that the functionality of dPiezo is similar to the mammalian version in that the channel directly transduces

mechanical stimuli into an electrical signal that can be used by the neuron. Larvae that are homozygous mutant for *piezo* have a severely reduced response to mechanical stimuli that is rescued with ectopic expression of *dPiezo* (Kim et al., 2012). Neither thermal nociception nor gentle touch response is affected by knockdown, implicating *dpiezo* exclusively to the detection of noxious mechanical stimuli (Kim et al., 2012). A remarkable finding is that heterozygous mutant larvae for both *dPiezo* and *painless* exhibited a significant defect in nociception while no defect was noted in larvae that were heterozygous mutants for either *dpiezo* or *painless*, separately (Kim et al., 2012). This finding suggests that the dPiezo and Painless ion channels carry out their function in a parallel pathway (Kim et al., 2012).

***Paralytic***

In *Drosophila*, the sodium voltage gated channel Paralytic (Para) is required for neurons to generate action potentials (Siddiqi & Benzer, 1976; Wu & Ganetzky, 1980). It has also been used in one of the foundational *Drosophila* nociception studies (Zhong et al., 2010). One of the experiments that established class IV md neurons as the nociceptors involved knocking down *para* via RNAi using the GAL4/UAS system (Zhong et al., 2010). After *para* was knocked down in nociceptors, larvae showed a very dramatic reduction in its nociceptive function toward both thermal and mechanical stimuli (Zhong et al., 2010). As a result, RNAi knockdown of *para* is commonly used as a positive control as it reliably generates a defective nociception phenotype. Though a reliable defective phenotype is produced in larvae, *para* RNAi knockdown has not been studied in adult flies.

## The Chronic Pain Model in *Drosophila* Larvae

The regulation of these ion channels is very important for nociceptive sensitization after injury. Nociceptive sensitization occurs when the threshold for the detection of noxious stimuli is lowered. This induces allodynia and hyperalgesia wherein stimuli that would normally not be noxious elicit nociceptive behavior and stimuli that are noxious elicit a much stronger response, respectively. The larval stage of *Drosophila* is useful to study sensitization. In this model, 20 mJ/cm$^3$ of UV exposure induces tissue damage and results in epidermal release of pro-inflammatory cytokines (Babcock et al., 2009). This lowers the activation threshold of nociceptors which simulates a chronic pain condition in humans (Babcock et al., 2009). Within this experimental paradigm, allodynia is observed when NEL occurs in response to an innocuous temperature. Hyperalgesia is characterized by an NEL latency to a noxious stimulus that is lower than when larvae are not in the UV-induced sensitized state. Both are indicative of nociceptive sensitization, but each may be influenced by different signaling pathways.

## Various Signaling Pathways Modulate Larval Nociceptor Sensitivity

Various signaling pathways are involved in the sensitization process that occurs in nociceptors after UV-induced injury. Two of these pathways involve Hedgehog (Hh) and Tumor Necrosis Factor α (Webster & Vucic) signaling, both of which involve regulation of the *dTrpA1* ion channel (Babcock et al., 2009, 2011; Follansbee et al., 2017; Gjelsvik et al., 2018; Im et al., 2015).

The Hedgehog signaling pathway has a critical role in development by providing spatial polarity (Collins & Cohen, 2005). For example, in the developing *Drosophila* wing,

Hh secreted by progenitor cells form a concentration gradient such that cells in the anterior segment are exposed to a higher concentration (Collins & Cohen, 2005). This induces the expression of genes that are not expressed in cells that are exposed to a lower concentration (Collins & Cohen, 2005). In addition to its role in development, Hh signaling is involved in nociceptor sensitization (Babcock et al., 2011; Im et al., 2015).

The role of Hh signaling in nociceptor sensitization after UV exposure has been extensively studied (Babcock et al., 2011). The average response latency of control larvae declined when tested at 45°C from around 7s to around 4s after being subjected to UV-induced injury (Babcock et al., 2011). After injury, Hh is released by nociceptors and binds to the receptor Patched (Ptc) in an autocrine manner, which activates the Smoothened (Smo) transmembrane protein (Babcock et al., 2011). Activation of Smo initiates a signaling cascade resulting in the activation of the Cubitus interruptus (Ci) transcription factor (Babcock et al., 2011). This then goes on to induce expression of *dpp*, the ligand involved in the BMP pathway, and the *engrailed* (*en*) gene for a transcription factor, though its target genes are not yet known (Babcock et al., 2011; Follansbee et al., 2017). However, in every instance that prevented expression of functional components of the Hh signaling pathway (Ptc, Smo, Ci, dpp, and en), the average latency of larvae (~7s) remained unchanged after UV exposure (Babcock et al., 2011). This indicates that Hh signaling is required for nociceptor plasticity after UV injury (Babcock et al., 2011).

A pathway characteristic of immune signaling, Tumor Necrosis Factor α (Webster & Vucic) is primarily involved in promoting apoptosis or survival of infected host cells (Webster & Vucic, 2020). TNFα also plays a significant and established role in nociceptive sensitization in vertebrates (Babcock et al., 2009). The *Drosophila* homolog of TNF is a

ligand called Eiger which binds to the TNF Receptor (TNFR) homolog, Wengen (Babcock et al., 2009; Jo et al., 2017). During UV-induced sensitization, pro-apoptotic genes *reaper*, *hid*, and *grim* are expressed in nociceptors and release Dronc from inhibition which allows its association with *Drosophila* IAP1 and Dark caspases to form the apoptosome (Babcock et al., 2009; Jo et al., 2017). This ultimately induces expression of NF-$_{K}$B, a nuclear-localized transcription factor, but its target genes are not yet known (Jo et al., 2017).

The Hh and TNF signaling pathways have a mutual requirement of Painless and dTRPA1 in order to induce nociceptive allodynia (Babcock et al., 2011). Interestingly, the thermal allodynia that results from ectopic activation of both the Hh and TNF pathways is stronger than the allodynia induced by either pathway alone, suggesting that they may be induced separately (Babcock et al., 2011). These pathways are discrete in that Hh signaling requires dTRPA1 to induce thermal hyperalgesia, perhaps by making modifications to the ion channel, but TNF does not (Babcock et al., 2011). The link between these various pathways and the actual ion channels indicates that there is some regulation or modification that occurs to nociceptor ion channels during sensitization. Though the exact mechanism remains elusive, it is possible that post-transcriptional control of gene expression plays a significant role in nociceptor plasticity.

**The Mechanisms of Adult Nociceptive Sensitization**

Nociceptive sensitization can be modeled in the adult fly with an amputation assay (Khuong et al., 2019). With this methodology, the middle leg on the right side (ipsilateral) of an adult fly is amputated at the midline of the femur (Khuong et al., 2019). After amputation, a significant sensitization to an innocuous 38°C is observed, even up to 21 days after

amputation (Khuong et al., 2019). No hyperalgesia is noted as a result of this sensitization (Khuong et al., 2019). This methodology more closely resembles how chronic pain conditions in humans are developed following a traumatic injury (Fernández-Moreno et al., 2007; Khuong et al., 2019). Importantly, normal locomotion is not affected by amputation, so any abnormal behavior is a result of nociceptive defect rather than locomotion (Khuong et al., 2019).

While the adult amputation model for nociceptive sensitization more closely resembles how neuropathic pain occurs in humans, much less is known about the mechanisms behind it (Khuong et al., 2019). This is due in part to no current study showing evidence of defects in adult thermal nociception resulting specifically from nociceptors, or the class IV md neurons that express *ppk* in adults (Khuong et al., 2019; Neely et al., 2010, 2011; Xu et al., 2006).

What is known about this heightened sensitivity is that a critical interaction occurs between the PNS and CNS (Khuong et al., 2019). Inhibitory neurotransmission is an important regulator of sensory circuits. The neurotransmitter that is responsible for relaying inhibitory signals is GABA (Khuong et al., 2019). In the context of nociception, nociceptors are subjected to an inhibitory signal from GABA-ergic neurons that project from the Ventral Nerve Cord (VNC), which is the equivalent structure to the vertebral spinal cord (Khuong et al., 2019). This provides important regulation of basal nociceptor activity. After injury, nociceptors begin to overstimulate these GABA-ergic neurons which leads to an excitotoxic response of cell death (Khuong et al., 2019). At the same time that GABA-ergic neurons go through apoptosis, the nociceptor in the leg that was amputated experiences severe neuropathy (Khuong et al., 2019). The intact nociceptor on the contralateral side exhibits a

much stronger response to stimulation, indicating that nociceptors are sensitized (Khuong et al., 2019). This sensitization is mediated by the release of stimulatory acetylcholine (ACh) neurotransmitters from nociceptors to the GABA-ergic VNC neurons and initiates a signaling cascade that is only somewhat understood (Khuong et al., 2019). Nociceptors release ACh which binds to and activates the nicotinic acetylcholine receptor alpha subunit (nAChRα) on GABA-ergic VNC neurons (Khuong et al., 2019). This induces a signaling cascade that expresses the twist transcription factor (Khuong et al., 2019). Twist is required to promote expression of pro-apoptotic genes, such as *caspase* which results in permanent GABA-ergic cell death in the VNC (Khuong et al., 2019). While this central neuropathy occurs, modifications are being made to the PNS due to the augmented nociceptor response to stimuli (Khuong et al., 2019). Thermal allodynia in injured flies is prevented with nociceptor-specific knockdown of *dTrpa1* and *painless (Khuong et al., 2019)*. Interestingly, blocking output from nociceptors completely prevented any GABA-ergic cell death, meaning that the mechanism behind sensitization may play a considerable role in modulating the circuitry of nociception (Khuong et al., 2019). Although it is possible that the same signaling pathways that have been previously described in the larval model and post-transcriptional regulation of gene expression may be involved in adult sensitization, it has yet to be shown and is therefore a rich area of investigation (Khuong et al., 2019).

**Translational Control Influences Neuronal Function and Plasticity**

Nociceptors are first and foremost neurons that detect sensory information from the external environment, which is constantly changing. Therefore, these neurons need to be able to adapt and fine-tune its sensitivity to dynamic stimuli through regulation of ion channels. This ability to modulate a nociceptor's sensitivity to stimuli is exemplified after injury, where

a heightened sensitivity to subnoxious stimuli prevents further injury and allows for heightened vigilance of the surrounding environment (Babcock et al., 2009; Khuong et al., 2019). It is because of the vital function of nociceptors that determining the cellular and molecular events that govern its plastic nature is important to discover potential treatments for chronic pain conditions.

It is possible that the translational control of proteins affects the function of a nociceptor by regulating expression of structural proteins or ion channels. These structural and functional changes influence the ability for a nociceptor to detect and transmit information. In chronic pain conditions, this manifests as an oversensitivity or inability to detect noxious stimuli. An early study into the cellular processes involved in hyperalgesia in mice provides strong evidence for this idea (Hou et al., 1997). In this study conducted by Wen-Yeong Hou and colleagues, mice were administered formalin was to induce nociceptive sensitization (Hou et al., 1997). However, when cycloheximide, a protein synthesis inhibitor, was co-administered, mice were less reactive to noxious stimuli (Hou et al., 1997). This indicates that de novo protein synthesis is a crucial aspect of nociceptor plasticity.

The ability for a cell to regulate translation for specific proteins is also important, particularly when the nociceptors need to respond quickly to dynamic stimuli using specialized ion channels. For example, when mice were chemically sensitized, the amount of TRPA1 channels that were localized to the membrane was significantly higher than those that were unsensitized (Schmidt et al., 2009). This could then explain the hypersensitive phenotype seen in mice when exposed to mechanical pressure that is dependent on TRPA1 (Petrus et al., 2007).

## General Methods of Translational Control

### *Nuclear mRNA Processing and Transcript Stability*

RNA processing is an important mechanism for post-mitotic cells, such as neurons, to respond to dynamic stimuli. Therefore, identifying specific proteins that are involved in RNA processing in nociceptors and how they affect nociceptive behavior are important steppingstones to elucidate the mechanisms by which chronic pain conditions occur. Nuclear RNA processing is crucial for the availability and expression of mRNA transcripts in response to neuronal activity and environmental stimuli. This can be influenced by 5' capping, polyadenylation, alternative splicing.

The general composition of an mRNA transcript includes the 5' and 3' untranslated regions (Andreassi et al.) and open reading frame (ORF) or coding sequence (CDS). The 5' cap is added at the start of translation by the addition of a modified methionine residue (Galloway & Cowling, 2019). The function of this cap is to protect the transcript from degradation and to be used as a binding site by Eukaryotic Initiation Factor 4E (eIF4E) (Bellato & Hajj, 2016; Galloway & Cowling, 2019). The purpose of capping is to prevent endonuclease-mediated decay which increases transcript stability (Galloway & Cowling, 2019). The 5'UTR follows the 5' cap and is composed of an RNA sequence that may contain an upstream ORF which influences its ability to be expressed during cellular stress scenarios (Bellato & Hajj, 2016). The 3' UTR is located after the stop codon and contains multiple polyadenylation start sites (Bolognani & Perrone-Bizzozero, 2008; Hachet & Ephrussi, 2004).

Another way that the efficacy of translation can be modulated is through the stability of the actual mRNA transcript. The stability of mRNA transcripts is important as the duration

of a transcript's half-life is associated with translation efficacy and the expressed protein's half-life (Bolognani & Perrone-Bizzozero, 2008). The alternative polyadenylation sites are important for mRNA stability because as the poly-A tails increase in length, so does the stability of the transcript (Andreassi et al., 2018). Motifs found within the 3'UTR can influence the stability of the transcript (Bolognani & Perrone-Bizzozero, 2008). The ARE motif is composed of AU-rich sequences which are associated with transcripts that are unstable and thus short-lived (Bolognani & Perrone-Bizzozero, 2008). Interestingly, there is a correlation between the half-life of a transcript and the half-life of the expressed protein (Hargrove & Schmidt, 1989). The relationship suggests that mRNA transcripts that are unstable result in fast-acting proteins that may be highly regulated to ensure that they are only expressed under certain conditions (Bolognani & Perrone-Bizzozero, 2008). Proteins that bind to 3'UTR AREs can either stabilize or destabilize the transcript (Bolognani & Perrone-Bizzozero, 2008).

There are two main forms in which an mRNA transcript can be spliced. In the first method of constitutive splicing, the precursor mRNA transcript is scanned and all introns are removed while the remaining exons are ligated together to form the final transcript (Wang et al., 2015). The second method, alternative splicing, occurs concurrently with transcription within the nucleus and specific exons or introns are excised from a precursor transcript (Wang et al., 2015). In order for alternative splicing to occur, the spliceosome must first be assembled. The U1 and U2 small nuclear ribonucleoproteins (snRNP) along with the U4/U6.U5 snRNPs are the main components (Wang et al., 2015). The spliceosome then scans the transcript for the 5' splice site (SS), the branch point sequence, and the 3' splice site. The SS are still elusive of any identifying characteristics, but represent specific points in

the transcript that are snipped (Wang et al., 2015). Various rearrangements of spliceosome complex snRNPs occur throughout the splicing process (Wang et al., 2015). Of note, the exons and introns that are removed or retained during splicing is dependent on the *cis*-regulatory elements within the transcript and *trans*-acting factors like SR proteins. Exon and intron retention is determined by the presence of exon/intron splicing enhancer sequences (ESE;ISE) and interactions with SR proteins such as SC35 (Wang et al., 2015). Conversely, exon and intron excision is determined by the presence of exon/intron splicing silencers (ESS;ISS) and heterogeneous nuclear ribonucleoproteins (hnRNPs) (Wang et al., 2015).

As a result of the various combinations of exons and introns included within the transcript, proteins with varying functions can be made from a single transcript. The importance of alternative splicing is exemplified in the sex-determination pathway in *Drosophila* (Burtis & Baker, 1989). For example, *doublesex* in *Drosophila* embryos can give rise to two mRNA transcripts for a transcription factor after alternatively splicing together different exons (Burtis & Baker, 1989). The specific transcription factor generated will dictate whether the larvae will develop as male or female (Burtis & Baker, 1989). While this is an extreme, binary example, *doublesex* clearly underscores the ability for a single gene to produce two proteins with vastly different end results.

### *mRNA Localization and Local Translation*

The idea that translation occurs outside of the neuronal soma is substantiated by the following evidence. Previous studies have found that poly-ribosome complexes are present at the base of dendritic spines (Steward & Levy, 1982). These polysome complexes also contain membranous components which indicates the ability to produce and process integral

membrane proteins such as ion channels and other receptors (Steward, 1983). Further, rough endoplasmic reticulum markers are found throughout dendrites, indicating that the machinery to process membrane proteins away from the soma is available (Steward, 1983). Granules found in neurons contain mRNA and in response to neuronal activation, are localized to specific cellular compartments (Oh et al., 2013). The mRNA transcripts in these granules are transcriptionally repressed by various RBPs so that expression is only induced when the cell deems it necessary (Oh et al., 2013). Altogether, these findings suggest that nociceptors may similarly be able engage in post-transcriptional regulation of gene expression that is modulated through various signaling pathways.

### *Translation Initiation*

Translation initiation serves as the rate limiting step of protein synthesis, so studying this process is critical for discovering important regulators that may be targeted. Initiation begins with the formation of the eukaryotic initiation factor 4F complex (4F complex) which is composed of three main eIFs: -4E, -4G, and -4A (Hinnebusch & Lorsch, 2012). eIF4E functions as a cap binding protein and binds to the 5'm7G mRNA cap with the aid of eIF4G, which serves as a scaffolding protein for poly-A binding protein (PABP), eIF4A, and eI4E (Hinnebusch & Lorsch, 2012). As the PABP binds to the poly-A tail of the transcript, it associates with eIF4G and a circularized mRNA structure is formed (Hinnebusch & Lorsch, 2012). eIF4A, which functions as a helicase, unwinds the transcript's secondary structure and allows for the pre-initiation complex (PIC) to bind (Hinnebusch & Lorsch, 2012). The PIC is composed of eIF2, the initiating tRNA containing methionine (Met-tRNA), and the 40S ribosomal subunit (Hinnebusch & Lorsch, 2012). Following the binding of the PIC and the

circularized mRNA-eIF4F complex, the start codon is found by the former, eIF2 is released after a conformational change through GTP hydrolysis, and the 60S ribosomal subunit is bound, forming the 80S initiation complex (Hinnebusch & Lorsch, 2012). Thus, cap-dependent translation begins. Under stressful conditions, the α subunit of eIF2 may be phosphorylated which will reduce global translation but enhance translation of stress-related genes (Bellato & Hajj, 2016). Additionally, there is an abnormal version of translation that does not require the 5' cap but instead uses the complex secondary structure created by the 5'UTR in certain mRNA transcripts, known as internal ribosomal entry sites (IRES), but the exact mechanism remains controversial (Shatsky et al., 2018).

**Translational Control in Nociceptors**

Currently, the direct relationship between a specific mRNA transcript and its dependence on post-transcriptional regulation in nociceptors is limited to Brain-Derived Neurotrophic Factor (Moy et al., 2017, 2018). The amount of BDNF mRNA transcripts remained the same in nociceptors before and after chemically inducing thermal hypersensitivity (Moy et al., 2018). However, when mice expressing a mutant eIF4E that cannot be phosphorylated were subjected to chemical sensitization, the amount of BDNF protein was significantly reduced compared to the control. Additionally, mice that were sensitized and expressed mutant eIF4E did not exhibit sensitized behavior in the early stages of sensitization. Therefore, phosphorylation of eIF4E is required for the efficient translation of BDNF in the early stages of hypersensitivity (Moy et al., 2017, 2018).

Previous work in the Bellemer lab by Amber Dyson identified *eIF2α*, *sc35,* and *larp4B* as a candidate genes that may be involved in thermal nociception (Dyson, 2017).

Each of these genes code for RBPs that can potentially be used for regulating expression of specific genes through varying mechanisms.

### *SC35*

As previously mentioned, the process of protein expression is generally conserved, but the specific RNA binding proteins and their target transcripts change depending on the cell of interest. One such protein that is involved in the alternative splicing process is SC35, a member of the family of serine/arginine-rich (SR) splicing factors that are highly conserved across metazoans (Tacke & Manley, 1999). The structure of SR proteins is considered modular with one to two RNA-recognizing motifs (RRMs) and an RS domain located at the carboxyl terminal that is responsible for direct protein-protein interactions (Tacke & Manley, 1999). Additionally, SR protein function is influenced by phosphorylation, indicating that they can be influenced by various signaling pathways (Qian et al., 2011). Although there are some splicing functions that are redundant across SR proteins, the mRNA transcript that each SR protein commits to splicing is more specific (Fu, 1993; Tacke & Manley, 1999). SC35 is used in pre-mRNA splicing, specifically exon inclusion, and transcriptional elongation, though its role in the latter is less understood (Lin et al., 2008). There seems to be some competition between different SR proteins in binding to transcripts. It is possible that this competition is utilized such that while the levels of the competing SR proteins are held within homeostatic levels, one SR protein is upregulated in response to a signaling cascade. This may then result in specific exons being included in a transcript, thus a particular isoform is upregulated (Pandit et al., 2013).

In the context of the nervous system, SC35 is known to regulate the inclusion of exon 10 in the *tau* transcript (Qian et al., 2011). Tau is an important structural protein with major neurological implications, most notably in Chronic Traumatic Encephalopathy (Katsumoto et al.) and Alzheimer's disease (Katsumoto et al., 2019). The inclusion/exclusion of exon 10 results in the formation of the 4R or 3R isoforms of tau, respectively (Qian et al., 2011). The ratio of each isoform is very important to normal neuronal function (Katsumoto et al., 2019; Liu & Gong, 2008; Qian et al., 2011). Therefore, disruption in the balance of Tau isoform abundance can cause neurodegeneration and dementia, indicating that regulation of splicing events is extremely important for normal function of the nervous system (Liu & Gong, 2008).

As it pertains to nociceptor function, SC35 as a splicing factor may influence neuron excitability by regulating the generation of specific, alternatively spliced mRNA transcripts. The exact mRNA transcripts that are affected by this process in nociceptors is not known. As the availability of the mRNA transcripts is altered, the ability for protein to be expressed changes as well. There is already evidence that SC35 is responsible for long-term changes in splicing pattern of acetylcholine esterase (Meshorer et al.), an enzyme that breaks down the acetylcholine neurotransmitter (Meshorer et al., 2005). The changes in AChE transcripts involves retention of an intron and inclusion of a variable carboxy-terminus sequence (Soreq & Seidman, 2001).

It is hypothesized that the SC35 splicing factor is involved in establishing baseline nociception. The implication if the hypothesis is valid would be that SC35 activity in splicing specific transcripts is required by nociceptors to function under basal conditions. The next step would be to identify which mRNA transcripts and specific introns/exons are being

spliced by SC35, what level of regulation SC35 is subjected to via phosphorylation, and what molecules are responsible for this regulation.

### *LaRP4B*

La ribonucleoprotein 4B, or LaRP4B, belongs to a family of La proteins which have varied function, but the genuine La protein, LaRP3, is involved in pre-tRNA processing (Maraia & Intine, 2001). LaRP4B is related to LaRP3, but is instead responsible for stimulating general translation (Schäffler et al., 2010). Its structure is composed of an N-terminal La module that contains a La motif and RNA recognizing motif (RRM) both of which are required for RNA binding (Alfano et al., 2004). Specifically, LaRP4B binds to the 3'UTR of mature mRNA transcripts as well as exons (Küspert et al., 2015). Additionally, LaRP4B has high binding affinity to transcripts that have a 3'UTR rich in adenosine and uracil (ARE elements) (Bolognani & Perrone-Bizzozero, 2008; Küspert et al., 2015).

In terms of function, LaRP4B is not well characterized, but there are some suggested purposes. With the findings that ARE elements are associated with mRNA instability, it is likely that LaRP4B serves to increase the half-life of specific mRNA transcripts that are generally unstable (Bolognani & Perrone-Bizzozero, 2008; Küspert et al., 2015). This increase in stability is particularly interesting as most of the RBPs that are associated with AREs tend to initiate mRNA decay (Barreau et al., 2005). LaRP4B binds to mature mRNA as well as the cytosolic poly-A binding protein 1 (CPABP1) and receptor for activated C kinase (RACK1) which is important during translation initiation (Küspert et al., 2015). In addition, LaRP4B binds to actively translating ribosomes and polyribosomes and exerts its influence on translation rather than transcription (Küspert et al., 2015). This is evidenced by

the fact that overexpression of LaRP4B resulted in an increase in enzymatic activity for a reporter gene while reporter's mRNA levels remained unchanged (Küspert et al., 2015). LaRP4B and another member of the La family LaRP4 may have redundant mRNA targets but differ in their ability to enhance the transcripts' expression (Küspert et al., 2015). This indicates that La proteins exhibit a stimulatory role in general translation but with varying levels of efficacy. It is still possible that there are unique mRNA targets between various La proteins, as this study used a human embryonic kidney cell line (Sternfeld et al., 2000) . For instance, another La protein, LARP1, had an mRNA target that was not shared with LaRP4 or LARP4B (Küspert et al., 2015).

***eIF2α***

The eIF2 subunit is a heterotrimer composed of α, β, and γ subunits (Krishnamoorthy et al., 2001). During normal translation initiation, the eIF2α within the ternary PIC (eIF2, 40S subunit, Met-tRNA) is bound to GTP (Krishnamoorthy et al., 2001). When the Met-tRNA binds to the correct AUG start codon, the PIC triggers GTP hydrolysis which causes eIF2 to dissociate from the PIC (Krishnamoorthy et al., 2001). When bound to GDP, eIF2α is not able to rejoin the ternary PIC complex (Krishnamoorthy et al., 2001). eIF2B is a guanine exchange factor (GEF) which will replace GDP with GTP so that eIF2 can bind to the PIC and once again scan an mRNA transcript for the start codon (Krishnamoorthy et al., 2001). Interestingly, phosphorylation of the α subunit of eIF2 at the 51$^{st}$ serine residue prevents any association with the catalytic domains of eIF2B GEF, locking eIF2 in an inhibited state (Krishnamoorthy et al., 2001). In fact, when eIF2α is phosphorylated, it is instead very strongly bound to the regulatory domains of eIF2B, which suggests that the phosphate group

competitively blocks eIF2 from associating with the eIF2B catalytic domains that are required for GDP/GTP exchange (Krishnamoorthy et al., 2001).

Under stress conditions such as hypoxia, amino acid starvation and high heat, eIF2α is phosphorylated which results in reduced global translation but increases the translation of stress response genes (Bellato & Hajj, 2016). Specifically, translation of Activating Transcription Factors 4 and 5 (ATF4; ATF5) is increased which are each effector transcription factors of the cellular stress response which can range from protective cell growth responses to programmed cell death (Bellato & Hajj, 2016). mRNA transcripts that contain ORFs within the 5'UTR (uORF) have been found to be preferentially translated during this stress scenario (Bellato & Hajj, 2016). The exact mechanism of this process is unclear, but it is likely that other proteins could be involved in the translation process that are activated under certain conditions, like the stress response (Bellato & Hajj, 2016; Khoutorsky et al., 2016; Meijer & Thomas, 2002).

Khoutorsky et al. found that the phosphorylated version of eIF2α (p-eIF2α) was present at much higher levels in mice experiencing chronic inflammation conditions, specifically in dorsal root ganglion (DRG) neurons (Khoutorsky et al., 2016). Interestingly, they also found that preventing eIF2α phosphorylation was enough to significantly reduce nociceptive sensitivity to noxious thermal stimuli, but not mechanical stimuli (Khoutorsky et al., 2016). They also found that it is likely that the function – and not expression – of the thermosensitive ion channel TRPV1 that is being modulated by p-eIF2α (Khoutorsky et al., 2016). This is inferred since actual levels of TRPV1 protein does not change when eIF2α is mutated to prevent phosphorylation compared to wildtype (Khoutorsky et al., 2016). However, when the phosphorylation of eIF2α was prevented, flow of ions through TRPV1

was reduced (Khoutorsky et al., 2016). It is expected that in *Drosophila*, RNAi-mediated knockdown of eIF2α will produce a similar, significant defect in baseline thermal nociception.

***eIF2Bα***

Previous work by Amber Dyson in the Bellemer lab validated the role of eIF2Bα in nociceptor hypersensitivity (Dyson, 2017). As previously shown, eIF2B is a guanine exchange factor that is crucial for eIF2 to associate with the pre-Initiation Complex (PIC) and begin translation (Krishnamoorthy et al., 2001). Therefore, any inhibition of eIF2B will result in decreased protein expression as eIF2 is unable to exchange GDP for GTP to achieve activation (Krishnamoorthy et al., 2001). eIF2B itself is a heterodecameric complex (Boone et al., 2022). It is composed of two major subcomplexes which are constituted by a combination of five subunits (Kashiwagi et al., 2017). The regulatory complex contains $\alpha_2\beta_2\delta_2$, which is nestled between two catalytic subcomplexes composed of γε (Kashiwagi et al., 2017). It is likely that this regulatory complex plays an important role in nociceptor plasticity. For example, recent research shows that a mutation in the β subunit of eIF2B resulting in decreased guanine exchange efficiency in turn caused an increase in translation of stress response genes (Boone et al., 2022). The eIF2Bα subunit has more freedom for movement compared to the other subunits in the regulatory subcomplex, and can potentially regulate eIF2B independently of eIF2α phosphorylation (Kashiwagi et al., 2017). When eIF2α is phosphorylated, it is tightly bound to eIF2Bα, which prevents eIF2α from replacing GDP with GTP and is associated with increased translation of genes involved in the stress response (Khoutorsky et al., 2016). It is thought that because eIF2 binds to the α subunit of

eIF2B, knocking out this subunit will prevent normal cap-dependent translation and instead upregulate stress-response genes that lead to hypersensitivity (Boone et al., 2022; Dyson, 2017; Krishnamoorthy et al., 2001; Williams et al., 2001).

**Objectives**

The objectives of this thesis are threefold, each with the purpose of investigating the role of eIF2α, SC35, and LaRP4B in nociception. First, the role of eIF2α, LaRP4B, and SC35 in thermal nociception will be confirmed through RNAi knockdown. These candidates were identified in a screen conducted in the Bellemer lab by Amber Dyson as potentially being involved in thermal nociception (Dyson 2017) . Therefore, it is expected that knockdown each of these target genes will result in a significant nociceptive defect.

Second, the utility of the *Drosophila* model system for nociception studies will be expanded through the creation and validation of a transgenic fly line expressing *ppk-GAL4;UAS-Cas9* to direct nociceptor-specific genetic knockouts. To test for effective knockout of target genes in thermal and mechanical nociception, Cas9-mediated knockout of *ppk* and *dTrpA1* will be induced. It is expected that Cas9 KO of *ppk* will result in significant defects in mechanical nociception. It is expected that Cas9 KO of *dTrpA1* will result in significant defects in both mechanical and thermal nociception. To rule out possible sgRNA-independent effects, Cas9 KO of *lk6* will be used as an experimental control. It is expected that Cas9 KO of *lk6* will not produce significant defects in mechanical or thermal nociception, as informed by previous work by Haley McGuirt in the Bellemer lab (McGuirt 2019).

Third, an adult thermal nociception assay will be validated using *painless* and *dTrpA1*$^{ins}$ genetic mutants with known defects in avoidance behavior (Neely et al., 2010). This assay could then potentially be used to identify the role of the RBPs eIF2α, SC35, and LaRP4B in adult thermal nociception.

## Materials and Methods

### Drosophila Maintenance and Care

Stocks of *Drosophila* were reared at room temperature. *Drosophila* adults and larvae that were used for crosses were reared in a climate-controlled incubator at 25°C on a 12h day/night cycle at approximately 50% humidity. All *Drosophila* species were fed via apple juice molasses media. In all crosses, 3 males were mated to 6 virgin females. The genotype of male and females in a cross will be specified for each experiment.

### Transgenic Fly Line Construction

In order to generate a transgenic fly line that would retain the desired ppk-GAL4;UAS-Cas9 genotype across generations, males of each half of the GAL4/UAS system were crossed to virgin females of a balancer line that expressed synthetic, inverted chromosomes which prevented recombination and have dominant physical markers. These flies express the genotype *w;* $\frac{Sp}{CyO}$ *;* $\frac{Sb}{Tm3,Ser}$ where balancer chromosomes are denoted by their physical markers: Sp (sternal pleura – abnormal hair growth between first and second limbs); CyO (CurlyO – curled wing phenotype); Sb (short bristle – shortened hair length) and Tm3, Ser (serrated – serrated wings). These flies are referred to as BOB flies. To begin, 3 adult males of the *ppk-GAL4* genotype were crossed to 6 adult female virgin BOB flies. The flies were allowed to seed the vial for 48h and were then flipped into a new cross vial every 24h for a week. Males of the desired phenotype were selected and organized based on phenotype (Table 1). Once 3 males of the desired phenotype of the $P_0$ cross were collected, they were mated with 6 BOB virgins. The same cross sequence was used for the *UAS-Cas9*

genotype. The process continued as shown in Table 1 until the final stock of *ppk-GAL4;UAS-Cas9* was generated.

**Larval Nociception Cross Setup – RNAi and Cas9**

In each RNAi experiment, two negative controls were made from one half of the GAL4/UAS system which does not allow expression of the target sequence. This is because both GAL4 and UAS are needed to activate transcription of the desired transgene.

The GAL4-only control for RNAi experiments was made by crossing 3 adult males of the *ppk-GAL4* driver line with 6 virgin females expressing a synthetic RNAi that did not target a transcript for degradation (Bloomington #36303). The UAS-only control for RNAi experiments was made by crossing 3 adult males that expressed the "gene X"-specific UAS-"X"-RNAi knockdown to 6 virgin females of the $w^{1118}$ genotype. The knockdown group for RNAi experiments was made by crossing 3 adult males that expressed the "gene X"-specific UAS-"X"-RNAi knockdown to 6 virgin females of the *ppk-GAL4* driver line.

In each Cas9 experiment, two negative controls were made from one half of the *ppk-GAL4/UAS-Cas9,U6-.sgRNA* system which does not allow expression of the target sequence. This is because both Cas9 and the sgRNA are needed to bind to a specific gene sequence and induce Cas9-mediated knockout.

The Cas9-only control for Cas9 experiments was made by crossing 3 males of the *ppk-GAL4;UAS-Cas9* line to 6 virgin females of the $w^{1118}$ genotype. Since there is no sgRNA expression, there is no Cas9-mediated mutagenesis. The sgRNA-only control for Cas9 experiments was made by crossing 3 adult males that expressed the "gene X"-specific *U6-X.sgRNA* to 6 virgin females of the $w^{1118}$ genotype.

**Table 1**

*Cross sequence for transgenic ppk-GAL4;UAS-Cas9 fly line*

| | *ppk – GAL4* | | *UAS – Cas9* | |
|---|---|---|---|---|
| Cross | ♂ Genotype | ♀ Genotype | ♂ Genotype | ♀ Genotype |
| $P_o$ | $w; \frac{ppk-GAL4}{+}; \frac{+}{+}$ | $w; \frac{Sp}{CyO}; \frac{Sb}{Tm3,Ser}$ | $w; \frac{+}{+}; \frac{UAS-Cas9}{+}$ | $w; \frac{Sp}{CyO}; \frac{Sb}{Tm3,Ser}$ |
| Desired Offspring | $w; \frac{ppk-GAL4}{CyO}; \frac{+}{Tm3,Ser}$ | | $w; \frac{+}{Sp}; \frac{UAS-Cas9}{Tm3,Ser}$ | |
| $F_1$ | $w; \frac{ppk-GAL4}{CyO}; \frac{+}{Tm3,Ser}$ | $w; \frac{Sp}{CyO}; \frac{Sb}{Tm3,Ser}$ | $w; \frac{+}{Sp}; \frac{UAS-Cas9}{Tm3,Ser}$ | $w; \frac{Sp}{CyO}; \frac{Sb}{Tm3,Ser}$ |
| Desired Offspring | $w; \frac{ppk-GAL4}{CyO}; \frac{Sb}{Tm3,Ser}$ *(Balanced GAL4)* | | $w; \frac{Sp}{CyO}; \frac{UAS-Cas9}{Tm3,Ser}$ *(Balanced Cas9)* | |
| $F_2$ | $w; \frac{ppk-GAL4}{CyO}; \frac{Sb}{Tm3,Ser}$ | $w; \frac{Sp}{CyO}; \frac{UAS-Cas9}{Tm3,Ser}$ | | |
| Final Stock | $(♂ x ♀)\ w; \frac{ppk-GAL4}{CyO}; \frac{UAS-Cas9}{Tm3,Ser}$ | | | |

*Note:* Genotypes are represented by *ppk-GAL4, UAS-Cas9* or + (wild type). Balancer chromosomes are denoted by their physical markers: CyO (CurlyO – curled wing phenotype); Sp (sternal pleura – abnormal hair growth between first and second limbs); Sb (short bristle – shortened hair length); Tm3, Ser (serrated – serrated wings).

The knockout group for Cas9 experiments was made by crossing 3 adult males that expressed the "gene X"-specific *U6-X.sgRNA* to 6 virgin females of the *ppk-GAL4;UAS-Cas9* genotype. After crosses were set up, flies were allowed to seed vials for 48h and were then flipped every 24h.

**Larval Thermal Nociception Assay – Basal and Hypersensitivity**

To collect wandering third instar larvae for thermal testing, distilled water was gently rinsed along the sides of cross vials. This water was then gently poured into a glass petri dish and excess water was removed. A small amount of dry yeast was added to disrupt surface tension. Larvae were allowed 3-5 minutes to acclimatize to the testing environment. A Variac Variable Transformer (Part No. ST3PN1210B) (ISE, Inc., Cleveland, OH) was used to control the temperature of the custom probe after being connected and set to 46°C for basal nociception experiments or 42°C for hypersensitivity experiments. The probe itself was made from a 6mm soldering iron with a chiseled tip. To monitor real-time changes in probe temperature to a tenth of a degree, an IT-23 thermistor and BAT-12 digital thermometer (Physitemp, Clifton, NJ) were used.

The probe was then used to apply the noxious stimulus to a lateral side of the larvae in a medial area of the body for 10 seconds. Each larvae tested counted as a trial and any trial wherein larvae lost contact with the probe before 10 seconds elapsed was discarded. Any trial wherein the probe temperature deviated by more than 1°C from 46°C in either direction was also discarded.

All thermal larval nociception trials were captured using a 30fps video camera that was mounted on a stereoscopic microscope. The videos of each experiment were analyzed

via Adobe Premiere Pro. The latency between exposure of larvae to the probe and completion of NEL was calculated to the frame. Any trial that did not elicit NEL after 10 seconds was automatically scored as 11 seconds.

**Larval Mechanical Nociception Assay**

A custom von Frey filament was constructed with 10mm of fishing line (Stren Original Monofilament 8 lb. line, Part #1304152, Pure Fishing, Inc., Columbia, SC) fixed to a glass Pasteur pipette using tape and clear acrylic nail polish. The fishing line delivered approximately 50mN of force. Larvae were prepared in the same manner as they were for thermal nociception assays. The von Frey filament was used to apply pressure to the middle of a larva's dorsal surface until the fishing line just began to bend. Larvae were tested three times and scored for the presence or absence of NEL after each trial. The total percentage of larvae that responded in any of the three trials was then calculated.

**Larval Nociceptor Imaging**

Confirmation of the inclusion of the *UAS-Cas9* transgene in the final *ppk-GAL4;UAS-Cas9* stock was done using a GFP negative tester line (Bloomington #81892) that expressed *md-GAL4;UAS-CD4-tdGFP,UAS-RedStinger,U6-GFP.gRNA*. This genotype produced GFP that was localized to the cell membrane, RedStinger fluorescence protein that localized to the nucleus, and a guide RNA strand that targeted GFP in all multidendritic neurons, including nociceptors.

The negative control group that did not induce Cas9 KO of GFP was created by crossing 3 males from the #81892 line to 6 virgin females. The positive control group that

did induce Cas9 KO of GFP was created by crossing 3 males from the #81892 line to 6 virgin females from the original UAS-Cas9 stock (Bloomington #54595). The experimental group that tested if Cas9 knocked-out GFP was created by crossing 3 males from the #81892 line to 6 virgin females from the final *ppk-GAL4;UAS-Cas9* stock.

To visualize nociceptor morphology of flies from the final *ppk-GAL4;UAS-Cas9* stock, two crosses were set up. In each, virgin females with the *ppk-GAL4,mCD8::GFP* genotype were used. These flies produced larvae with nociceptors that express the GFP-tagged mouse CD8 transmembrane protein, allowing visualization of nociceptor morphology. The negative control was made by crossing virgin females with the *ppk-GAL4,mCD8::GFP* genotype to $w^{1118}$ males. The experimental group was made by crossing virgin females of the *ppk-GAL4,mCD8::GFP* genotype to males with the *ppk-GAL4;UAS-Cas9* genotype.

Regardless of the experimental context, larvae from both experiments were prepared in the same way. Wandering third instar larvae were rinsed directly onto a glass petri dish. A single larva was immobilized via ligation near the A3 body segment by using a tied human hair and placed on a glass microscope slide. 3-5 drops of glycerol were used to fix larvae onto the slide before being covered with a glass coverslip. Mounted larvae were then subjected to confocal microscopy and Z-stacks were obtained of each larvae (Zeiss LSM 880, Oberkochen, Germany).

**Confocal Image Processing**

Z-stacks of images that required manual removal of frames due to larvae movement were processed with the open access ImageJ software and the TurboStack and StackReg plugins (Figure 6 only). Individual frames from the Z-stack were saved from the Zeiss

software and opened with ImageJ. The individual frames were converted to a Z-stack using the image to stacks function on ImageJ. The StackReg and TurboStack plugins were then executed to remove "ghosting" resulting from larvae movement. Individual frames that were not aligned by the plugins were individually removed. The processed frames were then merged into a maximum intensity projection for just red channel or green channel data. Data from red and green channels were then separated using the Split Channels function and separate maximum intensity projections were made for each channel.

**Fly DNA Extraction**

The protocol for fly DNA extraction was adapted from a protocol by George Dietzl in Barry Dickson's Lab, IMP Vienna 12/2002. 2 flies of a desired genotype were placed into a 1.5mL centrifuge tube and iced for 6 minutes. 200g/mL of proteinase K was added to squishing buffer. 100μL of the buffer was aspirated into the pipette tip and the pipette tip was used to grind the flies for a minute. Any remaining buffer was expelled after a minute of grinding the flies. The centrifuge tube with ground flies and buffer was incubated for 30 minutes at 37°C. The centrifuge tube was incubated for 10 minutes at 95°C to denature the proteinase K (Mini Heat Block, Fisher Scientific, Waltham, MA) The centrifuge tube was iced for 1 minute and then centrifuged at 1000RPM for no more than 5 seconds (Mini Centrifuge, Genesee Scientific, San Diego, CA) . The supernatant containing fly DNA was then transferred to a sterile centrifuge tube.

**Fly DNA PCR**

Amplification of the *ppk-GAL4* transgene was conducted via Polymerase Chain Reaction using Taq DNA Polymerase (New England BioLabs, #M0273S, Ipswich, PA). Primers were obtained from Invitrogen (Catalog number: 10336022, Waltham, MA). The forward primer sequence used to amplify the *ppk-GAL4* transgene was: GAATGGCCATATCATTGGGC. The reverse primer sequence was CAAGGGTGTTCCTTCAAC. PCR was automated with an Eppendorf 6331 Mastercycler thermocycler for 30 cycles (Hamburg, Germany). The denaturing, annealing, and extension temperatures were 95°C, 57°C, and 68°C, respectively. 2.5μL of fly template DNA and 1μL of *ppk-GAL4* template plasmid were used for PCR.

**Adult Thermal Nociception Cross Setup and Fly Collection**

Crosses used for adult thermal nociception assays were prepared about 12 days prior to testing. The basic setup of adult crosses was identical to those used for larval nociception assays, except $dTrpA1^{ins}$ and *painless* mutants were used as positive controls. Additionally, larvae were not collected and instead allowed to pupate. Careful monitoring of the vials was required after the pupae cases' color darkened as this indicated adults were about to eclose. Once this stage was reached, vials were checked twice daily at around 9AM and 5:30PM as these were the times in which most adults eclosed. If the first adults were present when checking at 9AM, then only virgins were collected, since it was impossible to guarantee that the non-virgins had eclosed that morning and not after 5:30PM the day before. If the first adults were present at 5:30PM, all adults were collected if the vial was checked that morning and there were no adults present.

Once the first adults eclosed, the vials were reared under room temperature and additional adults were collected for no more than 4 days. This was important to prevent genetic contamination from F1 progeny crossing. Adults of each genotype were collected with light $CO_2$ anaesthetization across multiple days until the vial was filled with 20 adults. After 20 adults were collected for a group, the flies were kept in their vial in room temperature for a week and flipped into new vials every 48h. After the week of recovery from $CO_2$ anaesthetization, flies could be subjected to the adult thermal nociception assay.

**Adult Thermal Nociception Assay**

The entire experiment was completed in the dark and a red colored light was used as a light source by taping a red test tube cap to a phone flashlight to minimize the flies' light-responsive behavior. A water bath (ISOTEMP, model: 205, FisherScientific, Waltham, MA), was set to 46°C and turned on 30 mins before starting the experiment. Pieces of cardboard were placed surrounding the water bath to minimize stray light from reaching the surface of the water. An insulated container was filled with ice. Adult flies from each individual group were flipped into separate, empty plastic vials with no food and labelled according to the blinded genotype. Two vials were placed on ice for 5 minutes to anesthetize the flies.

After five minutes, the vials were removed from the ice and carefully tilted at an angle of ~30°. The closed end of the tube was gently tapped to transfer the adult flies to small, empty petri dishes. The exact number of flies from each genotype was recorded and the petri dishes were immediately sealed with tape and labeled with the corresponding genotype symbol. Flies were allowed to recover for 30 minutes in complete darkness.

After the recovery period, all flies were ensured to be fully recovered by lightly inverting the dish and observing movement from all flies. The petri dish test chambers were placed on the surface of the water in the center of the water bath and a 4-minute timer was immediately started. After 4 minutes, the test chamber was immediately removed from the water bath and placed onto a white piece of paper. The number of flies that were incapacitated on the bottom surface was recorded. This process is repeated for the remaining genotypes.

**Statistical Analyses**

Significance in all thermal nociception assays was calculated using a two sided premutation t-test ($\alpha = 0.05$) and Cliff's $\Delta$ was used to estimate the effect size of two different groups (Ho et al., 2019). Significance in mechanical and adult thermal nociception assays was calculated using a chi-square test that compared the KO/KD/mutant to either one or two controls. For all comparisons, one degree of freedom was allocated and the $\chi^2_{crit}$ used was 5.024. Additionally, a Bonferroni correction to the $\alpha$ value was used in all experiments. For 2 comparisons, an $\alpha$ of 0.025 was used while an $\alpha$ of 0.0125 was used for 4 comparisons.

**Table 2**

*All* Drosophila *stocks used*

| Stock Number | Origin | Genotype | Notes |
|---|---|---|---|
| 44449 | Bloomington Drosophila Stock Center (BDSC) | y[1] v[1]; P{y[+t7.7] v[+t1.8]=TRiP.GLC01598}attP2/TM3, Sb[1] | Expresses RNAi targeting *eIF2α* |
| 65888 | | y[1] sc[*] v[1] sev[21]; P{y[+t7.7] v[+t1.8]=TRiP.HMC06150}attP40 | Expresses RNAi targeting *sc35* |
| 64937 | | y[1] sc[*] v[1] sev[21]; P{y[+t7.7] v[+t1.8]=TRiP.HMC05810}attP40 | Expresses RNAi targeting *larp4B* |
| 54595 | | w[1118]; P{y[+t7.7] w[+mC]=UAS-Cas9.C}attP2 | Expresses *UAS-Cas9.C* |
| 81892 | | w[*]; P{w[+mC]=GAL4}21-7, P{w[+mC]=UAS-CD4-tdGFP}8M2/CyO, P{Wee-P.ph0}2; P{w[+mC]=UAS-RedStinger}6, PBac{y[+mDint2] w[+mC]=U6-GFP.gRNA.ACDG}VK00027/TM6B, Tb[1] | Negative GFP Tester for Cas9 Function |
| 82690 | | y[1] v[1]; P{y[+t7.7] v[+t1.8]=TKO.GS05030}attP40 | Expresses sgRNA targeting *ppk* for Cas9 KO |
| 79764 | | y[1] sc[*] v[1] sev[21]; P{y[+t7.7] v[+t1.8]=TKO.GS01797}attP40 | Expresses sgRNA targeting *eIF2Bα* for Cas9 KO |
| 36342 | | TI{w[+mW.hs]=TI}TrpA1[1] | *dTrpA1* mutant |
| 6139 | | $w^{1118}$; P{UAS-paraRNAi} | Expresses RNAi targeting *para* |
| 342104 | Vienna Drosophila Resource Center (VDRC) | Not provided | Expresses sgRNA targeting *dTrpA1* for Cas9 KO |
| 341657 | | | Expresses sgRNA targeting *lk6* for Cas9 KO |

## Results

### Establishing the role of RBPs eIF2α, SC35, and LaRP4B using RNAi Knockdown

#### *eIF2α*

This experiment was conducted to determine the role of eIF2α's stimulation of translation on basal thermal nociception. It is expected that eIF2α plays an important role in nociception which would manifest as a significantly increased response latency compared to the GAL4- and UAS-only controls. To do this, the *ppk-GAL4;UAS-Dicer-2* line was crossed to the *UAS-eIF2α RNAi* line to induce nociceptor-specific knockdown of *eIF2α*.

In this experiment, three control groups were used as reference points for the experimental knockdown group. Each of the negative controls expressed either *ppk-GAL4* or *UAS-eIF2α*, but not both. Separating each half of the system prevents expression of the desired transgene. The GAL4-only control therefore expresses *ppk-GAL4* but not the RNAi needed to target eIF2α. The UAS-only control expresses *UAS-eIF2α* but without the *ppk-GAL4* driver. The experimental group then expresses both halves of the GAL4/UAS system and exhibits the *ppk-GAL4;UAS-eIF2α-RNAi* genotype. As a positive control, nociceptor-specific RNAi KD of *para* is induced as it is known to result in a virtually total loss of nociceptive function. All RNAi experiments are set up in a similar fashion with the UAS-RNAi being the only difference.

The latency for each group was as follows: GAL4-only – 3.082s, UAS-only – 2.844s, *eIF2α* RNAi – 5.751s, and *para* RNAi – 9.766s. The p-value of the difference between the GAL4 and UAS-only groups was 0.272 with a Cliff's Δ of -0.128. The range of the Cliff's Δ 95% confidence interval (CI) was -0.354, 0.112. The p-value of the difference between the *eIF2α* RNAi and GAL4-only groups was 0.0002 with a Cliff's Δ of -0.393. The range of the

Cliff's Δ 95% CI was -0.592, -0.16). The p-value of the difference between the *eIF2α* RNAi and UAS-only groups was 0.000 with a Cliff's Δ of 0.457. The range of the Cliff's Δ 95% CI was 0.23, 0.644. The p-value of the difference between the *eIF2α* and *para* RNAi groups was 0.000 with a Cliff's Δ of 0.593. The range of the Cliff's Δ 95% CI was 0.407, 0.735. These results show that the *eIF2α* RNAi group had a significantly higher latency than the two negative controls but was not as extreme as *para* RNAi. Thus, *eIF2α* knockdown results in a partial loss of nociception.

**Figure 2**

*Nociceptor-Specific RNAi Knockdown of* EIF2α *Significantly Impairs Nociceptive Function in* Drosophila *Larvae*

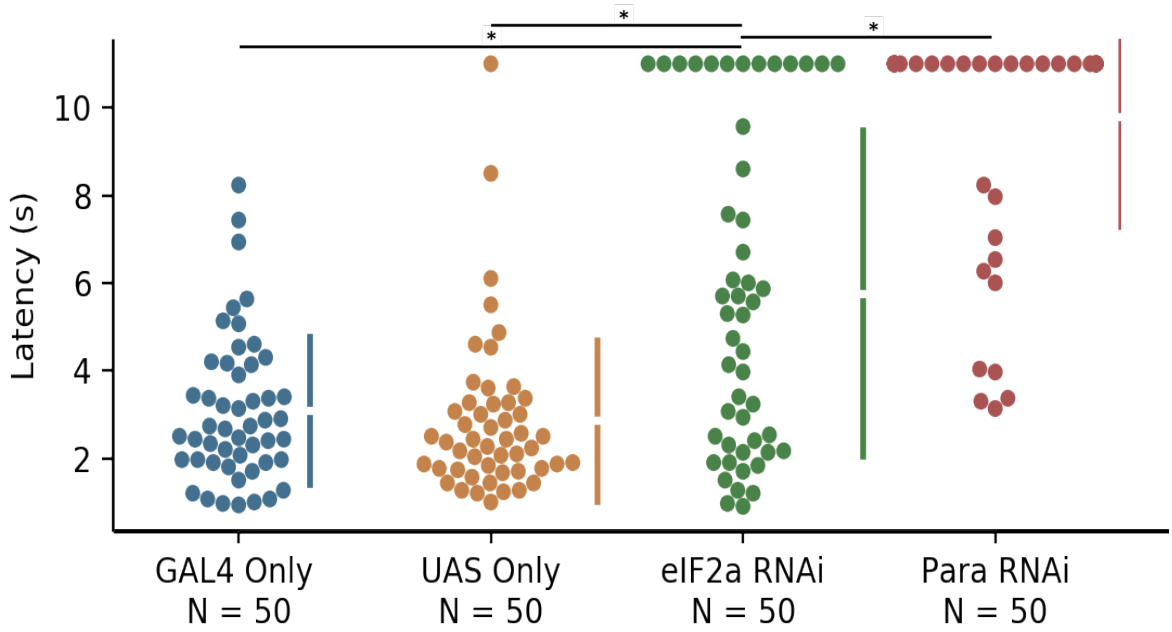


*Note*: Latency in seconds between contact with 46°C probe and complete NEL of individual larvae is shown as dots. Colored bars indicate interquartile ranges.

For each genotype, n = 50.

Significance was determined via two-sided permutation t-test. * = p = 0.00.

***SC35***

This experiment was conducted to determine the role of alternative splicing by the splicing factor SC35 in basal thermal nociception. It is expected that SC35 plays an important role in nociception which would manifest as a significantly increased response latency compared to the GAL4 and UAS-only controls. To do this, the *ppk-GAL4;UAS-Dicer-2* line was crossed to the *UAS-sc35-RNAi* line to induce nociceptor-specific knockdown of *sc35*. The GAL4-only, UAS-only, *para* RNAi controls and the experimental group were all set up similar to the eIF2α KD experiment (Figure 1), except the RNAi line used here targets SC35.

The latency for each group was as follows: GAL4-only – 2.810s, UAS-only – 2.717s, *sc35* RNAi – 4.778s, *para* RNAi – 10.468s. The p-value of the difference between the GAL4 and UAS-only control groups was 0.580 with a Cliff's Δ of 0.0644. The range of the Cliff's Δ 95% CI was -.0174, 0.295. The p-value of the difference between the *sc35* RNAi and GAL4-only groups was 0.000 with a Cliff's Δ of 0.518. The range of the Cliff's Δ 95% CI was 0.315, 0.682. The p-value of the difference between the *sc35* RNAi and UAS-only groups was 0.000 with a Cliff's Δ of 0.515. The range of the Cliff's Δ 95% CI was 0.327, 0.672. The p-value of the difference between the *sc35* RNAi and *para* RNAi groups was 0.000 with a Cliff's Δ of -0.661. The range of the Cliff's Δ 95% CI was -0.784, -0.492. These results show that the *sc35* RNAi group had a significantly higher latency than the two negative controls but was not as extreme as *para* RNAi. Thus, *sc35* knockdown results in a partial loss of nociception.

**Figure 3**

*Nociceptor-Specific RNAi Knockdown of* Sc35 *Significantly Impairs Thermal Nociception in* Drosophila *Larvae*

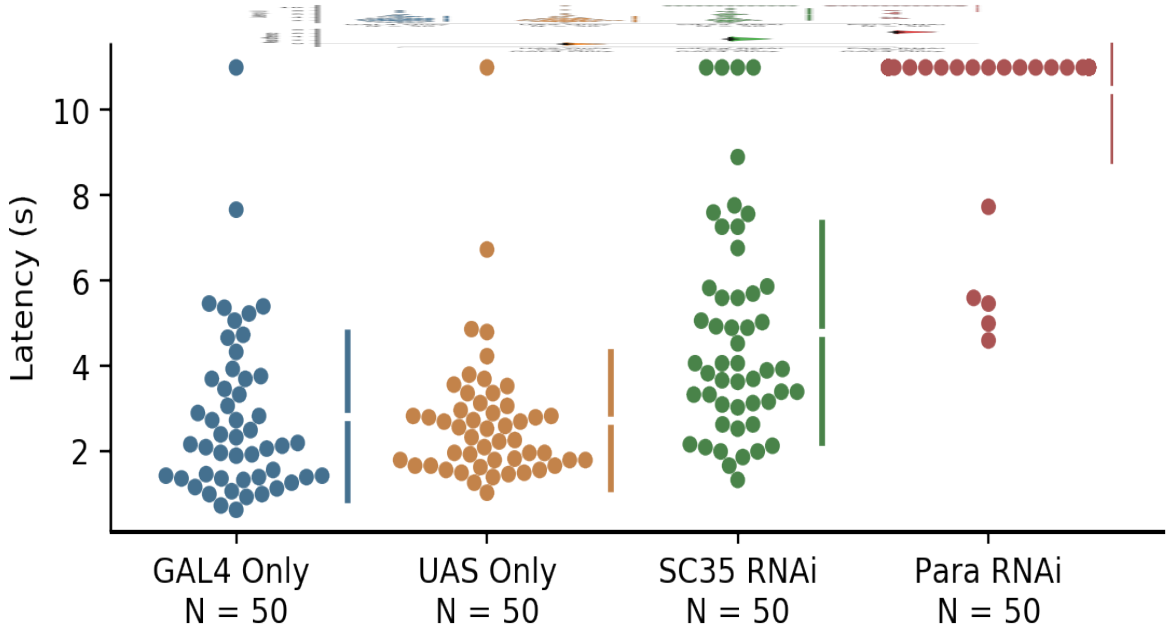


*Note:* Latency in seconds between contact with 46°C probe and complete NEL of individual larvae is shown as dots. Colored bars indicate interquartile ranges.

For each genotype, n=50.

Significance was determined via two-sided permutation t-test. * = p = 0.00.

***LaRP4B***

This experiment was conducted to determine the role that LaRP4B's stimulation of translation and stabilization of mRNA transcripts play in basal thermal nociception. It is expected that LaRP4B plays an important role in nociception which would manifest as a significantly increased response latency compared to the GAL4 and UAS-only controls. To do this, the *ppk-GAL4;UAS-Dicer-2* line was crossed to the *UAS-larp4b-RNAi* line to induce

nociceptor-specific knockdown of *larp4b*. The GAL4-only, UAS-only, *para* RNAi controls and the experimental group were all set up similar to the eIF2α KD experiment (Figure 1), except the RNAi line used here targets LaRP4B.

The latency for each group was as follows: GAL4-only – 3.615s, UAS-only – 3.502s, *larp4b* RNAi – 7.574s, *para* RNAi – 10.728s. The p-value of the difference between the GAL4 and UAS-only control groups was 0.244 with a Cliff's Δ of 0.126. The range of the Cliff's Δ 95% CI was -0.0932, 0.328. The p-value of the difference between the *larp4b* RNAi and GAL4-only groups was 0.000 with a Cliff's Δ of -0.664. The range of the Cliff's Δ 95% CI was -0.787, -0.491. The p-value of the difference between the *larp4b* RNAi and UAS-only groups was 0.000 with a Cliff's Δ of -0.687. The range of the Cliff's Δ 95% CI was -0.808, -0.519. The p-value of the difference between the *larp4b* RNAi and *para* RNAi groups was 0.000 with a Cliff's Δ of -0.537. The range of the Cliff's Δ 95% CI was -0.668, -0.389. Again, the knockdown of *larp4b* in nociceptors resulted in a partial loss in nociception compared to the controls.

**Figure 4**

*Nociceptor-Specific RNAi Knockdown of* Larp4B *Significantly Impairs Thermal Nociception in Drosophila Larvae*

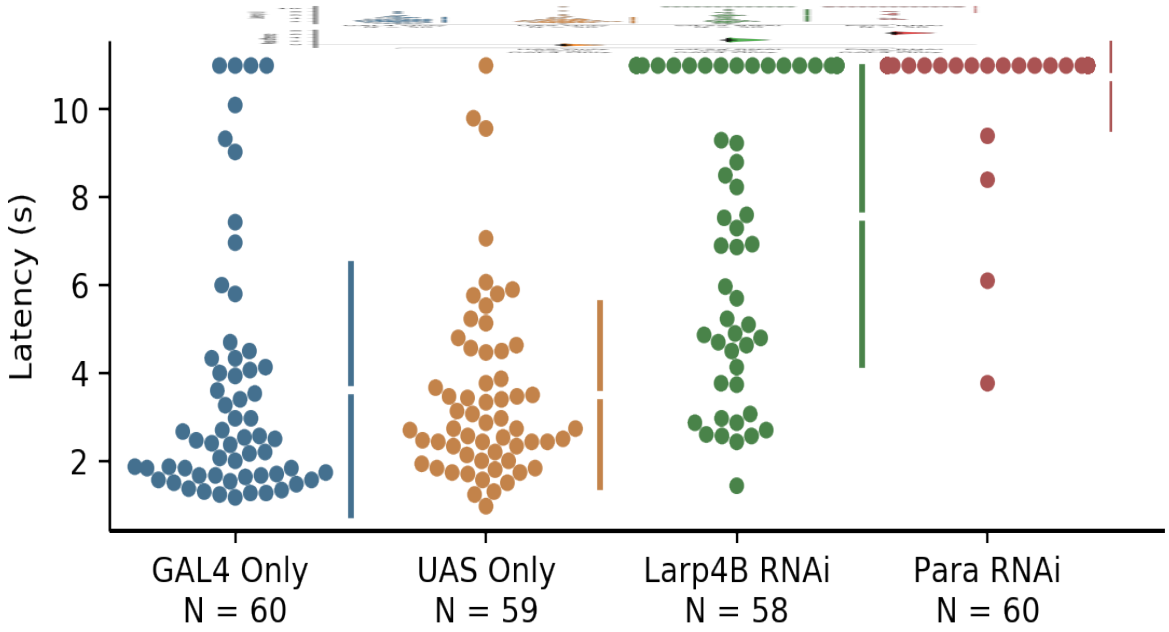


*Note:* Latency in seconds between contact with 46°C probe and complete NEL of individual larvae is shown as dots. Colored bars indicate interquartile ranges.

The n for each genotype is as follows: GAL4 Only – 60, UAS only – 59, Larp4B RNAi – 58, and Para RNAi – 60.

Significance was determined via two-sided permutation t-test. * = $p < 0.05$.

**Table 3**

*Larval Thermal Nociception Experiments Using RNAi Knockdown*

| Target | Genotype | n | Average Latency (s) | Comparison to GAL4 p-value | Comparison to UAS p-value |
|---|---|---|---|---|---|
| **eIF2α** | GAL4-only | 50 | 3.082 | | 0.262 |
| | UAS-only | 50 | 2.844 | 0.272 | |
| | *eIF2α* RNAi | 50 | 5.751 | 0.0002 | 0.000 |
| | Para RNAi | 50 | 9.776 | 0.000 | 0.000 |
| **SC35** | GAL4-only | 50 | 2.810 | | 0.580 |
| | UAS-only | 50 | 2.717 | 0.579 | |
| | *SC35* RNAi | 50 | 4.778 | 0.000 | 0.000 |
| | Para RNAi | 50 | 10.468 | 0.000 | 0.000 |
| **LaRP4B** | GAL4-only | 60 | 3.615 | | 0.244 |
| | UAS-only | 59 | 3.502 | 0.231 | |
| | *larp4B* RNAi | 58 | 7.574 | 0.000 | 0.000 |
| | Para RNAi | 60 | 10.728 | 0.000 | 0.000 |

*Note*: All experiments conducted at 46°C unless otherwise noted. p-values indicate comparison between the noted group and the GAL4-only control or UAS-only control. Significance determined via a two-sided permutation t-test.

## Confirmation of ppk-GAL4;UAS-Cas9 Genotype

In order to establish the homogenous genotype of *ppk-GAL4;UAS-Cas9* to be used as the driver of nociceptor-specific Cas9 expression, multiple generations of crosses were necessary. Two stocks each expressing either *ppk-GAL4* or *UAS-Cas9* were used to generate this line. Ideally, the final stock would be achieved in five generations of crosses. The inclusion of the desired *ppk-GAL4;UAS-Cas9* transgene was confirmed through a genetic analysis with PCR and gel electrophoresis or functional analysis via mutagenesis of a fluorescent reporter gene.

### *Confirming ppk-GAL4 Transgene Inclusion*

To confirm the presence of the *GAL4* transgene in the final genotype, PCR amplification of the *GAL4* sequence was conducted using genomic DNA samples isolated from single flies as templates. It is expected that in all DNA samples containing *the ppk-GAL4* transgene, PCR amplification will have succeeded, and visualization of the gel will indicate bands in the associated lanes. The contents of each lane are as follows, from left to right: 1000kb ladder, amplified DNA from adult flies with the *w;* $\frac{ppk-GAL4}{CyO}$ *;* $\frac{Sb}{Tm3,Ser}$ genotype as a positive control, amplified DNA from adult flies with the *w;* $\frac{Sp}{CyO}$ *;* $\frac{UAS-Cas9}{Tm3,Ser}$ genotype as a negative control, amplified DNA from the final stock of *w ppk-GAL4;UAS-Cas9*, and diluted plasmid containing the *ppk-GAL4* transgene as another positive control (Table 1). The absence of a band in the third lane indicates that there was no cross contamination during DNA extraction and that the primers only amplified the *ppk-GAL4* sequence. The presence of bands in the second and fifth lanes indicates that the ppk-GAL4 sequence was successfully amplified from sources known to contain the GAL4 sequence.

Therefore, the presence of a band in the fourth lane confirms that the *ppk-GAL4* transgene is present in the final fly stock.

**Figure 5**

*Gel Electrophoresis Visualization of Amplified* ppk-GAL4

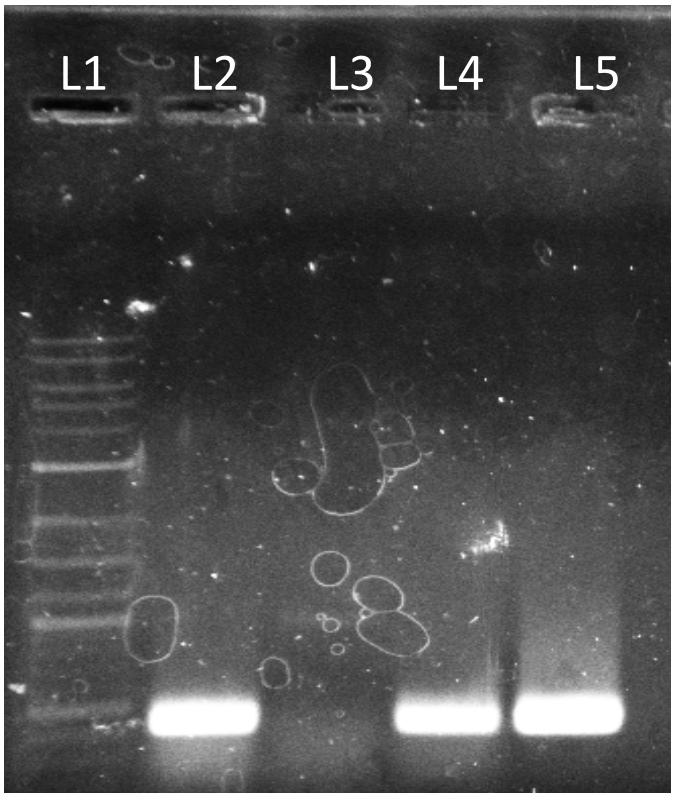


*Note*: L1 – Lane 1. L2 – Lane 2. L3 – Lane 3. L4 – Lane 4. L5 – Lane 5.

L1 contains 1000kb ladder. L2-5 contains DNA samples that were used as templates for PCR amplification of the *ppk-GAL4* sequence. L2 contains DNA from flies with the *w;* $\frac{ppk-GAL4}{CyO}$ ; $\frac{Sb}{Tm3,Ser}$ genotype. L3 contains DNA from flies with the the *w;* $\frac{Sp}{CyO}$ ; $\frac{UAS-Cas9}{Tm3,Ser}$ genotype. L4 contains DNA from flies with the *w;ppk-GAL4;UAS-Cas9* genotype. L5 contains control *ppk-GAL4* plasmid.

### *Confirming UAS-Cas9 Transgene Inclusion*

A functional Cas9 assay was used to confirm the expression and function of the Cas9 protein in the final stock. This was done using a tester line (Bloomington #81892) that expressed *md-GAL4;UAS-CD4-tdGFP,UAS-RedStinger,U6-GFP.gRNA*. This genotype produces GFP that is localized to the cell membrane, RedStinger fluorescent protein localized to the nucleus, and a guide RNA strand that targets GFP in all multidendritic neurons, including nociceptors, due to the *md* driver (Figure 6A-C, 7A-C).

Cas9 protein can use the GFP guide RNA that is provided within the tester line (*U6-GFP.gRNA*) to target GFP sequences. This induces mutagenesis that prevents any GFP from being expressed or visualized when Cas9 is present. Conversely, this assay would also reveal the absence or non-functionality of Cas9 by the presence of GFP after being crossed with a line that ostensibly expressed *UAS-Cas9*.

When adult flies of the #81892 tester line were crossed to adults of the *UAS-Cas9* stock (Figure 6D-F) or the final *ppk-GAL4;UAS-Cas9* stock (Figure 7D-F), all GFP fluorescence was eliminated in the md neurons of progeny larvae. Since there is no guide RNA for Cas9-mediated mutagenesis of the RedStinger fluorescence protein, all red fluorescence remained even after Cas9 KO of GFP.

**Figure 6**

*Confocal Microscopy Confirms the Functionality of Cas9-Mediated Knockout*

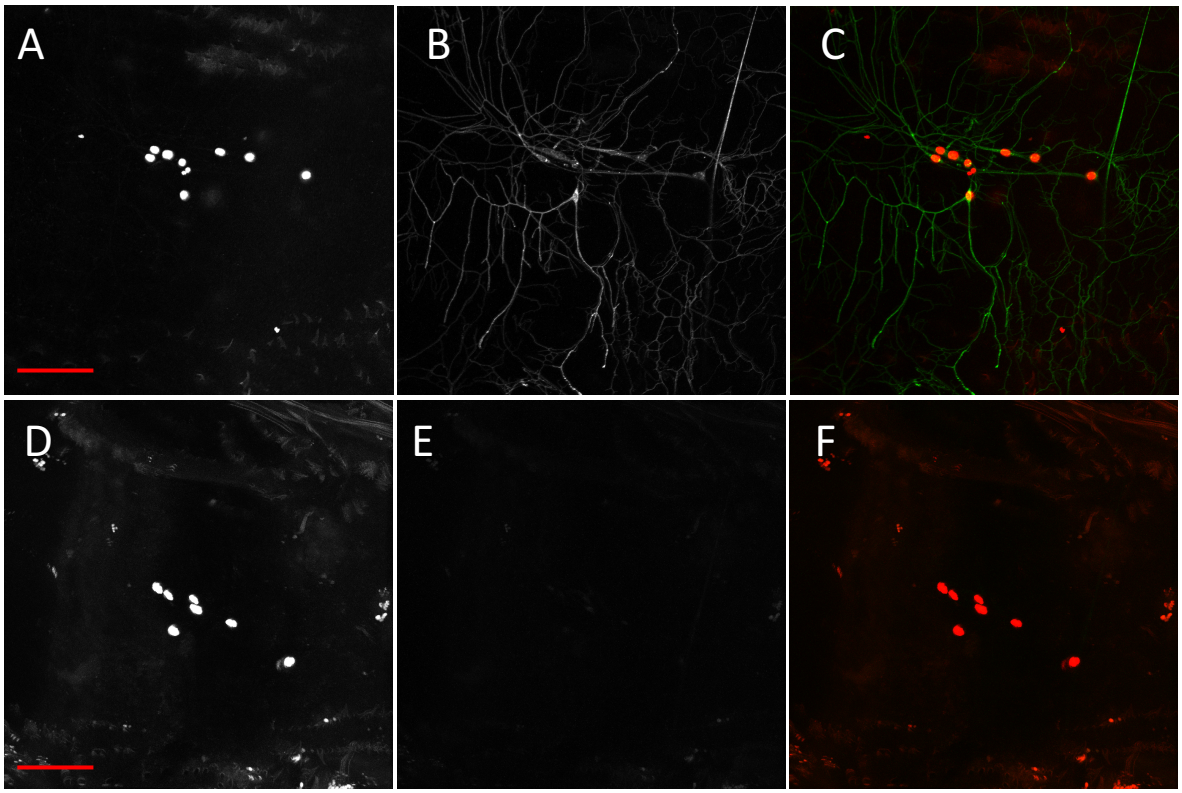


*Note:* Confocal microscopy of multidendritic neurons in larvae from a *dorsal* view. In all panels, GFP is tagged to the CD4 transmembrane protein and RFP is tagged to the Tra nuclear RBP. Red scale bar represents 200µm. Panels A and D show red channel fluorescence data. Panels B and E show green channel fluorescence data. Panels C and F show colorized composites. Panels A-C show control 81892 larvae. Panels D-F show larvae produced from crossing 81892 adults to stock *UAS-Cas9* adults. (**A-C**) RFP is intact and expressed in the nucleus and GFP is expressed in the membrane of all multidendritic neurons in a *dorsal* view of control larvae. (**D-F**) Cas9-mediated knockout of *cd4::GFP* prevents GFP expression in the membrane but retains red nuclear fluorescence in a *dorsal* view of stock *Cas9*-expressing larvae.

**Figure 7**

*Confocal Microscopy Confirms Incorporation of the UAS-Cas9 Transgene*

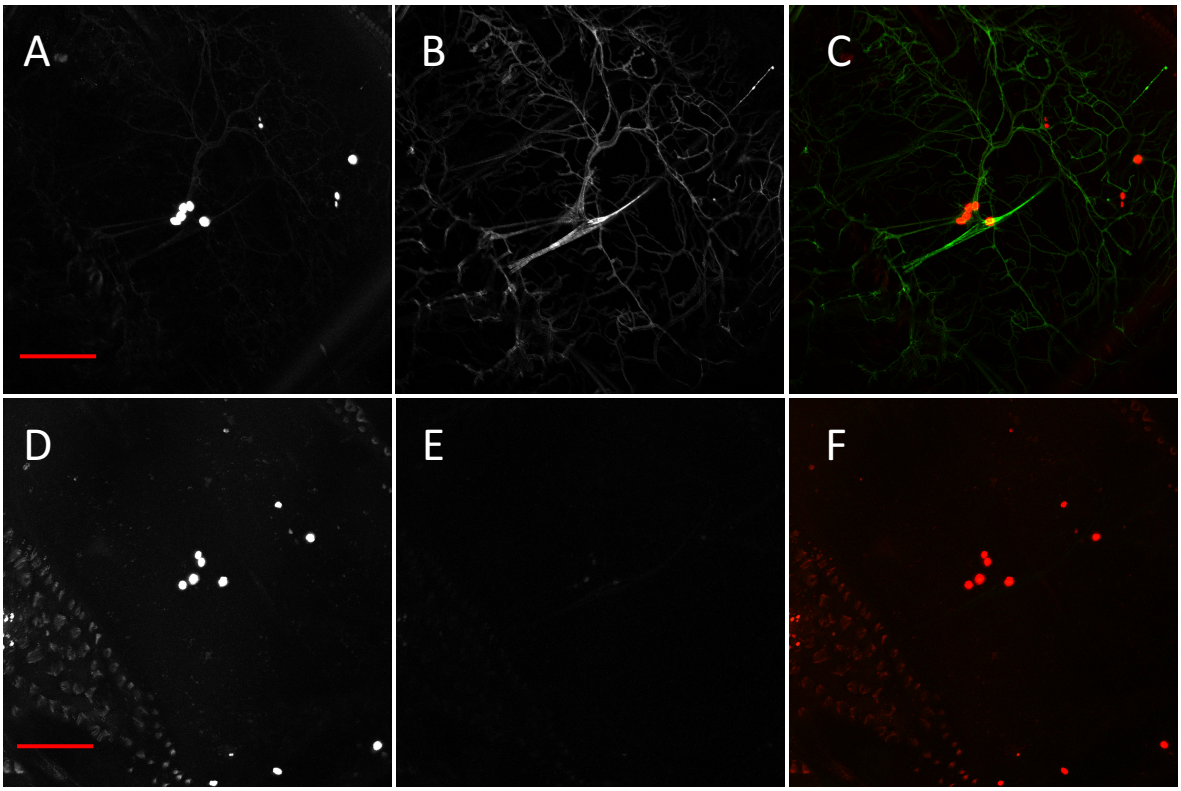


*Note:* Confocal microscopy of multidendritic neurons in larvae from a *ventral* view. In all panels, GFP is tagged to the CD4 transmembrane protein and RFP is tagged to the Tra nuclear RBP. Red scale bar represents 200µm. Panels A and D show red channel fluorescence data. Panels B and E show green channel fluorescence data. Panels C and F show colorized composites. Panels A-C show control 81892 larvae. Panels D-F show larvae produced from crossing 81892 adults to the final *ppk-GAL4;UAS-Cas9* stock. (**A-C**) Red nuclear fluorescence and green membrane fluorescence is present in all multidendritic neurons from a *ventral* view of control larvae. (**D-F**) Red nuclear fluorescence, but not green membrane fluorescence is present in all multidendritic neurons from a *ventral* view of larvae from the final *ppk-GAL4;UAS-Cas9* stock.

**Validating the Efficacy of Cas9-Mediated Knockout using Larval Nociception**

To confirm the efficacy of Cas9-mediated knockout (KO) in nociceptors, validation experiments targeting different genes in thermal and mechanical nociception contexts were conducted. In each experiment, the phenotype resulting from knocking out the target gene was previously established via RNAi or genetic mutants.

***Pickpocket – Mechanical Nociception***

This experiment was conducted to confirm the efficacy of Cas9-mediated KO of the *pickpocket* gene required for mechanical nociception (Zhong et al., 2010) . This is in turn to validate using the *ppk-GAL4;UAS-Cas9* system to investigate genes involved in larval mechanical nociception. It is known that *pickpocket* plays an important role in mechanical nociception, therefore, it is expected that Cas9-mediated KO of *ppk* will result in a significantly decreased response percentage compared to the Cas9- and sgRNA-only controls (Zhong et al., 2010). To do this, the *ppk-GAL4;UAS-Cas9* line was crossed with the *U6-ppk.gRNA* line to induce nociceptor-specific knockdown of *ppk*.

In this and all Cas9 KO experiments, three control groups were used as reference points for the experimental knockout group. Each of the negative controls expresses a one half of the GAL4/UAS system. The Cas9-only control expresses *ppk-GAL4;UAS-Cas9* but not the guide RNA needed to induce *ppk* mutagenesis. The sgRNA-only control expresses *U6-ppk.gRNA* but without the *ppk-GAL4;UAS-Cas9* driver. The experimental group then expresses both halves of the Cas9/sgRNA system and exhibits the *ppk-GAL4;UAS-Cas9,U6-ppk.gRNA* genotype. As a positive control, nociceptor-specific RNAi KD of *para* is induced as it is known to result in a virtually total loss of nociceptive function. In following

experiments using Cas9 KO, the only difference in set up is the use of different sgRNAs to target the gene indicated.

The percentage of larvae that respond for each group was as follows: Cas9-only – 61%, sgRNA-only – 63%, *ppk* KO – 37%, *para* RNAi – 4%. The significance of difference in response percentage between the *ppk* KO group and each Cas9/sgRNA-only control was tested via Chi-square. A Bonferroni correction to the α value was used to account for two comparisons, resulting in a corrected value of 0.025. The difference between the responding percentages of the *ppk* KO group and the Cas9-only control was significant with a $\chi^2$ of 9.442 and a p-value of 0.002123. The difference between the responding percentages of the *ppk* KO group and the sgRNA-only control was significant with a $\chi^2$ of 10.730 and a p-value of 0.001071. Cas9-mediated knockout of *ppk* significantly diminished larval mechanical nociception function.

**Figure 8**

*Nociceptor-Specific Cas9 Knockout of* Pickpocket *Significantly Impairs Mechanical Nociception in* Drosophila *Larvae*

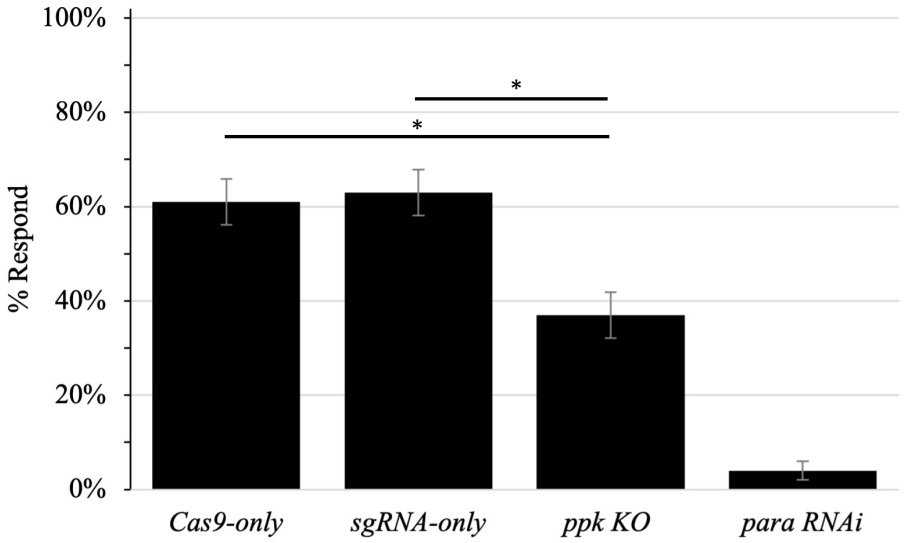


*Note:* The total percentage of larvae responding to 50mN of force is represented by bars. Error bars indicate standard error of the proportion.

For each group, n = 100.

Significance determined using a Chi-Square test with Bonferroni correction for two comparisons. * = $p < 0.025$.

***Lk6 – Mechanical Nociception***

This experiment was conducted to rule out the possibility of sgRNA-independent effects of Cas9 expression. Previous research in the Bellemer lab showed that knockout of *lk6* does not produce a noticeable phenotype in larval mechanical or thermal nociception, making it an ideal candidate for this control experiment. Therefore, a similar result of no difference between lk6 KO and control groups was expected. To do this, the *ppk-GAL4;UAS-*

*Cas9* line was crossed to the *U6-lk6.gRNA* line to induce nociceptor-specific KO of *lk6*. The Cas9-only, sgRNA-only, *para* RNAi controls and the experimental group were all set up similar to the *ppk* KO experiment (Figure 7), except the sgRNA line used in this experiment targets *lk6*.

Each group tested 100 larvae and the percentage of larvae that responded after three trials of mechanical stimulation with a 50mN von Frey filament was recorded. The percentage of larvae that respond for each group was as follows: Cas9-only – 67%, sgRNA-only – 70%, *lk6* KO – 70%, *para* RNAi – 10%. The significance of difference in response percentage between the *lk6* KO group and each Cas9/sgRNA-only control was tested via Chi-square. A Bonferroni correction to the α value was used to account for two comparisons, resulting in a corrected value of 0.025. The difference between the responding percentages of the *lk6* KO group and the Cas9-only control was not significant with a $\chi^2$ of 0.134 and a p-value of 0.7143. The difference between the responding percentages of the *lk6* KO group and the sgRNA-only control was not significant with a $\chi^2$ of 0.000 and a p-value of 1. Cas9-mediated knockout of *lk6* did not affect larval mechanical nociception.

**Figure 9**

*Nociceptor-Specific Cas9 Knockout of* Lk6 *does not Impair Mechanical Nociception in* Drosophila *Larvae*

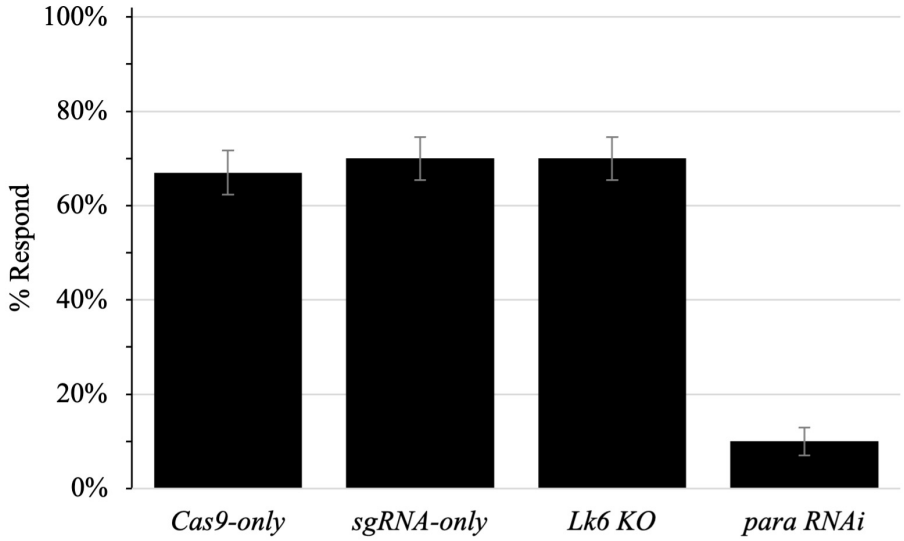


*Note:* The total rolling percentage of larvae in response to 50mN of force is represented by bars. Error bars indicate standard error of the proportion.

For each group, n = 100.

Significance determined using a Chi-Square test with Bonferroni correction for two comparisons.

***dTrpA1 – Mechanical Nociception***

The purpose of this experiment was to validate the use Cas9-mediated mutagenesis to knock out *dTrpA1*. This is in turn to validate using the *ppk-GAL4;UAS-Cas9* system to investigate genes involved in larval mechanical nociception. Since the role of dTrpA1 in larval nociception has been heavily studied, it is expected that Cas9-mediated KO of *dTrpA1* will result in a significantly decreased response percentage compared to the GAL4 and UAS-

only controls (Zhong et al., 2012). To do this, the *ppk-GAL4;UAS-Cas9* line was crossed to the *U6- dTrpA1.gRNA* line to induce nociceptor-specific knockout of *dTrpA1*. The Cas9-only, sgRNA-only, *para* RNAi controls and the experimental group were all set up similar to the *ppk* KO experiment (Figure 7), except the sgRNA line used in this experiment targets *dTrpA1*.

The sample size for each group was as follows: Cas9-only – 107, sgRNA-only – 112, *dTrpA1* KO – 102, *para* RNAi – 103. The percentage of larvae responding for each group was as follows: Cas9-only – 67.3%, sgRNA-only – 67.9%, *dTrpA1* KO – 57.8%, *para* RNAi – 4.85%. The significance of difference in response percentage between the *dTrpA1* KO group and each Cas9/sgRNA-only control was tested via Chi-square. A Bonferroni correction to the $\alpha$ value was used to account for two comparisons, resulting in a corrected value of 0.025. The difference between the responding percentages of the *dTrpA1* KO group and the Cas9-only control was not significant with a $\chi^2$ of 1.353 and a p-value of 0.2448. The difference between the responding percentages of the *dTrpA1* KO group and the sgRNA-only control was not significant with a $\chi^2$ of 1.507 and a p-value of 0.2195. Cas9-mediated knockout of *dTrpA1* in nociceptors did not effectively nor significantly impair nociception in larvae during mechanical nociception testing when compared to the controls.

**Figure 10**

*Effect of Nociceptor-Specific Cas9 Knockout of DTrpA1 on Mechanical Nociception in* Drosophila *Larvae*

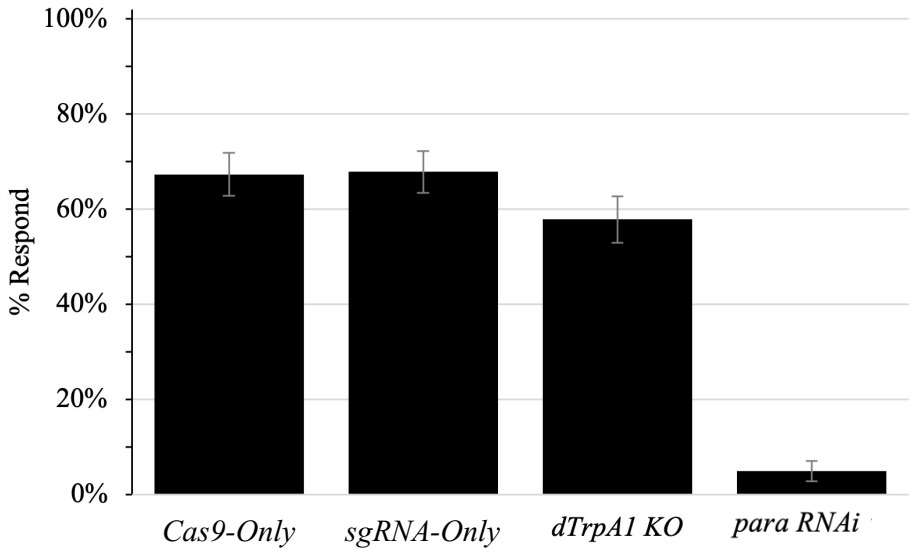


*Note:* The total rolling percentage of larvae in response to 50mN of force is represented by bars. Error bars indicate standard error of the proportion.

For each group, n = 107, 112, 102, and 103, respectively.

Significance determined using a Chi-Square test with Bonferroni correction for two comparisons.

**Table 4**

*Larval Mechanical Nociception Experiments Using Cas9 Knockout*

| Target | Genotype | n | % Response | Comparison | $\chi^2$ Test Stat. | p-value |
|---|---|---|---|---|---|---|
| ***ppk*** | Cas9-only | 100 | 61.0 | *ppk* KO | 9.442 | 0.002123 |
| | sgRNA-only | 100 | 63.0 | *ppk* KO | 10.730 | 0.001071 |
| | *ppk* KO | 100 | 37.0 | | | |
| | Para RNAi | 100 | 4.0 | | | |
| ***lk6*** | Cas9-only | 100 | 67.0 | *lk6* KO | 0.134 | 0.7143 |
| | sgRNA-only | 100 | 70.0 | *lk6* KO | 0.000 | 1 |
| | *lk6* KO | 100 | 70.0 | | | |
| | Para RNAi | 100 | 10.0 | | | |
| ***dTrpA1*** | Cas9-only | 107 | 67.3 | *dTrpA1* KO | 1.352 | 0.2448 |
| | sgRNA-only | 112 | 67.9 | *dTrpA1* KO | 1.507 | 0.2195 |
| | *dTrpA1* KO | 102 | 57.8 | | | |
| | Para RNAi | 103 | 4.85 | | | |

*Note:* All experiments conducted with 50mN force. Significance determined via $\chi^2$ test. Bonferroni correction resulted in an $\alpha$ value of 0.025 for comparison of the experimental group to each negative control. For all comparison calculations, df = 1 with a $\chi^2_{crit}$ of 5.024.

***dTrpA1 – Thermal Nociception***

The purpose of this experiment was to determine if Cas9-mediated knockout of *dTrpA1* in larvae would produce a significant defect in thermal nociception, as previously shown (Zhong et al., 2012). This would present as a significant increase in average latency and provide support to using Cas9 KO in nociceptors.

It is expected that Cas9-mediated KO of *dTrpA1* will result in a significantly decreased response percentage compared to the GAL4 and UAS-only controls. To do this, the *ppk-GAL4;UAS-Cas9* line was crossed with the *U6- dTrpA1.gRNA* line to induce nociceptor-specific knockout of *dTrpA1*. The Cas9-only, sgRNA-only, *para* RNAi controls and the experimental group are identical to those used in the *dTrpA1* KO experiment for mechanical nociception (Figure 9).

The average latency for each group was as follows: Cas9-only – 5.253s, UAS-only – 3.017s, *dTrpA1* KO – 5.133s, *para* RNAi – 10.807s. The p-value of the difference between the Cas9-only and sgRNA-only control groups was 0.000 with a Cliff's Δ of -0.55. The range of the Cliff's Δ 95% CI was -0.671, -0.405. The p-value of the difference between the *dTrpA1* KO and Cas9-only groups was 0.801 with a Cliff's Δ of -0.0205. The range of the Cliff's Δ 95% CI was -0.18, 0.142. The p-value of the difference between the *dTrpA1* KO and sgRNA-only groups was 0.000 with a Cliff's Δ of 0.548. The range of the Cliff's Δ 95% CI was 0.4, 0.664. The p-value of the difference between the *dTrpA1* KO and *para* RNAi groups was 0.000 with a Cliff's Δ of 0.903. The range of the Cliff's Δ 95% CI was 0.83, 0.951. The Cas9-only group had a significantly higher latency than the sgRNA-only group. The latency of the Cas9-only group was not significantly different from the *dTrpA1* KO group. There was a significant difference between latencies of the *dTrpA1* KO group and

sgRNA-only groups. Here, the *dTrpA1* KO latency being significantly higher than only the sgRNA-only group's latency and the significantly delayed Cas9-only latency does not allow for clear interpretation of the data. Additionally, the latency of the Cas9-only group is indicative of nociceptive defect.

**Figure 11**

*Effect of Nociceptor-Specific Cas9 Knockout of DTrpA1 on Thermal Nociception in* Drosophila *Larvae*

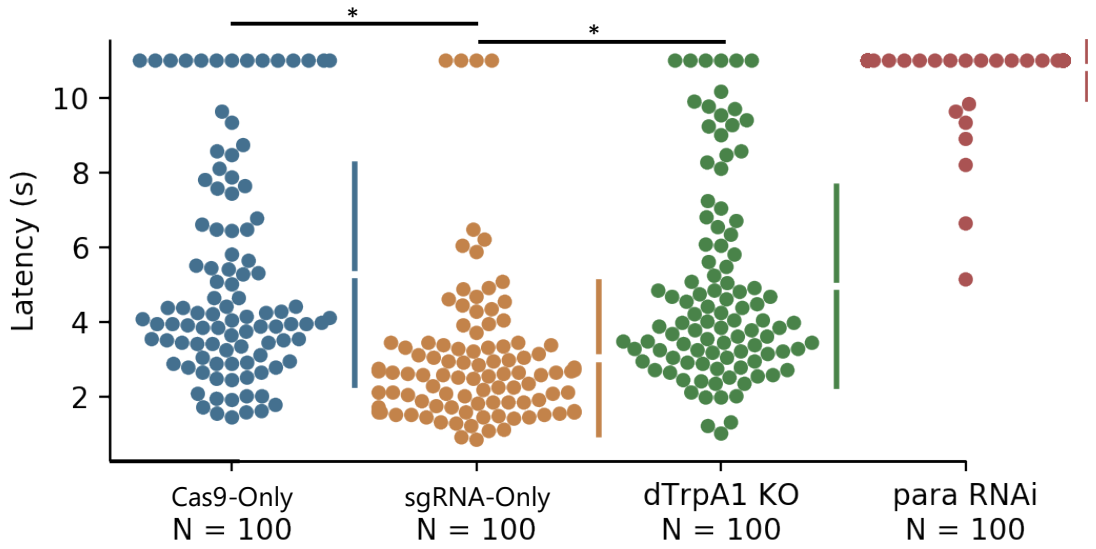


*Note:* Latency in seconds between contact with 46°C probe and complete NEL of individual larvae is shown as dots. Colored bars indicate interquartile ranges.

For each group, n = 100.

Significance was determined via two-sided permutation t-test. * = $p < 0.05$

***Lk6 – Thermal Nociception***

This experiment was conducted to rule out the possibility of off-target effects using Cas9-mediated KO of target genes in mechanical nociception. As previous research in the Bellemer lab showed that knockout of *lk6* does not produce a noticeable phenotype in larval mechanical nociception, a similar result of no difference between lk6 KO and control groups was expected. This is in turn to validate using the *ppk-GAL4;UAS-Cas9* system to investigate genes involved in larval thermal nociception. To do this, the *ppk-GAL4;UAS-Cas9* line was crossed to the *U6-lk6.gRNA* line to induce nociceptor-specific KO of *lk6*. The Cas9-only, sgRNA-only, *para* RNAi controls and the experimental group are identical to those used in the *dTrpA1* KO experiment for mechanical nociception (Figure 8).

The average latency for each group was as follows: Cas9-only – 4.162s, sgRNA-only – 3.601s, *lk6* KO – 3.185s, *para* RNAi – 11.000s. The p-value of the difference between the Cas9 and sgRNA-only control groups was 0.256 with a Cliff's Δ of -0.115. The range of the Cliff's Δ 95% CI was -0.309, 0.089. The p-value of the difference between the *lk6* and Cas9-only groups was 0.0316 with a Cliff's Δ of 0.213. The range of the Cliff's Δ 95% CI was 0.0178, 0.405. The p-value of the difference between the *lk6* and sgRNA-only groups was 0.366 with a Cliff's Δ of 0.0925. The range of the Cliff's Δ 95% CI was -0.111, 0.286. The p-value of the difference between the *lk6* KO and *para* RNAi groups was 0.000 with a Cliff's Δ of 7.82. The range of the Cliff's Δ 95% CI was 7.42, 8.14. The difference between the Cas9 and sgRNA-only control groups' latencies was not significant. The latency of the *lk6* KO group was significantly lower compared to the Cas9 control group's latency. However, the difference between the *lk6* KO and sgRNA control group's latencies was not significant.

Here, two conflicting comparisons of *lk6* KO latency to the controls' latencies does not allow for clear interpretation of the data.

**Figure 12**

*Effect of Nociceptor-Specific Cas9 Knockout of* Lk6 *on Thermal Nociception in* Drosophila *Larvae*

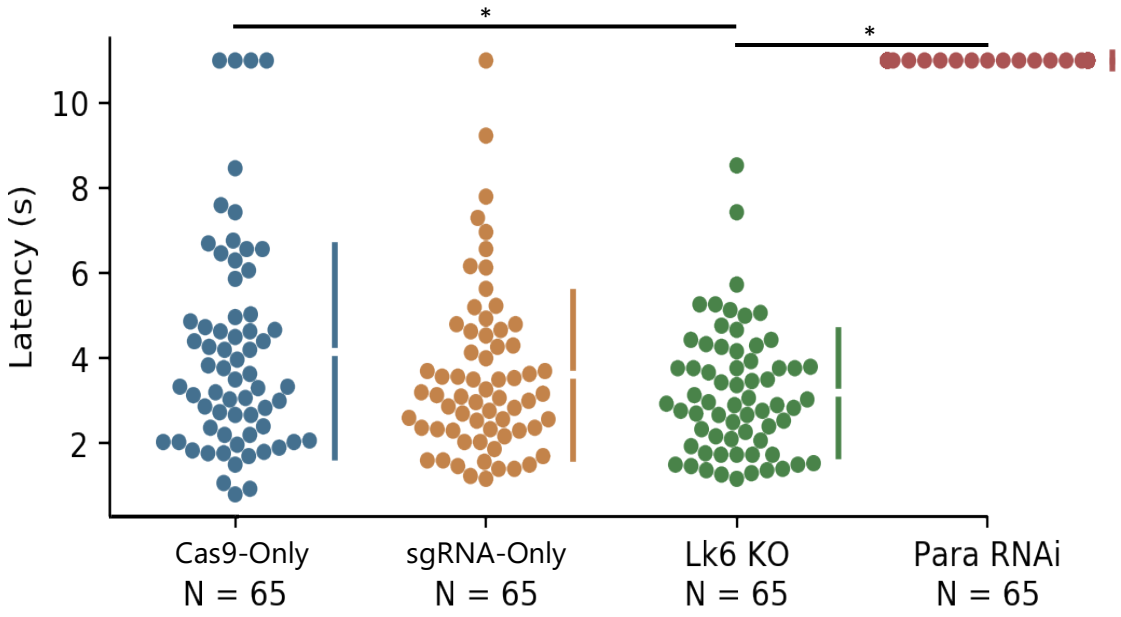


*Note:* Latency in seconds between contact with 46°C probe and complete NEL of individual larvae is shown as dots. Colored bars indicate interquartile ranges.

For each group, n = 65.

Significance was determined via two-sided permutation t-test. * = $p < 0.05$.

**Table 5**

*Summary of Larval Thermal Nociception Experiments Using Cas9 Knockout*

| Experiment | Genotype | n | Average Latency (s) | Comparison to Cas9-only p-value | Comparison to sgRNA-only p-value |
|---|---|---|---|---|---|
| **dTrpA1 Knockout** | Cas9-only | 100 | 5.253 | | 0.000 |
| | sgRNA-only | 100 | 3.017 | 0.000 | |
| | *dTrpA1* KO | 100 | 5.133 | 0.504 | 0.000 |
| | Para RNAi | 100 | 10.807 | 0.000 | 0.000 |
| **Lk6 Knockout** | Cas9-only | 65 | 4.162 | | 0.256 |
| | sgRNA-only | 65 | 3.601 | 0.265 | |
| | *lk6* KO | 65 | 3.185 | 0.0316 | 0.366 |
| | Para RNAi | 65 | 11.000 | 0.000 | 0.000 |

*Note:* All experiments conducted at 46°C unless otherwise noted. p-values indicate comparison between the noted group and the Cas9-only control or sgRNA-only control. Significance determined via a two-sided permutation t-test.

**Effect of Cas9 Expression on Nociceptor Dendrite Morphology**

A major concern was discovered during larval thermal nociception experiments using Cas9-mediated KO at 46°C (Figures 9-10). It was found that the GAL4-only control (*ppk-GAL4;UAS-Cas9*) had significantly delayed latency in thermal nociception assays compared to the UAS-only control which does not express Cas9. For example, in the *dTrpA1* KO experiment, the latency of the Cas9-only control was 5.253s and statistically delayed compared to the sgRNA-only control's latency of 3.017 ($p = 0.00$), but no different from the *dTrpA1* KO group's latency of 5.133 ($p = 0.504$) (Figure 10).

To help understand why the Cas9-only controls had significantly delayed latencies compared to the sgRNA-only controls, a qualitative morphological study of Cas9-only flies expressing *ppk-GAL4;UAS-Cas9* was conducted using a transgenic fly line that allows nociceptor visualization. Larvae containing the *ppk-GAL4,mCD8::GFP* transgene produce nociceptors that express the GFP-tagged mouse CD8 transmembrane protein, allowing visualization of nociceptor morphology. Two crosses were set up. The first was made by crossing virgin females with the *ppk-GAL4,mCD8::GFP* genotype to $w^{1118}$ males which produced larvae that would serve as a control group (Figure 13A-C). The second cross was made by crossing virgin females with the *ppk-GAL4,mCD8::GFP* genotype to males with the *ppk-GAL4;UAS-Cas9* genotype (Figure 13D-F). This cross would produce larvae that produced both Cas9 and GFP proteins to observe what, if any effects *UAS-Cas9* expression was having on dendrite morphology.

In 4 of 4 control larvae observed (3 shown), all observed nociceptors exhibited normal dendrite morphology with an elaborate branching pattern that tiled the larval body wall with no dendrite overlap (Figure 13A-C). In 3 of 3 experimental larvae, no observed

nociceptors exhibited normal dendrite morphology (Figure 13D-F). The nociceptors of larvae expressing *UAS-Cas9* exhibited numerous severe morphological defects. For example, little dendrite branching occurred in the nociceptors, such that very large portions of the larval body wall were not tiled. Additionally, in what few dendrite branches were present, the dendritic branches were extremely short and more closely resembled dendritic spines. No quantitative measurements were needed, as simple observation of the nociceptors revealed that Cas9 expression produced very dramatic and severe morphological defects, but follow-up experiments quantifying these defects would be worthwhile.

**Figure 13**

*Expression of UAS-Cas9 in Nociceptors Dramatically Impacts Larval Dendrite Morphology*

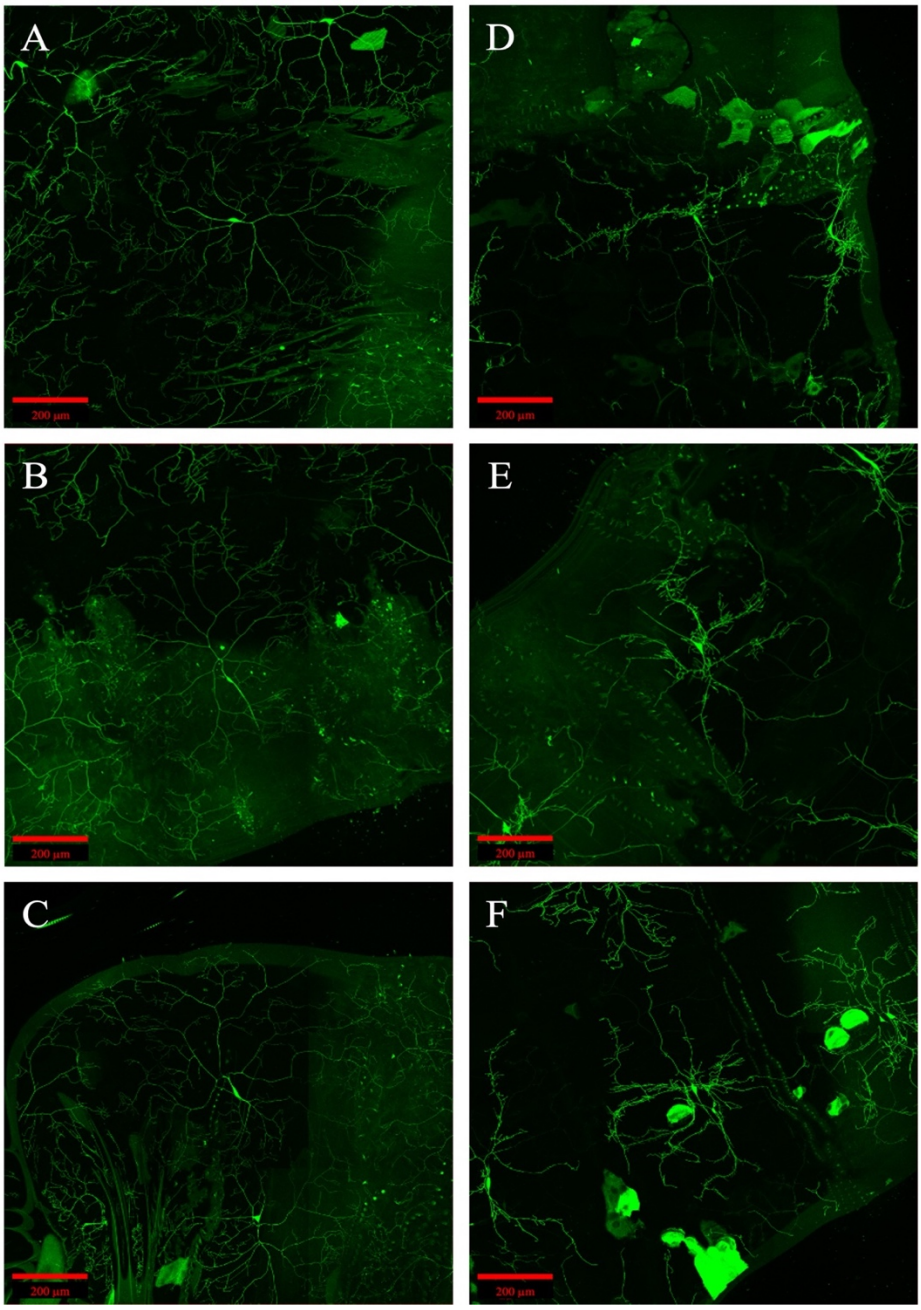


*Note:* (**A-C**) Confocal microscopy of nociceptors expressing *ppk-GAL4,mCD8::GFP*. (**D-F**) Confocal microscopy of nociceptors expressing *ppk-GAL4,mCD8::GFP; UAS-Cas9*.

For all images, red scale bar indicates 200µm.

**Validating the Adult Thermal Nociception Assay**

The following experiments were conducted to validate the use of the newly established adult thermal nociception assay by using *painless* and $dTrpA1^{ins}$ mutants as positive controls, which should exhibit significantly lower avoidance percentages compared to a $w^{1118}$ control (Neely et al., 2010). The role of these genetic mutants has been well-established in adult and larval thermal nociception, which is why they were used as positive controls (Neely et al., 2010, 2011). The significance of the difference between groups' avoidance percentage was determined with a Chi-square test. For all comparisons, 1 degree of freedom and a critical $\chi^2$ of 5.024 was used.

***Painless and $dTrpA1^{ins}$ – Adult Thermal Nociception***

Adult flies were exposed to a 46°C heat challenge and the percentage of flies that were able to avoid incapacitation by the heat were recorded. It is expected that the *painless* and $dTrpA1^{ins}$ groups would exhibit significantly lower avoidance percentages compared to the $w^{1118}$ controls. The avoidance percentage of each group was as follows: $w^{1118}$ – 93.64%, *painless* – 68.29%, $dTrpA1^{ins}$ – 75.25%. A Bonferroni correction to the α value was used to account for two comparisons, resulting in a corrected value of 0.025. The difference in the avoidance percentage of the $w^{1118}$ and *painless* groups was significant with a test $\chi^2$ of 5.62 and a p-value of 0.01776. The difference in the avoidance percentage of the $w^{1118}$ and $dTrpA1^{ins}$ groups was not significant with a test $\chi^2$ of 3.65 and a p-value of 0.05607. The *painless* mutants were able to show a significantly decreased avoidance percentage compared to the $w^{1118}$ control, which is consistent with previous findings. Surprisingly, $dTrpA1^{ins}$ mutants did not show a significant defect in avoidance behavior but did trend in that

direction. This warranted an additional experiment testing *dTrpA1$^{ins}$* adults as a positive control.

**Figure 14**

Painless *is Required for Adult Thermal Nociception*

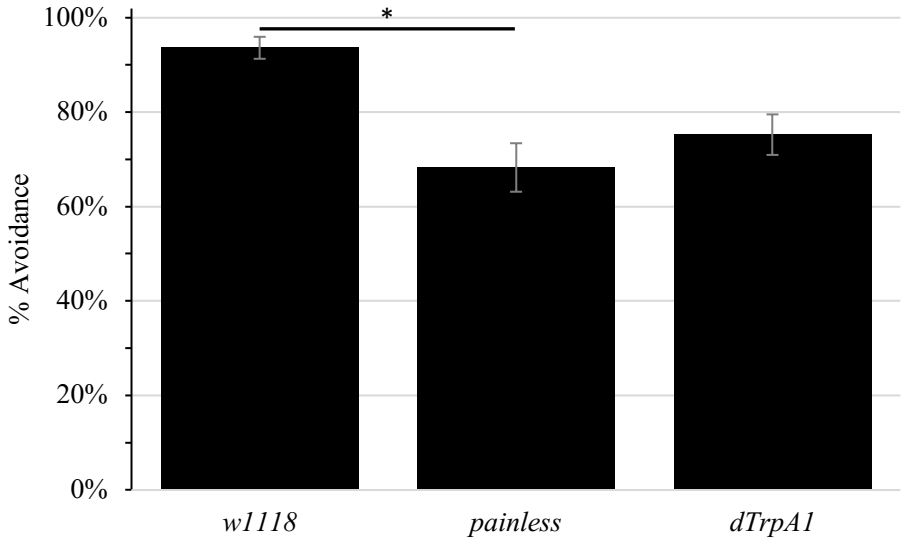


*Note:* The total avoidance percentage of flies against the 46°C heat challenge. Error bars indicate standard error of the proportion.

For each group, n = 110, 82, and 101, respectively.

Significance determined using a Chi-Square test with a Bonferroni correction for 2 comparisons.

***dTrpA1$^{ins}$ and dTrpA1 KO – Adult Thermal Nociception***

The purpose of this experiment was twofold. The first goal was to validate using the *dTrpA1$^{ins}$* adults as a positive control that would significantly decrease avoidance behavior. The second goal was to confirm the efficacy of Cas9-mediated KO of the *dTrpA1* gene,

which is required for adult thermal nociception. The percentage of adult flies that avoided a 46°C heat challenge after 4 minutes was recorded. The Cas9-only, sgRNA-only controls and the *dTrpA1* KO group are identical to those used in the *dTrpA1* KO experiment for mechanical nociception (Figure 9). As a positive control, $dTrpA1^{ins}$ adults were retested as they had been previously been shown in the original source of this assay to have a significantly lower avoidance percentage to noxious temperatures as adults (Neely et al., 2011).

The percentage of adults that avoided the heat challenge for each group was as follows: Cas9-only – 93.62%, sgRNA-only – 94.74%, *dTrpA1* KO – 88.66%, $dTrpA1^{ins}$ – 48.98%. A Bonferroni correction to the α value was used to account for four comparisons, resulting in a corrected value of 0.0125. The difference between the avoidance percentages of the *dTrpA1* KO group and the Cas9-only control was not significant with a $\chi^2$ of 0.255 and a p-value of 0.6136. The difference between the avoidance percentages of the *dTrpA1* KO group and the sgRNA-only control was not significant with a $\chi^2$ of 0.378 and a p-value of 0.5387.

Cas9-mediated knockout of *dTrpA1* did not effectively impair nociceptive function as evidenced by the similar avoidance percentage to the Cas9 and sgRNA-only controls. The difference between the avoidance percentages of the $dTrpA1^{ins}$ group and the Cas9-only control was significant with a $\chi^2$ of 20.9 and a p-value of 0.000004839. The difference between the avoidance percentages of the $dTrpA1^{ins}$ group and the sgRNA-only control was also significant with a $\chi^2$ of 21.7 and a p-value of 0.000003188. The $dTrpA1^{ins}$ mutant line but not Cas9-mediated KO of *dTrpA1* produced a significant defect in adult fly avoidance

behavior when subjected to a 46° heat challenge. This additional experiment supported using *dTrpA1*$^{ins}$ adults as a positive control for adult thermal nociception assays.

**Figure 15**

DTrpA1 *is Required for Adult Thermal Nociception and the Effect of Nociceptor-Specific Cas9 Knockout of* DTrpA1

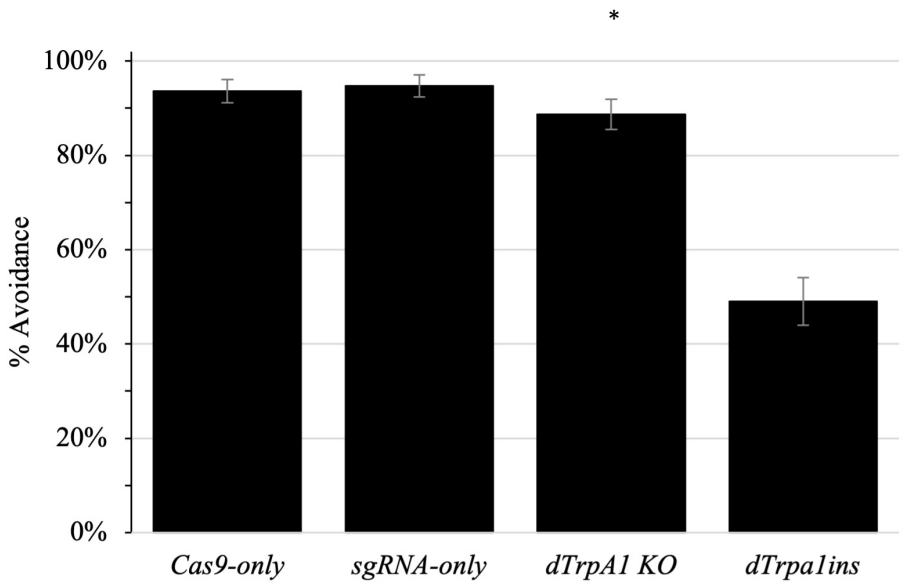


*Note*: This graph depicts the total avoidance percentage of flies against the 46°C heat challenge. Bars indicate standard error of the proportion.

For each group, n = 94, 95, 97, and 98, respectively.

Significance determined using a Chi-Square test with a Bonferroni correction for 4 comparisons. * = $p < 0.0125$.

***Para – Adult Thermal Nociception***

The purpose of this experiment was to investigate the role that the sodium voltage-gated ion channel Paralytic plays in *ppk*-expressing neurons in adult flies in response to a

46°C heat challenge. It is expected that the *para* KD group will exhibit significantly lower avoidance percentage compared to the GAL4 and UAS-only controls.

In this experiment, three control groups were used as reference points for the experimental knockdown group. Each of the negative controls expresses a non-functional half of the *ppk-GAL4/UAS-RNAi* system. The GAL4-only control therefore expresses *ppk-GAL4* but not the RNAi needed to target *para*. The UAS-only control expresses *UAS-para* RNAi but without the *ppk-GAL4* driver. The experimental group then expresses both halves of the GAL4/UAS system and exhibits the *ppk-GAL4;UAS-para-RNAi* genotype. As a positive control, $dTrpA1^{ins}$ adults were used as they had previously been shown to have a significantly lower avoidance percentage to noxious temperatures as adults (Neely et al., 2011).

The percentage of flies that were able to avoid incapacitation after being exposed to a 46°C heat challenge for 4 minutes was recorded for each group. The sample size for each group was as follows: GAL4-only – 123, UAS-only – 120, *para* RNAi – 113, *painless* – 83. The percentage of adults that avoided the heat challenge for each group was as follows: GAL4-only – 95.12%, UAS-only – 98.33%, *para* RNAi – 96.46%, *painless* – 62.65%. A Bonferroni correction to the α value was used to account for two comparisons, resulting in a corrected value of 0.025. The difference between the avoidance percentages of the *para* RNAi group and the GAL4-only control was not significant with a $\chi^2$ of 0.547 and a p-value of 0.4595. The difference in avoidance percentages between the *para* RNAi and UAS-only control groups was not significant with a $\chi^2$ of 0.686 and a p-value of 0.4075. The avoidance percentage of *painless* flies (~63%) was similar to the original validation experiment (~68%) (Figure 8).

**Figure 16**

*Para is not Required in Adult ppk+ Neurons for Adult Thermal Nociception*

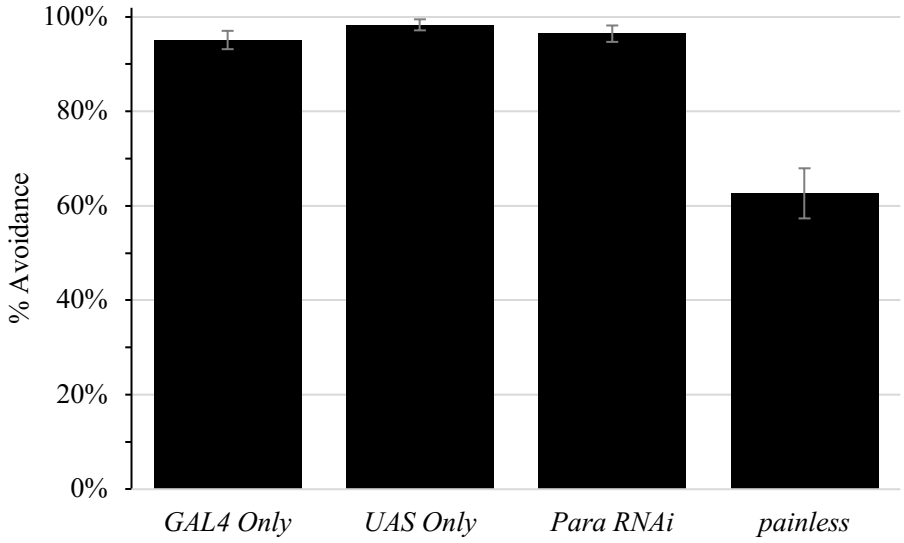


*Note:* The total avoidance percentage of flies against the 46°C heat challenge. Bars indicate standard error of the proportion.

For each group, n = 123, 120, 113, and 83, respectively.

Significance determined using a Chi-Square test with a Bonferroni correction for 2 comparisons.

**Table 6**

*Adult Thermal Nociception Experiments*

| Experiment | Genotype | n | % Avoidance | Comparison | $\chi^2$ Test Stat. | p-value |
|---|---|---|---|---|---|---|
| ***painless* and *dTrpA1* mutants** | $w^{1118}$ | 110 | 93.64 | | | |
| | *painless* | 82 | 68.29 | $w^{1118}$ | 5.62 | 0.01776 |
| | $dTrpA1^{ins}$ | 101 | 75.25 | $w^{1118}$ | 3.65 | 0.05607 |
| ***dTrpA1* Cas9 Knockout** | Cas9-only | 94 | 93.62 | *dTrpA1* KO | 0.255 | 0.6136 |
| | sgRNA-only | 95 | 94.74 | *dTrpA1* KO | 0.378 | 0.5387 |
| | *dTrpA1* KO | 97 | 88.66 | | | |
| | $dTrpA1^{ins}$ | 98 | 48.98 | Cas9-only | 20.9 | 0.000004839 |
| | | | | sgRNA-only | 21.7 | 0.000003188 |
| ***para* RNAi** | GAL4-only | 123 | 95.12 | *para* RNAi | 0.547 | 0.4595 |
| | UAS-only | 120 | 98.33 | *para* RNAi | 0.686 | 0.4075 |
| | Para RNAi | 113 | 96.46 | | | |
| | *painless* | 83 | 62.65 | | | |

*Note*: Significance determined via $\chi^2$ test. Bonferroni correction resulted in a one-tail $\alpha$ value of 0.025 and 0.0125 for 2 and 4 comparisons, respectively. For all comparison calculations, df = 1 with a $\chi^2_{crit}$ of 5.024.

## Discussion

This study aimed to validate three candidate genes' involvement in basal thermal nociception in larvae as detected in a screen by Amber Dyson (Dyson, 2017). Secondly, a custom-made *Drosophila* line that expressed *UAS-Cas9* in nociceptors using the GAL4/UAS system was subjected to a rigorous set of validation experiments using target genes with well-studied, defective nociception phenotypes. Third, an assay used to measure thermal nociception in adult *Drosophila* was replicated by using mutants that are known to produce defective avoidance behavior phenotypes. This assay was then used to investigate the role of the sodium voltage-gated channel Para in adult nociceptors. An additional goal of these latter two aims was to validate the role of eIF2α, SC35, and LaRP4B in thermal nociception.

### eIF2α is Required for Baseline Thermal Nociception

eIF2α is a translation initiation factor subunit that is regulated by the eIF2B guanine exchange factor (GEF). When eIF2α is phosphorylated, such that it cannot interact with eIF2B, global protein synthesis is decreased while the expression of stress response genes is upregulated (Bellato & Hajj, 2016). When RNAi knockdown of eIF2α was induced in nociceptors, a significant delay in latency was observed between the KD group and the GAL4-only and UAS-only controls (Figure 2 and Table 3). These data validate eIF2α as an RBP involved in thermal nociception as detected in Amber Dyson's RNAi screen (Dyson, 2017). It is likely that since RNAi knockdown of the α subunit of eIF2 is functionally mimicking phosphorylation in that guanine exchange activity cannot occur. This then leads to a global decrease in protein synthesis, including all of the proteins that are required for normal nociceptive function. Therefore, a hypersensitization and UV sensitization assay of

eIF2α would be worthwhile future directions to see if KD affects nociceptor plasticity following injury.

**SC35 is Required for Baseline Thermal Nociception**

SC35 is a splicing factor that is known for keeping balance between two isoforms of the structural Tau protein via exon inclusion (Lin et al., 2008; Liu & Gong, 2008; Qian et al., 2011). The knockdown of *sc35* via RNAi showed that the SC35 is required for basal nociceptive function (Figure 3 and Table 1). It is likely that SC35's exon inclusion activity impacts a very important mRNA transcript, which may be a structural protein. Indeed, in hippocampal neurons, SC35 alternatively splices transcripts of *tau* to maintain the appropriate proportion of 4R and 3R isoforms (Liu & Gong, 2008; Qian et al., 2011). A defect in the regulation of structural proteins would provide an explanation for the delayed latency of the KD group which was significantly higher compared to the GAL4-only and UAS-only controls (Figure 3). These data validate SC35 as an RBP involved in thermal nociception as detected in Amber Dyson's RNAi screen (Dyson, 2017). Further investigation into the effect that *sc35* KD has on dendrite morphology and injury-induced sensitization can be carried out to further characterize the role that SC35 plays in modulating nociceptor plasticity.

**LaRP4B is Required for Baseline Thermal Nociception**

LaRP4B is an RBP that is not well-characterized, but there are some lines of evidence that indicate it is involved in stimulating translation of specific mRNA transcripts (Küspert et al., 2015). This is presumably done by increasing the half-life of the transcripts themselves

(Küspert et al., 2015). An important aspect of mRNA metabolism and stability is that transcripts that are generally unstable tend to be only used in rare situations, such as cellular stress events (Bolognani & Perrone-Bizzozero, 2008; Hargrove & Schmidt, 1989). The role of LaRP4B in basal thermal nociception was investigated (Figure 4 and Table 1). After RNAi knockdown of LaRP4B, the average latency of larvae was significantly higher than both GAL4-only and UAS-only controls. These data validate LaRP4B as an RBP involved in thermal nociception as detected in Amber Dyson's RNAi screen (Dyson, 2017). This suggests that the stabilization of specific transcripts in nociceptors is indispensable to normal nociceptive function. A gain-of-function experiment investigating the effect that overexpression of LaRP4B would be a potential future direction. It could potentially result in a hypersensitivity phenotype since the mRNA transcripts with short half-lives are usually associated with the stress response (Bolognani & Perrone-Bizzozero, 2008; Hargrove & Schmidt, 1989). This would result in larvae tested at 42°C having a much faster latency compared to the control.

**Construction of a ppk-GAL4;UAS-Cas9 Fly Line**

Construction of the transgenic fly line that would express *ppk-GAL4;UAS-Cas9* occurred over 10 generations of crossing. Therefore, it was imperative to use molecular and microscopic techniques to confirm the presence of the *ppk-GAL4* and *UAS-Cas9* transgenes. Attempts to amplify the *UAS-Cas9* transgene via PCR were not fruitful, but amplification of the *ppk-GAL4* transgene was consistently successful. As shown in Figure 5, *ppk-GAL4* was present in the final *ppk-GAL4;UAS-Cas9* stock.

To test the presence, expression, and functionality of the *UAS-Cas9* transgene and Cas9 protein in the final stock, a functional assay was performed (Figures 6 and 7). The positive control cross used the initial *UAS-Cas9* stock to knock out GFP expression (Figure 6). This resulted in a complete elimination of GFP fluorescence (Figure 6E). As shown in Figure 7E, there is no green fluorescence present in the multidendritic neurons of larvae with the final *ppk-GAL4;UAS-Cas9* stock genotype. However, since there is no RFP.gRNA, the red nuclear fluorescence persists (Figure 7D,F).

Though the *ppk-GAL4* driver is included in the final *ppk-GAL4;UAS-Cas9* stock, the *md-GAL4* driver supersedes it since it covers a wider range of cell types. This means that it is not possible to knockout expression of GFP only in nociceptors. As the UAS-Cas9 transgene development is still new, a negative tester line that is specific to nociceptors is not yet available. Regardless, evidence from both PCR amplification of the *ppk-GAL4* driver (Figure 5) and functionality of the *UAS-Cas9* transgene (Figure 7) indicate that both transgenes were successfully incorporated into the final *ppk-GAL4;UAS-Cas9* stock and Cas9 was functional in the md neurons.

**Validating Cas9 Knockout Efficiency in Mechanical and Thermal Nociception**

Before using this newly constructed line to investigate the role of novel candidate genes that have not been studied before, it was important to test the *ppk-GAL4;UAS-Cas9* stock against target genes that have been thoroughly studied. Only after successfully validating this line through reproducing expected phenotypes could it be then used for novel investigations.

The first gene that was targeted for Cas9 KO was the mechanosensitive ion channel, *pickpocket* (Zhong et al., 2010). This ion channel is one of the first proteins that was studied in the context of *Drosophila* larval nociception and is required for normal mechanical nociception (Zhong et al., 2010). Therefore, Cas9 KO of *ppk* was expected to result in a significant defect in mechanical nociception. As shown in Figure 8, the *ppk* KO group had a significantly decreased response rate compared to the Cas9-only and sgRNA-only controls. Using Cas9-mediated gene KO seemed to work efficiently as these results were similar to those previously published (Zhong et al., 2010).

Next, the *lk6* gene's sequence was targeted for Cas9 KO. This protein has been studied previously in the Bellemer lab and the results showed that RNAi knockdown of *lk6* did not produce a significant defect in mechanical nociception (McGuirt, 2019). Therefore, the purpose of this experiment was to test if Cas9 overexpression inherently produced any sgRNA-independent effects. Consistent with previous findings, it appeared as though Cas9 KO did not produce any such effects during mechanical nociception. The *lk6* KO group had an identical response rate to the sgRNA-only control and was not statistically significant from the Cas9-only control (Figure 9).

As a final test of the efficiency of Cas9 KO in mechanical nociception, the *dTrpA1* ion channel was targeted. Similar to pickpocket, dTrpA1 is a foundational ion channel that has been extensively studied in nociceptors; therefore, significant defects in mechanical nociception were expected (Heber et al., 2019; Jordt et al., 2004; Neely et al., 2011; Saito & Tominaga, 2017; Zhong et al., 2012). Surprisingly, Cas9 KO of *dTrpA1* did not result in a significant decrease in rolling response when compared to the Cas9 and sgRNA-only controls (Figure 10 and Table 4). This was unexpected, so a thermal nociception assay was used to

determine if Cas9 KO of *dTrpA1* also resulted in an unexpected phenotype (Zhong et al., 2010, 2012)

Larvae that contained the GAL4/UAS system to direct Cas9 KO of *dTrpA1* had an average latency similar to what would be expected and was significantly higher than the sgRNA-only control (Table 5). However, the Cas9-only control also had a significantly delayed latency as well and was not statistically different from the KO group (Figure 11). These unexpected results indicate that there are sgRNA-independent effects of Cas9 overexpression. Therefore, Lk6 was revisited as a target gene for Cas9 KO using the thermal nociception assay as it could also be used to reveal sgRNA-independent effects (McGuirt, 2019).

A similar, but attenuated phenomenon was seen in the Lk6 thermal nociception experiment (Table 5 and Figure 12). Here, the latencies of the Cas9-only and sgRNA-only controls were not significantly different (Table 5). However, the Lk6 KO group had a latency that was significantly lower than the Cas9-only control (Figure 12). The inconsistent and varied latencies of the Cas9-only control that overexpressed *UAS-Cas9* was unexpected. It appeared as though *UAS-Cas9* overexpression was inherently causing nociceptive defects.

The experiments conducted in Figures 7-12 show that Cas9 overexpression in the Cas9-only control induces phenotypic abnormalities. For example, the significant defects in thermal nociception present in the Cas9-only group (Figures 11 and 12) was not detected during mechanical nociception assays targeting *ppk*, *dTrpA1*, or *lk6* (Figures 8-10). Ultimately it is not possible to make any conclusions from the Cas9 KO experiments, given the inconsistent phenotype of the Cas9-only controls.

To identify what was causing these results, a final experiment that involved driving expression of GFP in nociceptors was conducted (Figure 13). The purpose of this experiment was to observe what effect, if any, Cas9 overexpression using the GAL4/UAS system had on nociceptor morphology. Defects in nociceptor dendrite morphology is characterized in part by decreased branching and reduced surface area coverage. As expected, all observed nociceptors in 4 control larvae exhibited normal morphology (Figure 13A-C, fourth larvae not shown). A striking finding was made when the nociceptors of larvae overexpressing Cas9 were visualized. None of the nociceptors in these larvae exhibited normal dendrite morphology (Figure 13D-F). Indeed, these nociceptors exhibited numerous and severe morphological defects. For example, there was very little dendrite branching that occurred in the nociceptors. As a result, very large portions of the larval body wall were not tiled. This would explain the delayed latency as a decrease in coverage could result in a dampened ability to detect noxious thermal stimuli. Additionally, in what few dendrite branches were present, the stunted lengths were more closely resembled dendritic spines (Figure 13D-F). This microscopy data along with the defective phenotype of the Cas9-only control shown in thermal nociception assays indicate that Cas9 overexpression using the GAL4/UAS system is likely leading to morphological defects that severely impact dendrite morphology and function (Figure 13 and Tables 4 and 5).

**The GAL4/UAS System May Lead to Problematic Cas9 Overexpression**

The results shown here indicate that sgRNA-independent effects of Cas9 overexpression may be responsible for the severe defect in nociceptor function and dendrite morphology. One of the possible explanations for the observed results is that the GAL4/UAS

system inherently results in overexpression of the transgene linked to a UAS element (Brand & Perrimon, 1993; Johnson et al., 1995; Phelps & Brand, 1998; Vashee & Kodadek, 1995). GAL4 as a transcription factor is very efficient and recruits the machinery required for transcription (Brand & Perrimon, 1993; Phelps & Brand, 1998). Therefore, it is likely that Cas9 overexpression led to dysfunction that disrupted normal dendrite formation.

Additionally, there are multiple vectors and transgenic fly lines that are used to drive expression of Cas9 under the control of GAL4/UAS (Port et al., 2014, 2016, 2020). The *UAS-Cas9* transgene used in this thesis is known as the *Cas9.C* vector that is codon-optimized for expression in Drosophila and linked to 10 UAS elements (Port et al., 2014, 2020). One study from 2019 found that even after using the *Cas9.P2* transgene that is less potent and potentially less lethal than *Cas9.C*, unintended lethality was still induced through leaky Cas9 expression (Meltzer et al., 2019; Port & Bullock, 2016). The authors of the original source for the *UAS-Cas9* transgene also advise that Cas9 expression may behave differently in various cell and tissue contexts (Port et al., 2020).

As an example of *Drosophila*'s sensitivity to *Cas9* expression, it is important to note that the beginning of *UAS-Cas9* transgene development presented issues with organism viability (Port et al., 2014). For example, expression of *UAS-Cas9* alone resulted in high levels of lethality (Port et al., 2014). Surprisingly, even after expressing a version of Cas9 with mutated nuclease domains (dCas9), heightened lethality persisted, suggesting that Cas9 cytotoxicity is not a result of aberrant, nonspecific DSBs and NHEJR (Port et al., 2014). Interestingly, overexpression of dCas9 in *E. coli* results in abnormal cell morphology, downregulation of genes that code for chaperone proteins and proteases that are membrane-localized, and upregulation of genes involved in cell division (Cho et al., 2018). It is

therefore likely the Cas9 overexpression that is inherent to the GAL4/UAS system is causing defects in nociceptor development (Cho et al., 2018). As a result, further validation of eIF2α, SC35, and LaRP4B, or other novel investigations were not possible using CRISPR/Cas9 gene editing.

Various attempts and methods to further fine tune *UAS-Cas9* expression have been developed (Port et al., 2014, 2020). One of these involve inserting short upstream open reading frames (uORFs) of various lengths upstream of the UAS sequence to reduce translation rates of *Cas9* in an inverse manner (Port et al., 2020). This approach takes advantage of cells' existing regulation of translation through the consensus motif that has a high affinity for translation initiation factors (Ferreira et al., 2013). uORFs are engineered to contain a consensus motif that strongly enhances initiation, but the actual coding sequence only contains a few codons (Ferreira et al., 2013). As this uORFs is expressed, the ribosome remains on the transcript and reaches the ORF of the transgene that is being regulated through the uORFs. Thus, the longer the uORFs, the less likely it is that the ribosome reaches the transgene's ORF (Ferreira et al., 2013). Various version of the *UAS-Cas9* transgene was generated with this kind of uORFs regulation, however the *UAS-Cas9.C* vector tested in this study did not have this feature (Koreman et al., 2021; Port et al., 2014, 2020). Given the novel implementation of this technology, it is also likely that additional optimizations to Cas9 expression still need to be made.

Various questions are raised through this investigation. What processes are induced in nociceptors as a response to Cas9 expression that causes such a severe defect in dendrite morphology (Figure 13)? Could nociceptors be inherently subject to more stringent surveillance of double strand breaks in DNA? Are RNA molecules that are similar enough to

guide RNA strands expressed in nociceptors such that they induce Cas9-mediated mutagenesis absent the sgRNA molecules?

No other data on the effect of Cas9 expression on larval thermal and mechanical nociception is currently available. Thus, the data generated through this study indicates that choosing vectors for *UAS-Cas9* expression in nociceptors is much more complex than originally anticipated. A possible path to continue the development of CRISPR/Cas9 gene editing in *Drosophila* could involve creating a GAL4/UAS-independent expression system wherein a *Cas9* sequence is inserted downstream of the *pickpocket* promotor to drive expression of *Cas9* exclusively in nociceptors. This could avoid the concern of overexpression that is inherent to the GAL4/UAS system (Johnson et al., 1995; Phelps & Brand, 1998; Port & Bullock, 2016).

**Adult Thermal Nociception Protocol is Validated**

Since the third instar developmental stage of larvae only lasts for 24-48 hours, it is difficult to measure nociceptor plasticity over extended periods of time (Fernández-Moreno et al., 2007). Experiments investigating nociceptor plasticity in adult thermal nociception are only recently becoming a reality thanks to advances in protocol development (Khuong et al., 2019; Neely et al., 2011). Therefore, an additional goal of this project was to introduce one of these novel methods to measure adult thermal nociception to the lab (Neely et al., 2011). To validate the methodology, two positive controls were used: $dTrpA1^{ins}$ and *painless* mutants since their role has been shown as necessary for adult thermal nociception (Khuong et al., 2019; Neely et al., 2011; Xu et al., 2006). Surprisingly, only the *painless* mutants were able to indicate a significant defect in the avoidance response compared to $w^{1118}$ flies (Figure 14

and Table 6). The *dTrpA1*$^{ins}$ mutants did have a lower avoidance percentage but not significantly so (Figure 14 and Table 4).

Since there are multiple experiments showing that *dTrpA1*$^{ins}$ mutants exhibit significant defects in adult thermal nociception, *dTrpA1*$^{ins}$ mutants were tested again as a positive control (Figure 15 and Table 6). In this second experiment, Cas9 KO of *dTrpA1* was also tested to see if the same phenomenon seen in Cas9-only larvae expressing *UAS-Cas9* continued in adult thermal nociception. Perhaps unsurprisingly, given the evidence that *UAS-Cas9* expression results in severe defects in dendrite morphology (Figure 15), Cas9 KO of *dTrpA1* did not lead to a significant decrease in adult avoidance when compared the Cas9-only and sgRNA-only controls (Figure 15 and Table 6).

This experiment also showed that *dTrpA1*$^{ins}$ mutants had a very severe, significant decrease in avoidance rate compared to the Cas9-only and sgRNA-only controls (Figure 15 and Table 6). Thus, the water bath assay can be used in future experiments to gauge the effect of RNAi knockdown on adult thermal nociception with *dTrpA1*$^{ins}$ and *painless* mutants serving as positive controls. It is likely that the initial experiment that used *dTrpA1*$^{ins}$ mutants as a positive control did not produce clear results as the exact protocol was still being calibrated at the time. The adult flies used in this experiment were allowed to rest for 15 minutes after being anesthetized on ice for 5 minutes, though this recovery time was later increased to 30 minutes. This experiment successfully replicated the significantly decreased avoidance percentage of *dTrpA1*$^{ins}$ mutants when compared to two controls, which was shown in the original study using this methodology (Table 6) (Neely et al., 2011). Therefore, the use of *dTrpA1*$^{ins}$ mutants as a positive control for adult thermal nociception experiments

has been validated, and it is likely that the increase in recover time accounts for this discrepancy.

**Knockdown of Para in ppk+ Neurons Does Not Impact Adult Thermal Nociception**

The Paralytic (Para) sodium voltage-gated ion channel is necessary for the initiation and propagation of action potentials in *Drosophila* neurons (Siddiqi & Benzer, 1976; Wu & Ganetzky, 1980). RNAi knockdown of *para* has long been used as a positive control for larval thermal nociception assays (Zhong et al., 2010). Therefore, its role in adult thermal nociception was investigated. Surprisingly, RNAi knockdown of *para* in adult neurons expressing *pickpocket* (*ppk*+ neurons) resulted in a high avoidance percentage. When compared to the GAL4-only control, the difference in avoidance was insignificant and a similar comparison was true with the UAS-only control (Figure 16 and Table 6). As expected, the *painless* mutant had a low avoidance percentage as in the original validation experiment (Figure 14 and Table 6).

This is certainly a perplexing result, as an adult sensitization experiment which used an alternative method to completely block synaptic activity of *ppk*+ neurons via tetanus toxin, showed that sensitization to thermal stimuli was dependent on synaptic output from *ppk*+ neurons (Khuong et al., 2019). Though these are certainly separate states (basal vs. sensitized), it was not unwise to have predicted that *para*-RNAi KD would result in a significant decrease in avoidance behavior given the important role that *ppk*+ neurons play in adult sensitization and the consistent defective phenotype seen in larvae in mechanical and thermal nociception assays (Dyson, 2017; Khuong et al., 2019; McGuirt, 2019; Zhong et al., 2010). The lack of an observed defect in avoidance behavior after *para*-RNAi KD suggests

that adult *ppk*+ neurons either do not use Para in the same way they do in the larval stage, or that other ion channels like *dTrpA1* or *painless* have a stronger effect. Additionally, given its role in regulating injury-induced sensitization, it is possible that adult *ppk*+ neurons instead play a regulatory role in nociception rather than one that is strictly involved in the transduction of noxious sensory information.

An important consideration that must be made is that the *painless* and $dTrpA1^{ins}$ mutant genotypes result in loss of function of the corresponding protein in the entire organism. It is certainly possible that other structures in adult *Drosophila* regulate avoidance behavior to noxious heat, as investigations into the anatomical structures involved in thermal nociception are ongoing (Lin et al., 2022). Indeed, the original study that developed this technique found that removal of both antennae and the probiscis (feeding organ) resulted in a significant decrease in avoidance percentage (Neely et al., 2010). Therefore, it is possible that *dTrpA1* expression in these organs are what contribute to the detection and avoidance of noxious thermal stimuli.

Tangentially related, a study of ring neurons within the central complex of the adult *Drosophila* brain revealed incredibly intricate circuitry that gates thermoresponsive behavior and motor output as a response to increases in ambient temperature from a range of 25-31°C (Buhl et al., 2021). This finding may suggest that the circuitry involved in adult thermal nociception could be more complex than expected. Although some brain structures, such as the fan-shaped body within the central complex, have been identified to play some role in acute nociception, no study has explicitly implicated *ppk*+ sensory neurons (Hu et al., 2018; Khuong et al., 2019; Neely et al., 2010, 2011; Xu et al., 2006). Therefore, more anatomical studies that parse through specific sensory neuron subtypes using adult thermal nociception

assays are needed. Additionally, it is possible that these adult thermal assays are inadvertently involving other thermosensory organs in the adult fly. This would be remedied with the development of other protocols to measure the responsiveness of adult *Drosophila* to noxious temperatures.

Although the role of eIF2α, SC35, and LaRP4B in adult thermal nociception was not investigated due to time constraints, the foundation is set for future experiments validating the role of these, and other previously identified, RBPs using this additional experimental paradigm.

**Conclusions**

The data presented here show that RBP and post-transcriptional regulation of gene expression plays a strong role in nociception. This was shown through the significantly increased latencies of larvae that had eIF2α, a translation initiation factor, SC35, an alternative splicing regulator, and LaRP4B, a translation stimulator and mRNA stabilizer, knocked down via RNAi (Table 3). Though much optimization has been done to make CRISPR gene editing in *Drosophila* a reality, the results from multiple experiments here show that there is still more progress to be made, or that an approach that is different from the standard GAL4/UAS system is needed (Tables 4 and 5 and Figure 13). Additionally, adult thermal nociception may be more complex than anticipated and further experiments are needed to identify the role that *ppk*+ neurons play in adults (Figure 16). Ultimately, the *Drosophila* model system is one with seemingly infinite directions as research into the mechanisms of nociception and nociceptor plasticity progresses.

## References


Ainsley, J. A., Pettus, J. M., Bosenko, D., Gerstein, C. E., Zinkevich, N., Anderson, M. G., Adams, C. M., Welsh, M. J., & Johnson, W. A. (2003). Enhanced Locomotion Caused by Loss of the Drosophila DEG/ENaC Protein Pickpocket1. *Current Biology*, *13*(17), 1557–1563. https://doi.org/10.1016/s0960-9822(03)00596-7

Alfano, C., Sanfelice, D., Babon, J., Kelly, G., Jacks, A., Curry, S., & Conte, M. R. (2004). Structural analysis of cooperative RNA binding by the La motif and central RRM domain of human La protein. *Nat Struct Mol Biol*, *11*(4), 323-329. https://doi.org/10.1038/nsmb747

Andreassi, C., Crerar, H., & Riccio, A. (2018). Post-transcriptional Processing of mRNA in Neurons: The Vestiges of the RNA World Drive Transcriptome Diversity. *Front Mol Neurosci*, *11*, 304. https://doi.org/10.3389/fnmol.2018.00304

Babcock, D. T., Shi, S., Jo, J., Shaw, M., Gutstein, H. B., & Galko, M. J. (2011). Hedgehog signaling regulates nociceptive sensitization. *Curr Biol, 21*(18), 1525–1533. https://doi.org/10.1016/j.cub.2011.08.020

Babcock, D. T., Landry, C., & Galko, M. J. (2009). Cytokine signaling mediates UV-induced nociceptive sensitization in Drosophila larvae. *Curr Biol*, *19*(10), 799-806. https://doi.org/10.1016/j.cub.2009.03.062

Barreau, C., Paillard, L., & Osborne, H. B. (2005). AU-rich elements and associated factors: are there unifying principles? *Nucleic Acids Res*, *33*(22), 7138-7150. https://doi.org/10.1093/nar/gki1012

Bellato, H. M., & Hajj, G. N. (2016). Translational control by eIF2α in neurons: Beyond the stress response. *Cytoskeleton (Hoboken)*, *73*(10), 551-565. https://doi.org/10.1002/cm.21294

Bolognani, F., & Perrone-Bizzozero, N. I. (2008). RNA–protein interactions and control of mRNA stability in neurons. *Journal of Neuroscience Research*, *86*(3), 481-489. https://doi.org/10.1002/jnr.21473

Boone, M., Wang, L., Lawrence, R. E., Frost, A., Walter, P., & Schoof, M. (2022). A point mutation in the nucleotide exchange factor eIF2B constitutively activates the integrated stress response by allosteric modulation. *Elife*, *11*. https://doi.org/10.7554/eLife.76171

Brand, A. H., & Perrimon, N. (1993). Targeted gene expression as a means of altering cell fates and generating dominant phenotypes. *Development*, *118*(2), 401-415. https://doi.org/10.1242/dev.118.2.401

Breese, N. M., George, A. C., Pauers, L. E., & Stucky, C. L. (2005). Peripheral inflammation selectively increases TRPV1 function in IB4-positive sensory neurons from adult mouse. *Pain*, *115*(1-2), 37-49. https://doi.org/10.1016/j.pain.2005.02.010

Brewster, R., & Bodmer, R. (1995). Origin and specification of type II sensory neurons in Drosophila. *Development , 121*(9), 2923–2936. https://doi.org/10.1242/dev.121.9.2923

Buhl, E., Kottler, B., Hodge, J. J. L., & Hirth, F. (2021). Thermoresponsive motor behavior is mediated by ring neuron circuits in the central complex of Drosophila. *Scientific Reports*, *11*(1). https://doi.org/10.1038/s41598-020-80103-9

Burtis, K. C., & Baker, B. S. (1989). Drosophila doublesex gene controls somatic sexual differentiation by producing alternatively spliced mRNAs encoding related sex-specific polypeptides. *Cell*, *56*(6), 997-1010. https://doi.org/10.1016/0092-8674(89)90633-8

Caterina, M. J., Schumacher, M. A., Tominaga, M., Rosen, T. A., Levine, J. D., & Julius, D. (1997). The capsaicin receptor: a heat-activated ion channel in the pain pathway. *Nature*, *389*(6653), 816-824. https://doi.org/10.1038/39807

Cho, S., Choe, D., Lee, E., Kim, S. C., Palsson, B., & Cho, B. K. (2018). High-Level dCas9 Expression Induces Abnormal Cell Morphology in Escherichia coli. *ACS Synth Biol*, *7*(4), 1085-1094. https://doi.org/10.1021/acssynbio.7b00462

Collins, R. T., & Cohen, S. M. (2005). A Genetic Screen in Drosophila for Identifying Novel Components of the Hedgehog Signaling Pathway. *Genetics*, *170*(1), 173-184. https://doi.org/10.1534/genetics.104.039420

Dahlhamer, J., Lucas, J., Zelaya, C., Nahin, R., Mackey, S., DeBar, L., Kerns, R., Von Korff M., Porter, L., & Helmick, C. (2018). Prevalence of Chronic Pain and High-Impact Chronic Pain Among Adults - United States, 2016. *MMWR Morb Mortal Wkly Rep*, *67*(36), 1001-1006. https://doi.org/10.15585/mmwr.mm6736a2

Drissi, I., Woods, W. A., & Woods, C. G. (2020). Understanding the genetic basis of congenital insensitivity to pain. *Br Med Bull*, *133*(1), 65-78. https://doi.org/10.1093/bmb/ldaa003

Dubin, A. E., & Patapoutian, A. (2010). Nociceptors: the sensors of the pain pathway. *J Clin Invest*, *120*(11), 3760-3772. https://doi.org/10.1172/JCI42843

Dyson, A. (2017). *RNA-Processing Genes Control Sensory Neuron Function In Drosophila Melanogaster* [Master's thesis, Appalachian State University].

Fernández-Moreno, M. A., Farr, C. L., Kaguni, L. S., & Garesse, R. (2007). Drosophila melanogaster as a Model System to Study Mitochondrial Biology. In *Methods in Molecular Biology* (pp. 33-49). Humana Press. https://doi.org/10.1007/978-1-59745-365-3_3

Ferreira, J. P., Overton, K. W., & Wang, C. L. (2013). Tuning gene expression with synthetic upstream open reading frames. *Proceedings of the National Academy of Sciences*, *110*(28), 11284-11289. https://doi.org/10.1073/pnas.1305590110

Follansbee, T. L., Gjelsvik, K. J., Brann, C. L., Mcparland, A. L., Longhurst, C. A., Galko, M. J., & Ganter, G. K. (2017). Drosophila Nociceptive Sensitization Requires BMP Signaling via the Canonical SMAD Pathway. *The Journal of Neuroscience*, *37*(35), 8524-8533. https://doi.org/10.1523/jneurosci.3458-16.2017

Fu, X.-D. (1993). Specific commitment of different pre-mRNAs to splicing by single SR proteins. *Nature*, *365*(6441), 82-85. https://doi.org/10.1038/365082a0

Galloway, A., & Cowling, V. H. (2019). mRNA cap regulation in mammalian cell function and fate. *Biochim Biophys Acta Gene Regul Mech*, *1862*(3), 270-279. https://doi.org/10.1016/j.bbagrm.2018.09.011

Gasiunas, G., Barrangou, R., Horvath, P., & Siksnys, V. (2012). Cas9–crRNA ribonucleoprotein complex mediates specific DNA cleavage for adaptive immunity in bacteria. *Proceedings of the National Academy of Sciences*, *109*(39), E2579-E2586. https://doi.org/10.1073/pnas.1208507109

Gaskin, D. J., & Richard, P. (2012). The economic costs of pain in the United States. *J Pain*, *13*(8), 715-724. https://doi.org/10.1016/j.jpain.2012.03.009

Gjelsvik, K. J., Follansbee, T. L., & Ganter, G. K. (2018). Bone Morphogenetic Protein Glass Bottom Boat (BMP5/6/7/8) and its receptor Wishful Thinking (BMPRII) are required for injury-induced allodynia inDrosophila. *Molecular Pain*, *14*, 174480691880270. https://doi.org/10.1177/1744806918802703

Grueber, W. B., Jan, L. Y., & Jan, Y. N. (2002). Tiling of the Drosophila epidermis by multidendritic sensory neurons. *Development*, *129*(12), 2867-2878. https://doi.org/10.1242/dev.129.12.2867

Gu, P., Gong, J., Shang, Y., Wang, F., Ruppell, K. T., Ma, Z., Sheehan, A. E., Freeman M. R., & Xiang, Y. (2019). Polymodal Nociception in Drosophila Requires Alternative Splicing of TrpA1. *Current Biology*, *29*(23), 3961-3973.e3966. https://doi.org/10.1016/j.cub.2019.09.070

Hachet, O., & Ephrussi, A. (2004). Splicing of oskar RNA in the nucleus is coupled to its cytoplasmic localization. *Nature*, *428*(6986), 959-963. https://doi.org/10.1038/nature02521

Hargrove, J. L., & Schmidt, F. H. (1989). The role of mRNA and protein stability in gene expression. *FASEB J*, *3*(12), 2360-2370. https://doi.org/10.1096/fasebj.3.12.2676679

Heber, S., Gold-Binder, M., Ciotu, C. I., Witek, M., Ninidze, N., Kress, H.G., & Fischer, M. J. M. (2019). A Human TRPA1-Specific Pain Model. *The Journal of Neuroscience*, *39*(20), 3845-3855. https://doi.org/10.1523/jneurosci.3048-18.2019

Heigwer, F., Port, F., & Boutros, M. (2018). RNA Interference (RNAi) Screening in Drosophila. *Genetics*, *208*(3), 853-874. https://doi.org/10.1534/genetics.117.300077

Hinnebusch, A. G., & Lorsch, J. R. (2012). The Mechanism of Eukaryotic Translation Initiation: New Insights and Challenges. *Cold Spring Harbor Perspectives in Biology*, *4*(10), a011544-a011544. https://doi.org/10.1101/cshperspect.a011544

Ho, J., Tumkaya, T., Aryal, S., Choi, H., & Claridge-Chang, A. (2019). Moving beyond P values: data analysis with estimation graphics. *Nat Methods*, *16*(7), 565-566. https://doi.org/10.1038/s41592-019-0470-3

Hou, W. Y., Shyu, B. C., Chen, T. M., Shieh, J. Y., & Sun, W. Z. (1997). Protein synthesis inhibitor cycloheximide dose-dependently decreases formalin-induced c-Fos protein and behavioral hyperalgesia in rats. *Neurosci Lett*, *227*(2), 99-102. https://doi.org/10.1016/s0304-3940(97)00321-2

Hu, W., Peng, Y., Sun, J., Zhang, F., Zhang, X., Wang, L., Li, Q., & Zhong, Y. (2018). Fan-Shaped Body Neurons in the Drosophila Brain Regulate Both Innate and Conditioned Nociceptive Avoidance. *Cell Reports*, *24*(6), 1573-1584. https://doi.org/10.1016/j.celrep.2018.07.028

Hwang, R. Y., Zhong, L., Xu, Y., Johnson, T., Zhang, F., Deisseroth, K., & Tracey, W. D. (2007). Nociceptive Neurons Protect Drosophila Larvae from Parasitoid Wasps. *Curr Biol*, *17*(24), 2105-2116. https://doi.org/10.1016/j.cub.2007.11.029

Im, S. H., & Galko, M. J. (2012). Pokes, sunburn, and hot sauce: Drosophila as an emerging model for the biology of nociception. *Developmental Dynamics*, *241*(1), 16-26. https://doi.org/10.1002/dvdy.22737

Im, S. H., Takle, K., Jo, J., Babcock, D. T., Ma, Z., Xiang, Y., & Galko, M. J. (2015). Tachykinin acts upstream of autocrine Hedgehog signaling during nociceptive sensitization in Drosophila. *eLife*, *4*. https://doi.org/10.7554/elife.10735

Jo, J., Im, S. H., Babcock, D. T., Iyer, S. C., Gunawan, F., Cox, D. N., & Galko, M. J. (2017). Drosophila caspase activity is required independently of apoptosis to produce active TNF/Eiger during nociceptive sensitization. *Cell Death & Disease*, *8*(5), e2786-e2786. https://doi.org/10.1038/cddis.2016.474

Johnson, R. L., Grenier, J. K., & Scott, M. P. (1995). patched overexpression alters wing disc size and pattern: transcriptional and post-transcriptional effects on hedgehog targets. *Development*, *121*(12), 4161-4170. https://doi.org/10.1242/dev.121.12.4161

Jordt, S. E., Bautista, D. M., Chuang, H. H., McKemy, D. D., Zygmunt, P. M., Högestätt, E. D., Meng, I. D., & Julius, D. (2004). Mustard oils and cannabinoids excite sensory nerve fibres through the TRP channel ANKTM1. *Nature*, *427*(6971), 260-265. https://doi.org/10.1038/nature02282

Kashiwagi, K., Ito, T., & Yokoyama, S. (2017). Crystal structure of eIF2B and insights into eIF2–eIF2B interactions. *The FEBS Journal*, *284*(6), 868-874. https://doi.org/10.1111/febs.13896

Katsumoto, A., Takeuchi, H., & Tanaka, F. (2019). Tau Pathology in Chronic Traumatic Encephalopathy and Alzheimer's Disease: Similarities and Differences. *Front Neurol*, *10*, 980. https://doi.org/10.3389/fneur.2019.00980

Kawai, K., Kawai, A. T., Wollan, P., & Yawn, B. P. (2017). Adverse impacts of chronic pain on health-related quality of life, work productivity, depression and anxiety in a community-based study. *Fam Pract*, *34*(6), 656-661. https://doi.org/10.1093/fampra/cmx034

Khoutorsky, A., Sorge, R. E., Prager-Khoutorsky, M., Pawlowski, S. A., Longo, G., Jafarnejad, S. M., Tahmasebi, S., Martin, L. J., Pitcher, M. H., Gkogkas, C. G.,

Sharif-Naeini, R., Ribeiro-da-Silva, A., Bourque, C. W., Cervero, F., Mogil, J. S., & Sonenberg, N. (2016). eIF2α phosphorylation controls thermal nociception. *Proc Natl Acad Sci U S A*, *113*(42), 11949-11954. https://doi.org/10.1073/pnas.1614047113

Khuong, T. M., Wang, Q.-P., Manion, J., Oyston, L. J., Lau, M.-T., Towler, H., Lin, Y. Q., & Neely, G. G. (2019). Nerve injury drives a heightened state of vigilance and neuropathic sensitization in Drosophila. *Science Advances*, *5*(7), eaaw4099. https://doi.org/10.1126/sciadv.aaw4099

Kim, S. E., Coste, B., Chadha, A., Cook, B., & Patapoutian, A. (2012). The role of Drosophila Piezo in mechanical nociception. *Nature*, *483*(7388), 209-212. https://doi.org/10.1038/nature10801

Koltzenburg, M., Stucky, C. L., & Lewin, G. R. (1997). Receptive properties of mouse sensory neurons innervating hairy skin. *J Neurophysiol*, *78*(4), 1841-1850. https://doi.org/10.1152/jn.1997.78.4.1841

Koreman, G. T., Xu, Y., Hu, Q., Zhang, Z., Allen, S. E., Wolfner, M. F., Wang, B., & Han, C. (2021). Upgraded CRISPR/Cas9 tools for tissue-specific mutagenesis in Drosophila. *Proceedings of the National Academy of Sciences*, *118*(14), e2014255118. https://doi.org/10.1073/pnas.2014255118

Krishnamoorthy, T., Pavitt, G. D., Zhang, F., Dever, T. E., & Hinnebusch, A. G. (2001). Tight Binding of the Phosphorylated α Subunit of Initiation Factor 2 (eIF2α) to the Regulatory Subunits of Guanine Nucleotide Exchange Factor eIF2B Is Required for Inhibition of Translation Initiation. *Molecular and Cellular Biology*, *21*(15), 5018-5030. https://doi.org/10.1128/mcb.21.15.5018-5030.2001

Kuhfittig-Kulle, S., Feldmann, E., Odersky, A., Kuliczkowska, A., Goedecke, W., Eggert, A., & Pfeiffer, P. (2007). The mutagenic potential of non-homologous end joining in the absence of the NHEJ core factors Ku70/80, DNA-PKcs and XRCC4-LigIV. *Mutagenesis*, *22*(3), 217-233. https://doi.org/10.1093/mutage/gem007

Küspert, M., Murakawa, Y., Schäffler, K., Vanselow, J. T., Wolf, E., Juranek, S., Schlosser, A., Landthaler, M., & Fischer, U. (2015). LARP4B is an AU-rich sequence associated factor that promotes mRNA accumulation and translation. *RNA*, *21*(7), 1294-1305. https://doi.org/10.1261/rna.051441.115

Liao, C., & Beisel, C. L. (2021). The tracrRNA in CRISPR Biology and Technologies. *Annu Rev Genet*, *55*, 161-181. https://doi.org/10.1146/annurev-genet-071719-022559

Lin, S., Coutinho-Mansfield, G., Wang, D., Pandit, S., & Fu, X. D. (2008). The splicing factor SC35 has an active role in transcriptional elongation. *Nature Structural & Molecular Biology*, *15*(8), 819-826. https://doi.org/10.1038/nsmb.1461

Lin, W. Y., Liu, C. H., Cheng, J., & Liu, H. P. (2022). Alterations of RNA-binding protein. *Front Mol Neurosci*, *15*, 1006455. https://doi.org/10.3389/fnmol.2022.1006455

Liu, F., & Gong, C.-X. (2008). Tau exon 10 alternative splicing and tauopathies. *Molecular Neurodegeneration*, *3*(1), 8. https://doi.org/10.1186/1750-1326-3-8

Maraia, R. J., & Intine, R. V. A. (2001). Recognition of Nascent RNA by the Human La Antigen: Conserved and Divergent Features of Structure and Function. *Molecular and Cellular Biology*, *21*(2), 367-379. https://doi.org/10.1128/mcb.21.2.367-379.2001

McGuirt, H. (2019). The Role of Translation Initiation Regulating Kinases, Lk6 and Tor, on Nociceptor Development and Function in *Drosophila Melanogaster* [Master's thesis, Appalachian State University].

Meijer, H. A., & Thomas, A. A. M. (2002). Control of eukaryotic protein synthesis by upstream open reading frames in the 5'-untranslated region of an mRNA. *Biochemical Journal*, *367*(1), 1-11. https://doi.org/10.1042/bj20011706

Meijering, E., Jacob, M., Sarria, J.-C. F., Steiner, P., Hirling, H., & Unser, M. (2004). Design and validation of a tool for neurite tracing and analysis in fluorescence microscopy images. *Cytometry*, *58A*(2), 167-176. https://doi.org/10.1002/cyto.a.20022

Meltzer, H., Marom, E., Alyagor, I., Mayseless, O., Berkun, V., Segal-Gilboa, N., Unger, T., Luginbuhl, D., & Schuldiner, O. (2019). Tissue-specific (ts)CRISPR as an efficient strategy for in vivo screening in Drosophila. *Nat Commun*, *10*(1), 2113. https://doi.org/10.1038/s41467-019-10140-0

Meshorer, E., Bryk, B., Toiber, D., Cohen, J., Podoly, E., Dori, A., & Soreq, H. (2005). SC35 promotes sustainable stress-induced alternative splicing of neuronal acetylcholinesterase mRNA. *Mol Psychiatry*, *10*(11), 985-997. https://doi.org/10.1038/sj.mp.4001735

Moy, J. K., Khoutorsky, A., Asiedu, M. N., Black, B. J., Kuhn, J. L., Barragán-Iglesias, P., Megat, S., Burton, M. D., Burgos-Vega, C. C., Melemedjian, O. K.,Boitano, S., Vagner, J., Gkogkas, C. G., Pancrazio, J. J., Mogil, J. S., Dussor, G., Sonenberg, N., & Price, T. J. (2017). The MNK–eIF4E Signaling Axis Contributes to Injury-Induced Nociceptive Plasticity and the Development of Chronic Pain. *The Journal of Neuroscience*, *37*(31), 7481-7499. https://doi.org/10.1523/jneurosci.0220-17.2017

Moy, J. K., Khoutorsky, A., Asiedu, M. N., Dussor, G., & Price, T. J. (2018). eIF4E Phosphorylation Influences BDNF mRNA Translation in Mouse Dorsal Root

Ganglion Neurons. *Front Cell Neurosci*, *12*, 29. https://doi.org/10.3389/fncel.2018.00029

Neely, G. G., Hess, A., Costigan, M., Keene, A. C., Goulas, S., Langeslag, M., Griffin, R. S., Belfer, I., Dai, F., Smith, S. B., Diatchenko, L., Gupta, V., Xia, C-P., Amann, S., Kreitz, S., Heindl-Erdmann, C., Wolz, S., Ly, C. V., Arora, S., … Penninger, J. M. (2010). A Genome-wide Drosophila Screen for Heat Nociception Identifies α2δ3 as an Evolutionarily Conserved Pain Gene. *Cell*, *143*(4), 628-638. https://doi.org/10.1016/j.cell.2010.09.047

Neely, G. G., Keene, A. C., Duchek, P., Chang, E. C., Wang, Q.-P., Aksoy, Y. A., Rosenzweig, M., Costigan, M., Woolf, C. J., Garrity, P. A., & Penninger, J. M. (2011). TrpA1 Regulates Thermal Nociception in Drosophila. *PLoS ONE*, *6*(8), e24343. https://doi.org/10.1371/journal.pone.0024343

Oh, J.-Y., Kwon, A., Jo, A., Kim, H., Goo, Y.-S., Lee, J.-A., & Kim, H. K. (2013). Activity-dependent synaptic localization of processing bodies and their role in dendritic structural plasticity. *Journal of Cell Science*, *126*(9), 2114-2123. https://doi.org/10.1242/jcs.125690

Padgett, R. W., Wozney, J. M., & Gelbart, W. M. (1993). Human BMP sequences can confer normal dorsal-ventral patterning in the Drosophila embryo. *Proceedings of the National Academy of Sciences*, *90*(7), 2905-2909. https://doi.org/10.1073/pnas.90.7.2905

Pandit, S., Zhou, Y., Shiue, L., Coutinho-Mansfield, G., Li, H., Qiu, J., Huang, J., Yeo, W. G., Ares, M., & Fu, X.-D. (2013). Genome-wide Analysis Reveals SR Protein

Cooperation and Competition in Regulated Splicing. *Molecular Cell*, *50*(2), 223-235. https://doi.org/10.1016/j.molcel.2013.03.001

Petrus, M., Peier, A. M., Bandell, M., Hwang, S. W., Huynh, T., Olney, N., Jegla, T., & Patapoutian, A. (2007). A role of TRPA1 in mechanical hyperalgesia is revealed by pharmacological inhibition. *Mol Pain*, *3*, 40. https://doi.org/10.1186/1744-8069-3-40

Phelps, C. B., & Brand, A. H. (1998). Ectopic Gene Expression in Drosophila Using GAL4 System. *Methods*, *14*(4), 367-379. https://doi.org/10.1006/meth.1998.0592

Poe, A. R., Wang, B., Sapar, M. L., Ji, H., Li, K., Onabajo, T., Fazliyeva, R., Gibbs, M., Qiu, Y., Hu, Y., & Han, C. (2019). Robust CRISPR/Cas9-Mediated Tissue-Specific Mutagenesis Reveals Gene Redundancy and Perdurance in Drosophila. *Genetics*, *211*(2), 459-472. https://doi.org/10.1534/genetics.118.301736

Port, F., & Bullock, S. L. (2016). Augmenting CRISPR applications in Drosophila with tRNA-flanked sgRNAs. *Nature Methods*, *13*(10), 852-854. https://doi.org/10.1038/nmeth.3972

Port, F., Chen, H.-M., Lee, T., & Bullock, S. L. (2014). Optimized CRISPR/Cas tools for efficient germline and somatic genome engineering in Drosophila. *Proceedings of the National Academy of Sciences*, *111*(29), E2967-E2976. https://doi.org/10.1073/pnas.1405500111

Port, F., Strein, C., Stricker, M., Rauscher, B., Heigwer, F., Zhou, J., Beyersdörffer, C., Frei, J., Hess, A., Kern, K., Lange, L., Langner, N., Malamud, R., Pavlović, B., Rädecke, K., Schmitt, L., Voos, L., Valentini, E., & Boutros, M. (2020). A large-scale resource for tissue-specific CRISPR mutagenesis in Drosophila. *eLife*, *9*. https://doi.org/10.7554/elife.53865

Qian, W., Liang, H., Shi, J., Jin, N., Grundke-Iqbal, I., Iqbal, K., Gong, C. X., & Liu, F. (2011). Regulation of the alternative splicing of tau exon 10 by SC35 and Dyrk1A. *Nucleic Acids Res*, *39*(14), 6161-6171. https://doi.org/10.1093/nar/gkr195

Robertson, J. L., Tsubouchi, A., & Tracey, W. D. (2013). Larval Defense against Attack from Parasitoid Wasps Requires Nociceptive Neurons. *PLoS ONE*, *8*(10), e78704. https://doi.org/10.1371/journal.pone.0078704

Roper, S. D., & Chaudhari, N. (2017). Taste buds: cells, signals and synapses. *Nat Rev Neurosci*, *18*(8), 485-497. https://doi.org/10.1038/nrn.2017.68

Saito, S., & Tominaga, M. (2017). Evolutionary tuning of TRPA1 and TRPV1 thermal and chemical sensitivity in vertebrates. *Temperature*, *4*(2), 141-152. https://doi.org/10.1080/23328940.2017.1315478

Schmidt, M., Dubin, A. E., Petrus, M. J., Earley, T. J., & Patapoutian, A. (2009). Nociceptive Signals Induce Trafficking of TRPA1 to the Plasma Membrane. *Neuron*, *64*(4), 498-509. https://doi.org/10.1016/j.neuron.2009.09.030

Schäffler, K., Schulz, K., Hirmer, A., Wiesner, J., Grimm, M., Sickmann, A., & Fischer, U. (2010). A stimulatory role for the La-related protein 4B in translation. *RNA*, *16*(8), 1488-1499. https://doi.org/10.1261/rna.2146910

Scully, R., Panday, A., Elango, R., & Willis, N. A. (2019). DNA double-strand break repair-pathway choice in somatic mammalian cells. *Nature Reviews Molecular Cell Biology*, *20*(11), 698-714. https://doi.org/10.1038/s41580-019-0152-0

Shatsky, I. N., Terenin, I. M., Smirnova, V. V., & Andreev, D. E. (2018). Cap-Independent Translation: What's in a Name? *Trends Biochem Sci*, *43*(11), 882-895. https://doi.org/10.1016/j.tibs.2018.04.011

Siddiqi, O., & Benzer, S. (1976). Neurophysiological defects in temperature-sensitive paralytic mutants of Drosophila melanogaster. *Proc Natl Acad Sci U S A*, *73*(9), 3253-3257. https://doi.org/10.1073/pnas.73.9.3253

Soreq, H., & Seidman, S. (2001). Acetylcholinesterase – new roles for an old actor. *Nat Rev Neurosci*, *2*(4), 294-302. https://doi.org/10.1038/35067589

Sternfeld, M., Shoham, S., Klein, O., Flores-Flores, C., Evron, T., Idelson, G. H., Kitsberg, D., Patrick, J. W., & Soreq, H. (2000). Excess "read-through" acetylcholinesterase attenuates but the "synaptic" variant intensifies neurodeterioration correlates. *Proceedings of the National Academy of Sciences*, *97*(15), 8647-8652. https://doi.org/10.1073/pnas.140004597

Steward, O. (1983). Polyribosomes at the base of dendritic spines of central nervous system neurons--their possible role in synapse construction and modification. *Cold Spring Harb Symp Quant Biol*, *48 Pt 2*, 745-759. https://doi.org/10.1101/sqb.1983.048.01.077

Steward, O., & Levy, W. (1982). Preferential localization of polyribosomes under the base of dendritic spines in granule cells of the dentate gyrus. *The Journal of Neuroscience*, *2*(3), 284-291. https://doi.org/10.1523/jneurosci.02-03-00284.1982

Story, G. M., Peier, A. M., Reeve, A. J., Eid, S. R., Mosbacher, J., Hricik, T. R., Earley, T. J., Hergarden, A. C., Andersson, D. A., Hwang, S. W., Mcintyre, P., Jegla, T., Bevan, S., & Patapoutian, A. (2003). ANKTM1, a TRP-like Channel Expressed in Nociceptive Neurons, Is Activated by Cold Temperatures. *Cell*, *112*(6), 819–829. https://doi.org/10.1016/s0092-8674(03)00158-2

Tacke, R., & Manley, J. L. (1999). Determinants of SR protein specificity. *Curr Opin Cell Biol*, *11*(3), 358-362. https://doi.org/10.1016/S0955-0674(99)80050-7

Tracey, W. D., Wilson, R. I., Laurent, G., & Benzer, S. (2003). painless, a Drosophila gene essential for nociception. *Cell*, *113*(2), 261-273. https://doi.org/10.1016/s0092-8674(03)00272-1

Ugur, B., Chen, K., & Bellen, H. J. (2016). Drosophila tools and assays for the study of human diseases. *Disease Models & Mechanisms*, *9*(3), 235-244. https://doi.org/10.1242/dmm.023762

Vashee, S., & Kodadek, T. (1995). The activation domain of GAL4 protein mediates cooperative promoter binding with general transcription factors in vivo. *Proceedings of the National Academy of Sciences*, *92*(23), 10683-10687. https://doi.org/10.1073/pnas.92.23.10683

Wang, H., La Russa, M., & Qi, L. S. (2016). CRISPR/Cas9 in Genome Editing and Beyond. *Annu Rev Biochem*, *85*, 227-264. https://doi.org/10.1146/annurev-biochem-060815-014607

Wang, Y., Liu, J., Huang, B., Xu, Y.-M., Li, J., Huang, L.-F., Lin, J., Zhang, J., Min, Q.-H., Yang, W.-M., & Wang, X.-Z. (2015). Mechanism of alternative splicing and its regulation. *Biomedical Reports*, *3*(2), 152-158. https://doi.org/10.3892/br.2014.407

Webster, J. D., & Vucic, D. (2020). The Balance of TNF Mediated Pathways Regulates Inflammatory Cell Death Signaling in Healthy and Diseased Tissues. *Front Cell Dev Biol*, *8*, 365. https://doi.org/10.3389/fcell.2020.00365

Williams, D. D., Pavitt, G. D., & Proud, C. G. (2001). Characterization of the Initiation Factor eIF2B and Its Regulation in Drosophila melanogaster. *Journal of Biological Chemistry*, *276*(6), 3733-3742. https://doi.org/10.1074/jbc.m008041200

Wu, C.-F., & Ganetzky, B. (1980). Genetic alteration of nerve membrane excitability in temperature-sensitive paralytic mutants of Drosophila melanogaster. *Nature*, *286*(5775), 814-816. https://doi.org/10.1038/286814a0

Xu, S. Y., Cang, C. L., Liu, X. F., Peng, Y. Q., Ye, Y. Z., Zhao, Z. Q., & Guo, A. K. (2006). Thermal nociception in adult Drosophila: behavioral characterization and the role of the painless gene. *Genes, Brain and Behavior*, *5*(8), 602-613. https://doi.org/10.1111/j.1601-183x.2006.00213.x

Zhong, L., Bellemer, A., Yan, H., Ken, H., Jessica, R., Hwang, R. Y., Pitt, G. S., & Tracey, W. D. (2012). Thermosensory and nonthermosensory isoforms of Drosophila melanogaster TRPA1 reveal heat-sensor domains of a thermoTRP Channel. *Cell Rep*, *1*(1), 43-55. https://doi.org/10.1016/j.celrep.2011.11.002

Zhong, L., Hwang, R. Y., & Tracey, W. D. (2010). Pickpocket is a DEG/ENaC protein required for mechanical nociception in Drosophila larvae. *Curr Biol*, *20*(5), 429-434. https://doi.org/10.1016/j.cub.2009.12.057

## Appendix: Cas9 KO of eIF2Bα Results

### eIF2Bα – Thermal Hypersensitization

The purpose of this experiment was to determine if Cas9-mediated knockout of *eIF2Bα* in larvae would produce expected results in a hypersensitive thermal nociception context, as previously seen in the Dyson thesis (Dyson, 2017). It is expected that Cas9-mediated KO of *eIF2Bα* will result in a significantly *decreased* response latency compared to the Cas9 and sgRNA-only controls. To do this, the *ppk-GAL4;UAS-Cas9* line was crossed to the *U6-eIF2Bα.gRNA* line to induce nociceptor-specific knockout of *eIF2Bα*. The Cas9-only, sgRNA-only, *para* RNAi controls and the experimental group were all set up similar to the *ppk* KO experiment (Figure 7), except the sgRNA line used in this experiment targets *eIF2Bα*.

The average latency for each group was as follows: Cas9-only – 9.399s, sgRNA-only – 9.801s, *eIF2Bα* KO – 8.327s, *para* RNAi – 10.875s. The p-value of the difference between the Cas9 and sgRNA-only control groups was 0.462 with a Cliff's Δ of 0.0472. The range of the Cliff's Δ 95% CI was -0.0794, 0.177. The p-value of the difference between the *eIF2Bα* KO and Cas9-only groups was 0.0058 with a Cliff's Δ of -0.201. The range of the Cliff's Δ 95% CI was -0.339, -0.0595. The p-value of the difference between the *eIF2Bα* KO and sgRNA-only groups was 0.0002with a Cliff's Δ of -0.25. The range of the Cliff's Δ 95% CI was -0.382, -0.113. The p-value of the difference between the *eIF2Bα* KO and *para* RNAi groups was 0.000 with a Cliff's Δ of 0.464. The range of the Cliff's Δ 95% CI was 0.361, 0.57. The Cas9 and sgRNA-only control groups had similar latencies around 9 seconds (Figure 17). The *eIF2Bα* KO group had a significantly decreased latency to the 42°C stimulus (8.327s) compared to either the Cas9-only (9.399s) or sgRNA-only (9.801) control.

Cas9-mediated mutagenesis of eIF2Bα had a significant, but modest effect of inducing injury-independent thermal hypersensitization. Due to the observed cytotoxicity of Cas9 overexpression using the GAL4/UAS system, these results cannot be considered a validation or replication of the RNAi phenotype (Table 3 and Figure 13).

**Figure 17**

*Effect of Nociceptor-Specific Cas9 Knockout of EIF2Bα on Thermal Hypersensitivity in* Drosophila *Larvae*

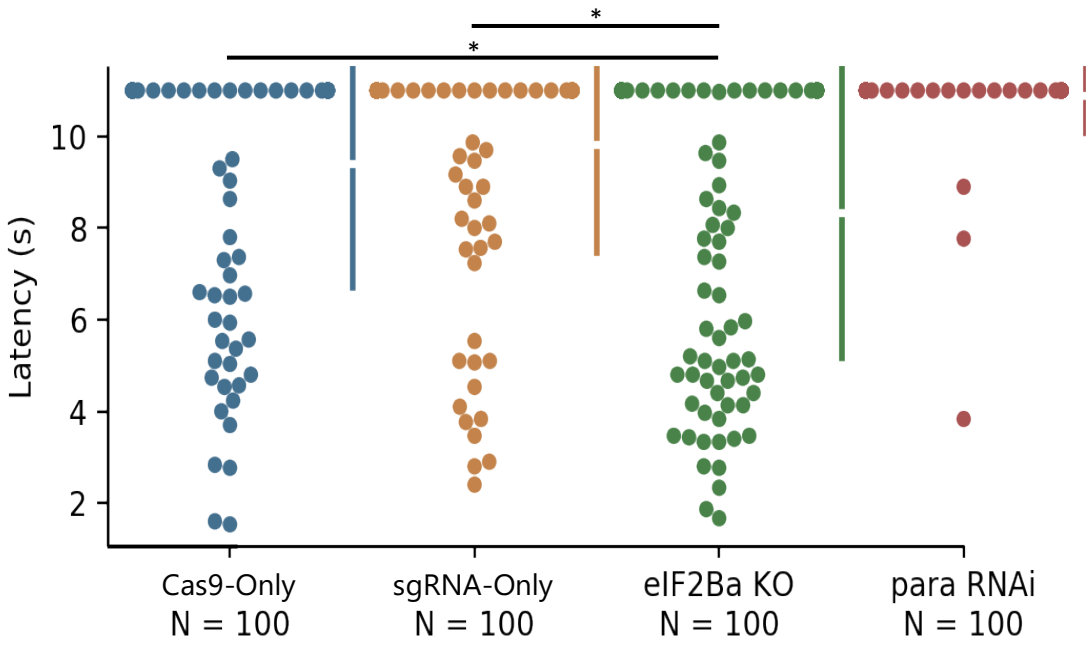


*Note:* Latency in seconds between contact with 42°C probe and complete NEL of individual larvae is shown as dots. Colored bars indicate interquartile ranges.

For all groups, n = 100.

Significance was determined via two-sided permutation t-test. * = $p < 0.05$.

## Vita

Erik Fernando Rangel Silva was born in Ecatepec de Morelos, Mexico, in 1997. His parents are Jose Martinez and Liliana Silva. In 2019, he graduated from Wingate University with a Bachelor of Science in Biology and a minor in Spanish. His undergraduate research experience led him to pursue graduate level study of Biology. In the Fall of 2020, he began the Master of Biology program at Appalachian State University. After graduation, he will work as a clinical research associate for a stem cell therapy project at a biopharmaceutical company. He plans to eventually pursue a doctoral degree to explore the pathology and progression of neuroHIV disorders.